JOHNSON CREEK LANDSLIDE RESEARCH PROJECT, LINCOLN COUNTY, OREGON

FINAL REPORT TO THE OREGON DEPARTMENT OF TRANSPORTATION

by G.R. Priest, J.C. Allan, A.R. Niem, W.A. Niem, and S.E. Dickenson

Special Paper 40
Oregon Department of Geology and Mineral Industries
2008

Cover photo: Looking south from the top of the northeast headwall of the Johnson Creek landslide, January 4, 2001. Pleistocene marine terrace deposits (tan) are exposed in the fresh escarpment.

State of Oregon
Department of Geology and Mineral Industries
Vicki S. McConnell, State Geologist

Special Paper 40

JOHNSON CREEK LANDSLIDE RESEARCH PROJECT, LINCOLN COUNTY, OREGON
FINAL REPORT TO THE OREGON DEPARTMENT OF TRANSPORTATION

By
George R. Priest[1], Jonathan C. Allan[1], Alan R. Niem[2], Wendy A. Niem[2], and Stephen E. Dickenson[3]

2008

[1]Oregon Department of Geology and Mineral Industries, Coastal Field Office, 313 SW 2nd Street, Suite D, Newport, Oregon 97365
[2]formerly with Department of Geosciences, 104 Wilkinson Hall, Oregon State University, Corvallis, Oregon 97331-5506
[3]School of Civil and Construction Engineering, 220 Owen Hall, Oregon State University, Corvallis, Oregon 97331-3212

NOTICE

THE RESULTS AND CONCLUSIONS OF THIS REPORT ARE NECESSARILY BASED ON LIMITED GEOLOGIC AND GEOPHYSICAL DATA. AT ANY GIVEN SITE IN ANY MAP AREA, SITE-SPECIFIC DATA COULD GIVE RESULTS THAT DIFFER FROM THOSE SHOWN IN THIS REPORT. **THIS REPORT CANNOT REPLACE SITE-SPECIFIC INVESTIGATIONS.** THE HAZARDS OF AN INDIVIDUAL SITE SHOULD BE ASSESSED THROUGH GEOTECHNICAL OR ENGINEERING GEOLOGY INVESTIGATION BY QUALIFIED PRACTITIONERS.

Oregon Department of Geology and Mineral Industries Special Paper 40
Published in conformance with ORS 516.030

For copies of this publication or other information about Oregon's geology and natural resources, contact:

Nature of the Northwest Information Center
800 NE Oregon Street #5, Suite 177
Portland, Oregon 97232
(503) 872-2750
http://www.naturenw.org

or these DOGAMI field offices:

Baker City Field Office
1510 Campbell Street
Baker City, OR 97814-3442
Telephone (541) 523-3133
Fax (541) 523-5992

Grants Pass Field Office
5375 Monument Drive
Grants Pass, OR 97526
Telephone (541) 476-2496
Fax (541) 474-3158

For additional information:
Administrative Offices
800 NE Oregon Street #28, Suite 965
Portland, OR 97232
Telephone (971) 673-1555
Fax (971) 673-1562
http://www.oregongeology.com
http://egov.oregon.gov/DOGAMI/

TABLE OF CONTENTS

LIST OF FIGURES

LIST OF PLATES

LIST OF TABLES

ABSTRACT

A five-year study indicates that the Johnson Creek landslide moves in response to intense rainfall that raises pore water pressure throughout the slide in the form of pulses of water pressure traveling from the headwall graben down the axis of the slide at rates of 1.4 to 2.5 m/hr in the upper part and 3.5 m/hr to virtually instantaneous in the middle part. Vertical arrays of piezometers measured infiltration at rates of only 50 mm/hr, so infiltration is too slow to affect saturated water pressure except in the headwall graben. The hydraulic gradient through the slide mass is small and groundwater flow appears to be nearly horizontal, roughly parallel to the slide plane. These observations and the rapidity of pressure transmission are consistent with a high effective hydraulic conductivity throughout the slide mass. Westward slope of the piezometric surface is consistent with better drainage in the western part of the slide. Movement episodes proceed by en masse movement when threshold pore pressures are reached followed by faster and faster movement of the middle portion of the slide when pore water pressure there rises above ~9.4 to 10.8 m head above the slide plane. In January 2003, slide velocity increased by an order of magnitude when head above the slide plane at the middle observation site reached 11.4 m while the western site reached ~9 m, ~2 m above its maximum for the following four winter seasons. Antecedent rainfall correlating with this accelerated movement was mean precipitation of 0.84 m in the previous 60 days and 2.1 mm/hr in the 62 hours immediately before the movement. Antecedent deformation correlating with the accelerated movement was extension of 1 cm in the lower part of the slide, possibly raising effective hydraulic conductivity there. This increased hydraulic conductivity may have caused a uniquely rapid pore pressure response in the lower part of the side and the unique 2-m increase in head. With respect to engineering solutions for slide mitigation, the reduction of water pressures at the headwall graben by dewatering (e.g., drains or pumps) should be effective given the inferred high hydraulic conductivity of the slide and sensitivity to pressure change at the graben. Limit equilibrium stability analyses indicate that 3 m of erosion would destabilize the slide for most of the winter season. This finding suggests that buttressing the toe of the slide is an effective long-term remediation option.

EXECUTIVE SUMMARY

This report presents and interprets data acquired during a five-year study by the Oregon Department of Geology and Mineral Industries (DOGAMI) and the Oregon Department of Transportation (ODOT).

The Johnson Creek landslide moves in response to prolonged, intense rainfall that raises water pressure throughout the slide over a period of 30 to 50 hours. The sequence of events that leads to movement starts with vertical infiltration through the unsaturated zone at ~50 mm/hr (~1.5 to 3.0 m depth in 30 to 50 hours). Infiltration rapidly raises pore water pressure in the headwall graben. Pressure is then transmitted down the axis of the slide at speeds of 1.4 to 2.5 m/hr in the upper part and 3.5 m/hr to virtually instantaneous in the middle part of the slide. Arrival time of this translating pulse, or "wave," of pressure is similar at different levels in the saturated zone in the middle of the slide mass, producing about the same total head at each level monitored; therefore the vertical hydraulic gradient is small. Seepage analyses from recorded piezometer data demonstrated nearly horizontal flow roughly parallel to the slide plane. These observations and the rapidity of pressure transmission are consistent with a high effective hydraulic conductivity throughout the slide. The lower piezometric elevation in the western part of the slide is probably indicative of better drainage there. A structure of unknown strike but with 2 m of down-to-the-east displacement lies in the middle of the slide where piezometric gradient changes and may be a groundwater barrier.

The slide begins to move en masse when threshold pore pressures are reached, the middle portion of the slide moving more rapidly than those portions to the east and west when pore water pressure there rises above ~9.4 to 10.8 m head above the slide plane. Head above the slide plane is persistently higher at the middle monitoring site than east and west of it at all times of the year, perhaps in response to the groundwater barri-

er. For most of the small creeping movements observed during the four winters, the middle site appeared to control movement for the slide as a whole. Slide velocity in January 2003 reached a minimum of 3-6 mm/hr in the middle of the slide when head above the slide plane at the middle site reached 11.4 m while the western site reached ~9 m, ~2 m above its maximum head over the following four winter seasons. The eastern site lagged behind at a steady rate of ~0.3 mm/hr during this event. These were the highest rates of movement during the five winter seasons. The conditions for accelerated movement were 0.84 m of rainfall in the previous 60 days and 62 hours of rain at a mean rate of 2.1 mm/hr. Other instances of rain at these intensities for 33 and 15 hours did not trigger the unique response at the western site, although in January of 2006 head rose as high as 10.9 m at the middle site, resulting in creeping movements averaging 0.24–0.27 mm/hr. Pore water pressure increase at the western site occurred 5 hours before the middle site in January 2003 but 28 hours after the middle site in January 2006. Antecedent movement in December 2002 of the western site 1 cm farther than the middle site created extension between the two and possibly raised effective hydraulic conductivity. Increased hydraulic conductivity may have caused the early pressure response and the unique increase in head at the western site. Understanding the complex groundwater hydraulics within and below the slide mass will be facilitated by continued monitoring of the slide with the newly installed vertical arrays of piezometers. Additional vertical arrays of piezometers installed in other parts of the slide would be beneficial. It is recommended that if these arrays are installed, they be grouted. Grouted piezometers installed at the same depth as the adjacent sand-packed piezometers recorded water pressures 1-2 m higher. Pressures from sand-packed piezometers were lower than the hydrostatic gradient.

Erosion at the toe of the slide along the beach due to wave action was also found to impact significantly the margin of stability of the slide. Limit equilibrium stability analyses found that factor of safety (FOS) declines 2.3 percent for every meter of erosion from the passive wedge formed by the back-tilted toe of the slide. The same analysis found that 1 m rise in head at the middle monitoring site caused a 2 percent decline in FOS, and that the slide reaches instability when head rise at the middle site rises 1.1 m above normal winter levels. Removal of 3 m from the toe could thus destabilize the slide during most of the winter season.

Remediation of the water pressures at the headwall graben by drainage through French drains or other means (vertical wells, surface collection, and drainage of rainwater) would be a valuable demonstration project. The high hydraulic conductivity of the slide mass inferred from rapid pore pressure transmission should make dewatering schemes particularly effective. Buttressing the toe of the slide is an effective long-term remediation option, as it eliminates erosion that can trigger movement regardless of pore water pressures. The chief environmental costs for hard revetments are loss of dry sand beach from rising sea level and creating an unnatural shoreline feature. Both of these can be mitigated by buttressing only the southern part of the slide where the most damaging movement has occurred. Understanding whether a partial buttress could stabilize other parts of the slide is an important objective for further research.

INTRODUCTION

This is the final report for a five-year investigation of the Johnson Creek landslide, Lincoln County, Oregon, by Oregon Department of Geology and Mineral Industries (DOGAMI) and Oregon Department of Transportation (ODOT) (Figure 1). The ODOT Research Program sponsored the project in cooperation with the Federal Highway Administration in order to gain a better understanding of the mechanics of large translational landslides affecting Tertiary sedimentary rocks along the U.S. west coast. The U.S. Geological Survey (USGS) Landslide Hazards Program became a partner in the project in 2005 with similar aims. The slide is less than 0.5 km (¼ mile) south of Otter Rock, Oregon, and impacts U.S. Highway 101, two private structures, and local utilities. It is clearly visible on 1939 aerial photos and causes a westward deflection of Highway 101. ODOT installed six inclinometers between 1972 and 1976 (Figure 2). In this investigation ten boreholes, three soil moisture probes, and a rain gauge were installed to monitor rainfall, movement, and water pressure (Figures 2 and 3).

OBJECTIVES

The objectives of the investigation are to determine:

- Relative importance of groundwater pressure and coastal erosion as driving forces for translational landslides.
- Thresholds of water pressure and erosion that trigger movement.
- Potential effectiveness of remediation alternatives.
- Costs of remediation alternatives in terms of money and effect on beach sand supply.
- Application of the information to other coastal translational landslides.

REGIONAL GEOLOGIC SETTING

The Johnson Creek landslide is one of several similar translational slides on coastal bluffs of Lincoln County that cut through seaward dipping Tertiary sedimentary rocks. Where these bluffs form sea cliffs 20 to 60 m high, translational slides are common with single block failures up to ~100 m wide (Priest and Allan, 2004). The bluff at Johnson Creek has all of these characteristics: It is ~30 m high, is composed of seaward dipping sedimentary rocks of the Astoria Formation, and is affected by a large translational landslide ~200 m wide (Figure 2). Like many of the sedimentary rock bluffs on the Pacific coast, a flight of Pleistocene marine terraces creates a steplike landscape with a veneer of beach and dune sand (Figures 1 and 4). The landslide cuts through the second terrace in this sequence (Figure 1).

PREVIOUS WORK

The geotechnical engineering firm Landslide Technology installed inclinometers and piezometers in winter 2002-2003, analyzed movement and water pressure data, and produced a summary report (Landslide Technology, 2004). The summary report documented observations from December 2002 to March 2003:

- There were three movement events: December 13 to 16, 2002; January 31 to February 3, 2003; and March 20 to 24, 2003. The second event had 24-cm movement in the central part of the slide; the movement sheared off all inclinometers and one piezometer cable installed below the slide plane. The other two movements were ≤ 4 cm.
- Resurvey of marker pins on the slide surface revealed that the southern part of the slide moved faster than the central and northern part during this period.
- Piezometric level measured in a sand pack 3–6 m below the central part of the slide plane was lower than in the slide mass, but shearing of the piezometer cable by the January 27 to February 3, 2003, movement limited data collection to 24 days. Landslide Technology concluded that groundwater levels in the slide mass are primarily influenced by surface water, with less influence from a deeper groundwater source.
- A minimum level of approximately 10 m of head above the slide plane in the central part of the slide was reached before ground movement was triggered.
- Factor of safety declined 2.3 percent for every 1 m of erosion of the slide toe.

Landslide Technology (2004) recommended several remediation options (Appendix M) based on a limit equilibrium analysis of stability that identified

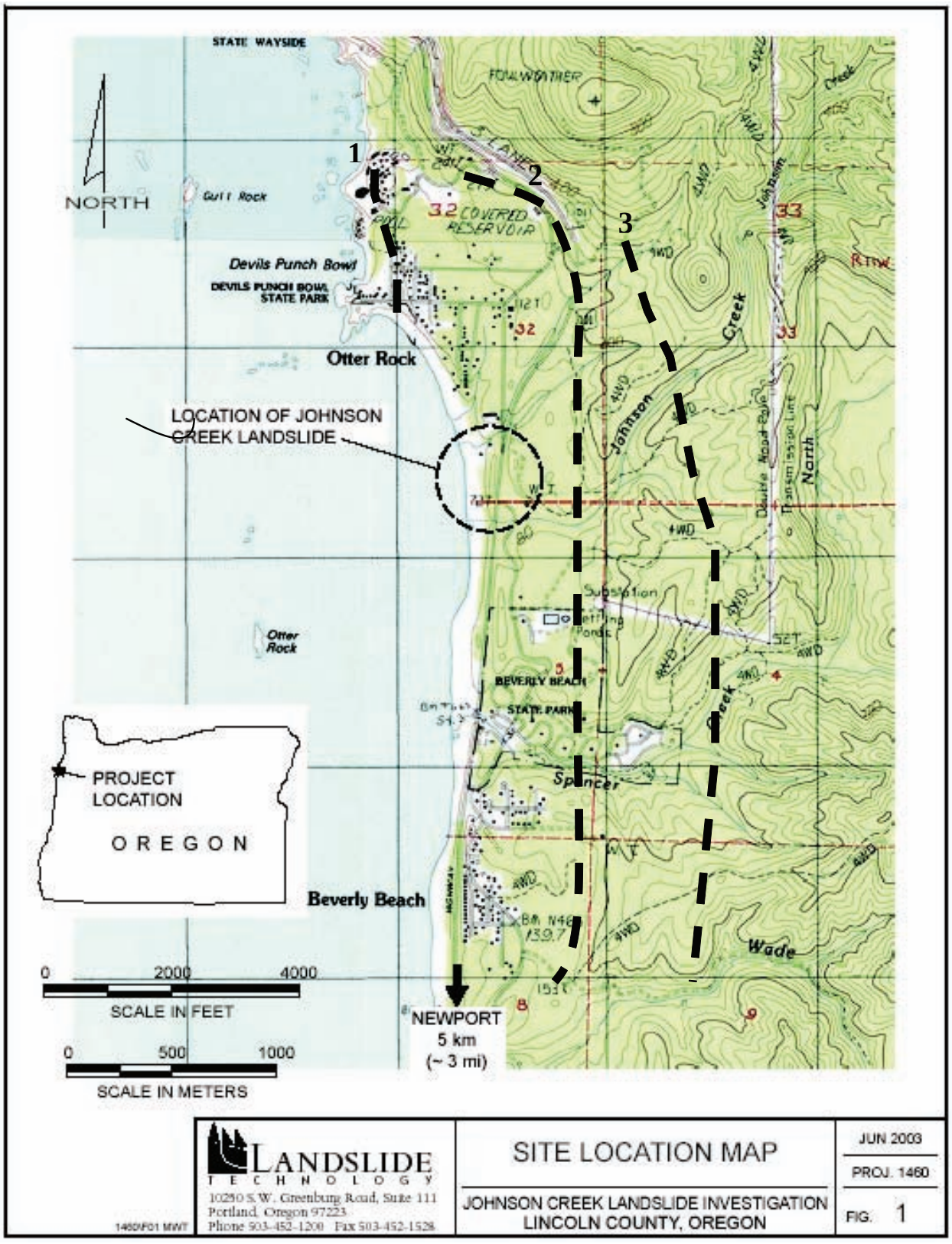

Figure 1. Location of the study area showing the backstops (eastern reach of coastal retreat) of three Pleistocene marine terraces numbered from youngest (1) to oldest (3). The remnant of a fourth terrace is preserved east of the third backstop at the ridge top between Spencer Creek and Johnson Creek. The Johnson Creek landslide displaces the second youngest terrace. Figure is modified from Landslide Technology (2004).

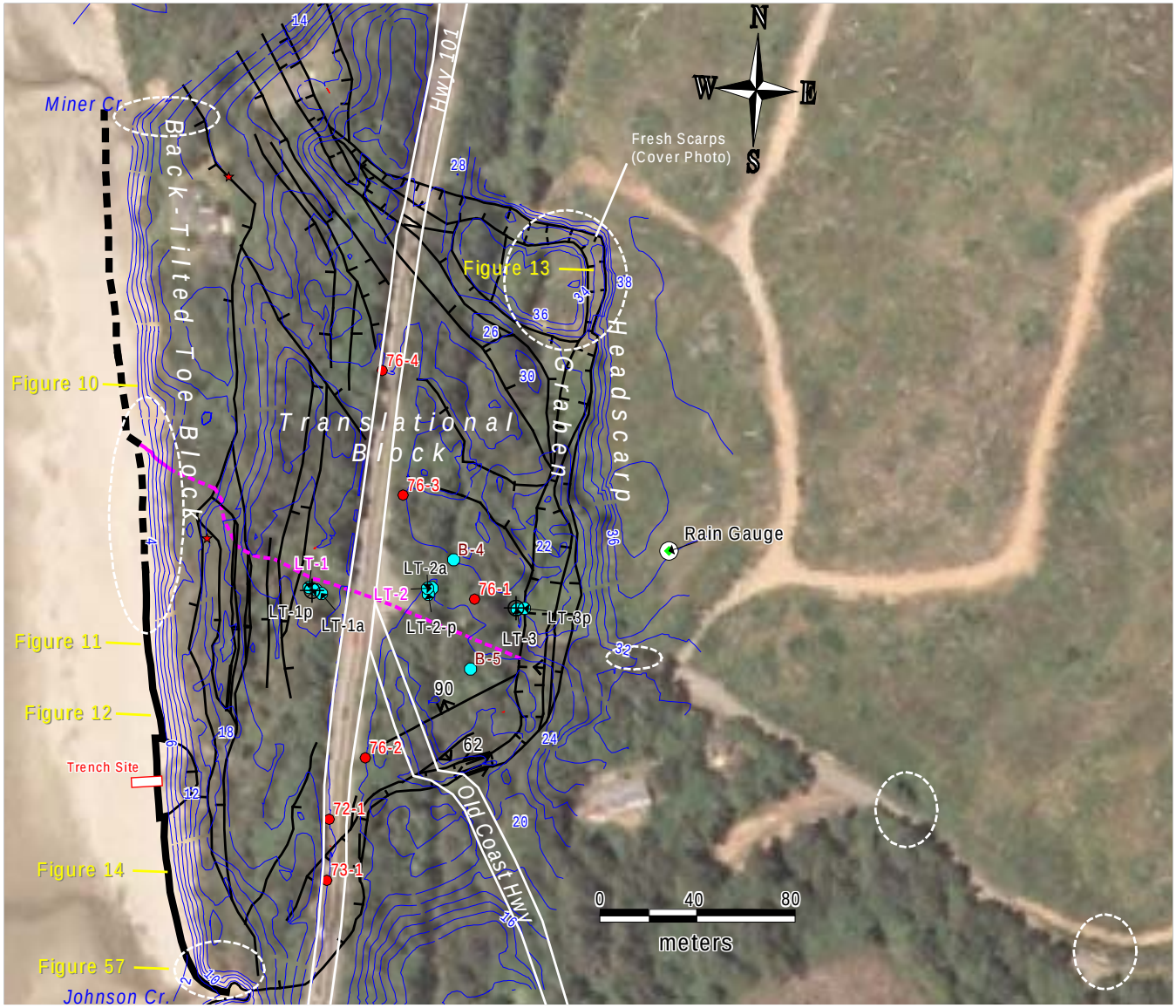

Figure 2. Site map of the Johnson Creek landslide showing 2002–2006 drill sites (blue dots), 1972–1976 Oregon Department of Transportation inclinometer sites (red dots), and the rain gauge. Blue dots with black circle and cross have soil moisture probes installed. Borehole labels in black are piezometer holes; purple labels indicate inclinometers; brown labels indicate groundwater observation wells. Base map is a 2005 U.S. Geological Survey digital orthophoto quadrangle (DOQ). Blue lines are topographic contours at 2-m intervals; black lines are major slide block boundaries. Black teeth on slide boundaries point toward the down thrown side; dashed purple line is highly speculative structure connecting an exposed fault or internal scarp at the toe to a similar structure located somewhere between boreholes LT-1 and LT-2. White dotted ellipses mark localities of detailed fracture and joint observations.

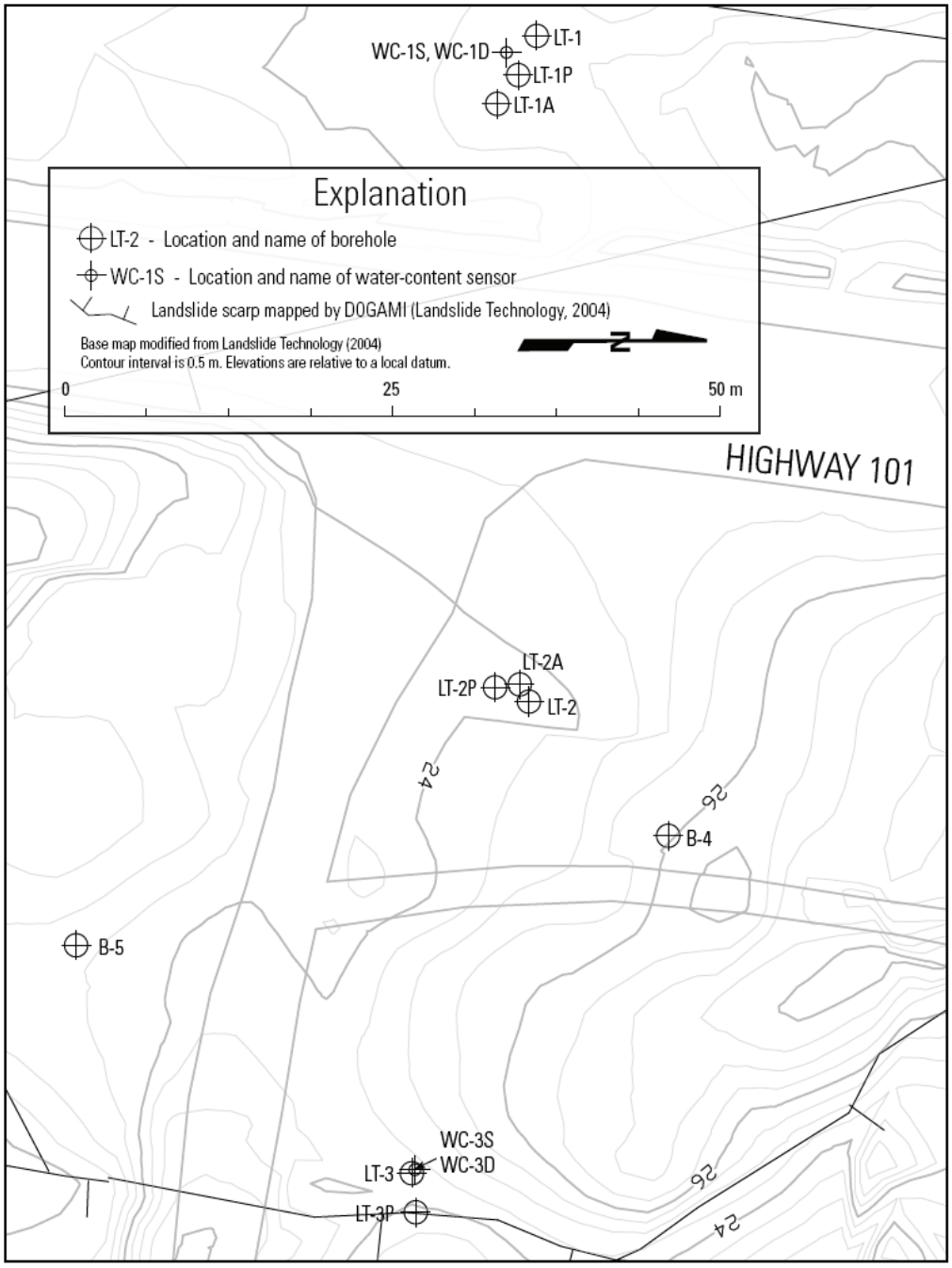

Figure 3. Location of soil moisture probes. Probe locations are labeled WC-1S, WC-1D, WC-3S, and WC-3D; probe depths are 1.5 m, 2.4 m, 1.6 m, and 3.1 m, respectively. Other labels are as in Figure 2. Figure is from Schulz and Ellis (2007).

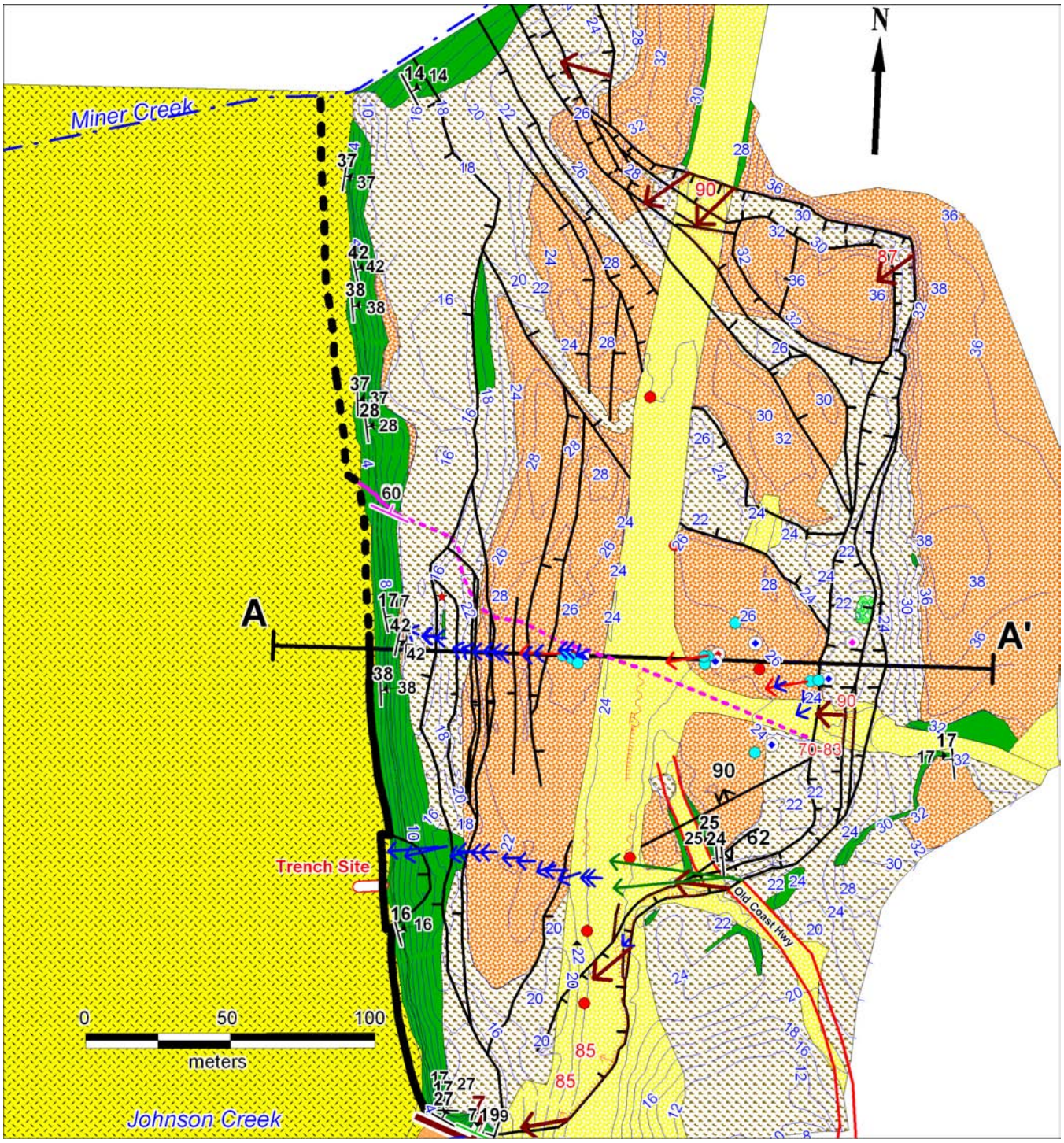

Figure 4. Geologic map of the Johnson Creek landslide. See Figure 5 for explanation and Figure 7 for cross section A-A'. Large green arrows depict direction of movement on the southeast margin of the slide based on offset of the east embankment of the Old Coast Highway; the two arrows illustrate uncertainty. Red arrows are directions of slide movement from inclinometer data; blue arrows are direction of movement from re-survey of survey markers between October 24, 2002, and April 17, 2003 (see Appendix E); brown arrows are in direction of movement from marker nails on fresh slide scarps monitored for small March 2003 slide movement (see Appendix G).

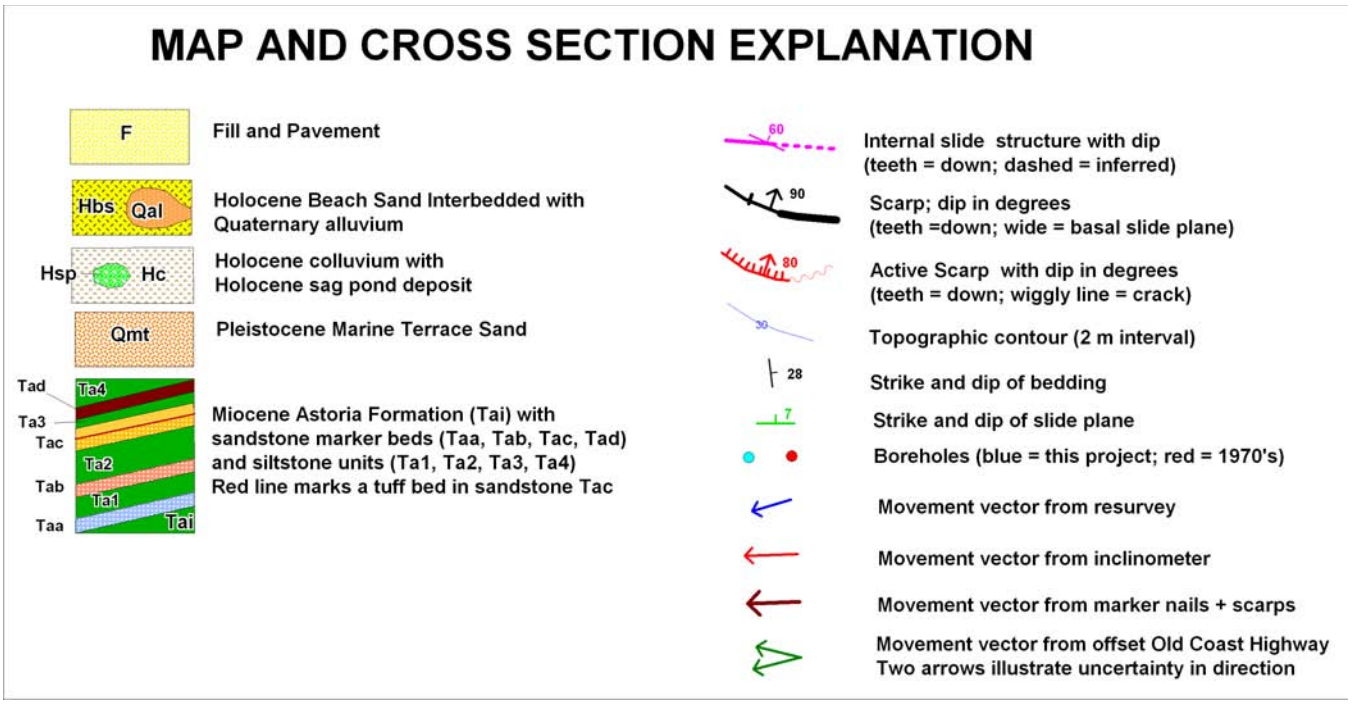

Figure 5. Map explanation for geologic map (Figure 4).

groundwater pressure as the primary cause of movement, aided by erosion of the slide toe. Additional slope stability analyses performed by Dickenson and Christie of Oregon State University (Priest and others, 2006; Appendix N) supplemented the limit equilibrium analyses of Landslide Technology (2004) with additional parametric evaluations of the influence of groundwater conditions, toe erosion, and geotechnical parameters on the computed margins of stability. Landslide Technology concluded that a buttress at the toe of the slide would be the most cost-effective remediation option.

An interim report by Priest and others (2006) summarized previous work plus additional data available through November 20, 2004. They concluded that

- Small movements of a few centimeters appeared to affect the entire slide equally and nearly simultaneously.
- Differential movement between internal slide blocks occurred between January 27 and February 3, 2003, when the central part of the slide moved 24 cm.
- Head above the slide plane was largest in the central part of the slide where the largest movement occurred.
- The Astoria Formation below the basal shear zone is much less permeable than the fractured materials in and above the shear zone.
- East-to-west migration of pore water pressure increases accompanying rainfall events might be caused by (a) pressure transmission and flow from infiltration of water at the head of the slide or (b) vertical infiltration throughout the slide. East-to-west lag of pressure increases in the latter case would be from greater depth of the water table in the western part of the slide.
- The highly fractured slide probably has relatively high effective hydraulic conductivity.
- Buttressing the southern, fastest moving part of the slide may be a cost-effective remediation option relative to buttressing the entire slide.
- Dewatering with vertical, pumped wells may slow movement significantly.

In December 2005 the U.S. Geological Survey (USGS) Landslide Hazards Program upgraded instrumentation for hourly (or shorter) collection of movement, water pore pressure, and rainfall data. Ellis and others (2007a) summarized December 2005 to January 2006 observations, concluding that:

- Rapid response of pore pressures near the basal slip plane to rainfall events suggests either relatively high hydraulic conductivity along the slide plane or rapid infiltration of rainfall through fractures from the ground surface in the upper part of the slide.

- Reduction in pore pressure thresholds from previous movement episodes indicates that rainfall or pore-pressure thresholds may not be entirely reliable or precise indicators of potential landslide movement.

In 2006 USGS installed soil moisture probes and vertical arrays of piezometers (Schulz and Ellis, 2007) in part to test the hypothesis of Priest and others (2006) that vertical infiltration of meteoric water may have a role in east-to-west migration of water pressure increases. Ellis and others (2007b) concluded from observation of water pressures during small (≤ 4 cm) movements between December 12, 2006, and April 1, 2007, that:

- The primary source of groundwater pressure increases throughout the slide is from infiltration of water near the head of the slide where the water table is shallow and from lateral groundwater flow.
- When the basal shear-zone groundwater pressure near the center of the slide reaches an approximate threshold value, the slide begins to creep almost uniformly.
- Groundwater flow within the slide is approximately parallel to the slide base.
- There is a very weak vertical hydraulic gradient, even across the basal shear zone, and relatively high hydraulic conductivity throughout the slide mass. Ellis and others (2007b) emphasized that this conclusion contradicts the conclusion of Landslide Technology (2004) that there is a hydraulic gradient to lower total head below the basal shear zone.

Schulz (2007, p. 362) similarly concluded that "vibrating-wire-piezometer nests show nearly horizontal groundwater pressure transmission from the head of the landslide toward the toe, and suggest that the landslide basal rupture surface has no effect on groundwater flow." The inferences by Ellis and others (2007b) and Schulz (2007) were from observation of piezometric pressures from grouted piezometers at depths up to 0.5 m below the base of the basal shear zone. The inferences of Landslide Technology (2004) were from piezometric pressures observed in a sand pack 3-6 m below the base of the basal shear zone, so the observational database is not exactly equivalent.

GENERAL APPROACH

We examine hydrologic, geologic, and slide movement data from November 23, 2002, to April 1, 2007, to gain insight into how the hydrologic regime triggers slide movement. Although still preliminary, ground-based light detection and ranging (lidar) surveys of wave erosion of the landslide toe provide additional insight into the potential importance of erosion in triggering movement. We use slope stability analyses to understand the how much erosion and water pressure is required to cause slide movement. We briefly summarize general conclusions from slope stability analyses of Landslide Technology (2004) and Priest and others (2006); also see Appendices M and N.

GENERAL FINDINGS

We verify previous findings that intense rainfall events cause all observed movements. Water infiltrates rapidly into the shallow water table at the head of the slide, transmitting pore water pressure through the saturated zone to the rest of the slide. Except at the headwall graben, wetting fronts from these rainfall events reach the water table after pore water pressure rises from lateral pressure transmission and flow. The key role of pore water pressure in triggering movement and the high hydraulic conductivity of the slide inferred from pore water pressure transmission suggests that dewatering may be an effective remediation option in these kinds of slides. The upper part of the slide with highest water table and highest head above the slide plane is the most critical target for dewatering. Erosion of the slide toe can trigger movement regardless of water pressure, if it proceeds far enough, so long-term remediation of coastal slides of this type will require some means of stopping erosion. An erosion resistant buttress would be the most effective means of stopping both movement and erosion.

METHODS

GEOLOGIC MAPPING

Geologic mapping was conducted by George Priest with assistance from Alan Niem. Dense vegetation and deep soil hindered bedrock mapping. A 1-m steel split tube punch coring device was used to penetrate the soils where bedrock was poorly exposed. Some areas had such dense brushy vegetation that they were virtually inaccessible. The most accurate geologic data were gathered at the sea cliff, the two bounding drainages, and in the northeast quadrant of the landslide where a recent movement created many fresh exposures (see cover photo). Johnson Creek exposed bedrock below the slide during winter 2002-2003. General spacing, width, and orientation of fractures were carefully measured at representative sites in all of these exposures and in road cuts (Figure 2). The Old Coast Highway and Highway 101 were convenient markers for measurement of lateral and vertical offset by the slide. Surface water, seeps, and springs were also mapped.

TOPOGRAPHIC SURVEY

Dennison Surveying of Newport, Oregon, performed a survey of topography in fall 2002 and a resurvey of selected points (steel rods) in spring 2003. Survey control outside the landslide area was established by tying the survey to at least four ODOT Global Positioning System (GPS) control points including ODOT points 9303-1, 9303-2, 9303-3 and 9303-4. Coordinates and elevations were established by static GPS methods and were verified (GPS site calibration procedures) against Lincoln County Geodetic control points and National Geodetic Survey High Accuracy Reference Network (HARN) control monuments. The vertical datum for all topographic data was the North American Vertical Datum of 1988 (NAVD 1988). The horizontal datum was originally a local reference system used by ODOT but was transformed to Oregon State Plane 3601 North Zone, North American Datum of 1983 (NAD 1983) meters.

The survey was expressed in topographic contours at 0.5-m intervals that generally yielded an excellent representation of the morphology of the landslide. A few areas of particularly dense vegetation prevented access in the western part of the slide.

SUBSURFACE EXPLORATION

Drilling

Exploratory drilling program began with six borings completed between November 18 and December 5, 2002 (first phase) and January 6 to January 10, 2003 (second phase). Borings completed as part of phase one are designated, from west to east (lower to upper part of the slide), LT-1, LT-2, and LT- 3 (Figure 2). Companion borings drilled in the second-phase installation of piezometers are designated LT-1p, LT-2p, and LT-3p (Figure 2; Table 1).

Geo-Tech Explorations, Inc. of Tualatin, Oregon, performed the exploratory drilling using a track-mounted CME 850 drill rig. A combination of 15-cm (57/8-in) outer diameter (O.D.) tricone mud-rotary, casing installation through overburden, and PQ3-wireline diamond core drilling techniques were used to drill the slope inclinometer borings to final depth. Hollow-stem auger techniques were used to drill the piezometer borings to final depth. Soil samples in the inclinometer borings (LT-1, LT-2, and LT-3) were obtained at approximately 0.76- or 1.52-m (2.5- or 5-ft) intervals using a 7.6-cm (3-in) O.D. split-spoon sample barrel driven by a 63.5-kg (140-lb) auto-trip hammer. The underlying bedrock was sampled by obtaining rock cores using 1.52-m (5-ft) long, triple barrel coring techniques. The quality of the bedrock was recorded using Rock Quality Designation (RQD) and core recovery indices. Samples were also collected in the piezometer borings in the zones of measured slide movement, using 7.6-cm (3-in) diameter thin-walled Shelby tubes. In addition, select soil samples were obtained in Boring LT-3p using Standard Penetration Test (SPT) procedures.

Four boreholes were drilled in November 2006 in order to install additional piezometers (Table 1; Figure 2): One (LT-1a) at the west site, one (LT-2a) at the middle site, and two between the middle and east sites (B-4 and B-5). William H. Schulz of the USGS supervised drilling and described cores from the B-4 and B-5 boreholes (Schulz and Ellis, 2007). No samples were described from the LT-1a or LT-2a boreholes, which were rapidly drilled utilizing a rotary bit. Boreholes for the water-content sensors were made by driving a 0.6-m-long, 5.1-cm-diameter, cylindrical steel sampler using a 22-kg electric breaker hammer to depths of 1.5

Table 1. Borehole, piezometer, soil moisture probe, depths and elevations relative to the base of the Johnson Creek landslide basal shear zone ("slide plane" in the table).

Hole	Borehole Elevation (m)	Total Depth (m)	Depth to Probe Tip (m)	Probe Elevation (m)	Slide Plane Depth (m)	Slide Plane Elevation (m)	Sand Pack Depth Interval (m)
LT-1p piezometer @ 23.80 m	25.179	26.8	24.80	0.38	26.2	–1.1	23.8–26.8
LT-1 inclinometer	25.048	33.8			26.5	–1.5	-
LT-2p piezometer @ 16.70 m	24.698	25.0	16.70	8.00	18.4	6.3	15.2–18.2
LT-2p piezometer @ 24.70 m	24.698	25.0	24.70	0.00	18.4	6.3	21.8–25.0
LT-2 inclinometer	25.028	34.7			18.6	6.4	-
LT-3p piezometer @ 5.5 m	24.472	7.0	5.50	18.97	5.8	18.7	3.9–7.0
LT-3 inclinometer	24.746	28.7			7.0	17.7	-
LT-1a piezometer hole @ 3.35 m	25.201	26.5	3.35	21.85	25.9	-0.7	cement
LT-1a piezometer hole @ 9.14 m	25.201	26.5	9.14	16.06	25.9	-0.7	cement
LT-1a piezometer @ 15.24 m	25.201	26.5	15.24	9.96	25.9	-0.7	cement
LT-1a piezometer @ 21.34 m	25.201	26.5	21.34	3.86	25.9	-0.7	cement
LT-1a piezometer @ 24.08 m	25.201	26.5	24.08	1.12	25.9	-0.7	cement
LT-1a piezometer @ 26.21 m	25.201	26.5	26.21	–1.01	25.9	-0.7	cement
LT-2a piezometer @ 3.05 m	24.792	19.4	3.05	21.74	18.8	6.0	cement
LT-2a piezometer @ 6.10 m	24.792	19.4	6.10	18.69	18.8	6.0	cement
LT-2a piezometer @ 10.67 m	24.792	19.4	10.67	14.12	18.8	6.0	cement
LT-2a piezometer @ 13.72 m	24.792	19.4	13.72	11.07	18.8	6.0	cement
LT-2a piezometer @ 16.76 m	24.792	19.4	16.76	8.03	18.8	6.0	cement
LT-2a piezometer @ 19.29 m	24.792	19.4	19.29	5.50	18.8	6.0	cement
B-4 piezometer hole 20.12 m	26.736	20.6	20.12	6.62	18.2	8.5	cement
B-5 piezometer hole @ 10.67 m	23.199	12.0	10.67	12.53	9.8	13.4	cement
LT-1 soil moisture probe @ 1.5 m	25.048	1.50	1.50	23.55	26.5	–1.5	-
LT-1 soil moisture probe @ 3.0 m	25.048	2.40	2.40	22.65	26.5	–1.5	-
LT-3 soil moisture probe @ 1.50 m	24.396	1.60	1.60	22.80	7.0	17.4	-
LT-3 soil moisture probe @ 3.0 m	24.396	3.10	3.10	21.30	7.0	17.4	-
72-1 (1972 ODOT inclinometer)	23.50	21.3	-	-	9.1	14.4	-
73-1 (1973 ODOT inclinometer	23.50	29.0	-	-	16.8	6.7	-
76-1 (1976 ODOT inclinometer)	25.66	21.3	-	-	14.6	11.0	-
76-1 (1976 ODOT inclinometer)	25.00	21.3	-	-	14.6	10.4	-
76-2 (1976 ODOT inclinometer)	24.00	21.3	-	-	20.1	3.9	-
76-3 (1976 ODOT inclinometer)	25.50	26.2	-	-	24.4	1.1	-
76-4 (1976 ODOT inclinometer)	25.50	25.9	-	-	26.8	–1.3	-

Slide plane depths and elevations from Oregon Department of Transportation (ODOT) inclinometers installed in the 1970s are highly uncertain; see text for explanation. @ = at depth of; all elevations are relative to the North American Vertical Datum of 1988 (NAVD 1988).

to 3.1 m, two at the western (LT-1) and two at the eastern (LT-3) site (Figure 3; Schulz and Ellis [2007]). Table 1 summarizes borehole depths and collar elevations.

Test Pits

On March 24, 2003, two exploratory test pits were excavated in an east-west line through the slide toe to examine the geometry and composition of the slide plane. The backhoe reached ~1.5 m depth in each pit. Pit locations are shown in Figure 2 as the trench site.

MONITORING

Surface Displacement

Movement of the slide surface between October 2002 and April 2003 was determined by resurveying survey pins along a line-of-sight parallel to Highway 101 (Appendix F), resurveying steel stakes in three east-west lines through the slide (Appendix E), and detailed measurements across the heads of marker nails installed on both sides of well defined scarps (Appendix G). Movement at survey pins for the line-of-site survey and the steel stakes was determined by comparison to stable survey points outside the slide. Vertical and horizontal separation of marker nails installed with nail heads touching allowed precise measurement of direction and amount of movement at individual fresh scarps. Vulnerability of marker nails to burial or removal by mass wasting limited measurement to one movement episode in March 2003.

Subsurface Displacement

Inclinometers and extensometers provided slide movement data at three sites (LT-1, LT-2, and LT-3; Figure 2). Borehole depths are listed in Table 1.

Slope inclinometer casings were installed in borings LT-1, LT-2, and LT-3. The inclinometers consist of 3.048-m (10-ft) lengths of Slope Indicator Company 7.0-cm (2.75-in) O.D. acrylonitrile-butadiene-styrene (ABS) casings with quick-connect couplings. The annular space between the casings and boring sidewalls was backfilled with cement bentonite grout, and each inclinometer was capped with a protective surface monument and concrete. Details of the inclinometer installations are included on the summary boring logs, Appendix B. Coaxial cable was attached to the downslope exterior of the slope indicator casings. The RG59U coaxial cable is commonly used for home electronics. The cable can allow the use of time domain reflectometry (TDR) technology for measurement of additional information on slide movement at depth after the casing has been sheared, but no TDR logging device was available for that experiment before the cables were sheared by the large slide movement in 2003. Coaxial cables were installed in 2006 on casings of groundwater monitoring wells B-4 and B-5 (Figure 2), so these data may be collected at those sites some time in the future.

Manual boring extensometers were installed within the slope inclinometer casings after the inclinometer probe was unable to pass the shear zone. The extensometers allow for continued slide monitoring, although at a reduced accuracy and with no directional information as compared to the inclinometer. The extensometer consisted in the original installation of a braided steel rope anchored with an attached chain in a 3-m (10-ft) long concrete and sand plug at the bottom of the casing. A 0.6- to 0.9-m (2- to 3-ft) section of steel rope extended from the top of the casing with a crimped ferrule attached near the end of the rope. The distance between the top of the casing and the bottom of the ferrule became the gauge length of the extensometer during the first two years of observations.

In November 20, 2004, the USGS installed new data acquisition systems to monitor existing instrumentation at the site, and new instrumentation was added that allowed simultaneous recording of precipitation, groundwater pressure and landslide movement. PsiTronix extension transducers (80-in range) were attached with a pulley and reel assembly to the braided wire in each of the three extensometer holes (Figure 2). USGS replaced the three GEOKON dataloggers with two Campbell Scientific CR10X dataloggers, one at the LT-1 site and one at the LT-3 site.

Measurement error varied with the method. Inclinometers have a high precision (0.25 mm) compared to that of the extensometers (1 cm) used prior to installation of the cable and pulley system. Cable extension of 0.05 cm can be resolved with the cable and pulley system (Schulz and Ellis, 2007).

Rainfall

A rain gauge was installed above the headscarp at the location shown in Figure 2 about 80 m northeast of the LT-3 site. The instrument is a Global Water, Inc., RG200 tipping bucket rain gauge initially connected to a Global

Water model GL400-1-1 pulse type datalogger. As of November 20, 2004, the new Scientific CR10X logger at the LT-3 site also receives data through a wire from the rain gauge. Both current and former dataloggers were originally programmed to record rainfall amounts every hour; however, since March 9, 2006, data from the rain gauge, extensometers, and piezometers has been recorded every 15 minutes. On January 7, 2003, a wind shield was installed on the rain gauge. Prior to that high winds created some false readings.

Estimates of precipitation for periods of time when local rain gauge data were lacking were compiled from the Hatfield Marine Science Center archives (http://hmsc.oregonstate.edu/weather/archives/guinlib/). The rain gauge for these data is located ~12 km south of the landslide.

Groundwater

Groundwater pore pressures were monitored by vibrating wire piezometers, and soil moisture was monitored by soil moisture probes. Table 1 summarizes borehole depths and elevations of all piezometers and probes. Piezometers and moisture probes were installed in phases.

In December 2002, four vibrating wire pressure transducers, manufactured by Slope Indicator Company, were installed next to the LT-1, LT-2, and LT-3 inclinometer holes; these boreholes are labeled LT-1p, LT-2p, and LT-3p in Figure 2. In each boring, the pressure transducers were installed within 2 m above the slide plane identified from inclinometer data. The sand pack around the transducer penetrated the slide plane. An additional pressure transducer was installed 5.1 m below the basal shear zone at the middle drill site (LT-2p) in a sand pack 3–6 m below the slide plane. This transducer lost communication with the datalogger due to slide movement on February 1, 2003.

Between November 7 and November 14, 2006, the USGS Landslide Hazards Program supervised installation of 12 vibrating wire piezometers in two boreholes, consisting of two vertical arrays of six piezometers (boreholes LT-1a and LT-2a, Figure 2; Table 1). All were grouted with a bentonite-cement mixture (see Schulz and Ellis, 2007, for further details).

Also installed November 2006 were two single piezometers inside slotted casing near the bottom of two groundwater monitoring wells (boreholes B-4 and B-5, Figure 1; Table 1). The groundwater monitoring wells consisted of Johnson Screens 1.25-in (3.15-cm) diameter, schedule 80 PVC pipe with 10-slot screened sections. Coaxial cable was taped to the outside of the B-4 and B-5 well casings and extends to the bottom of each borehole. The cable permits possible identification of the depth of shearing in the two wells (Kane and Beck, 1996). The annular space around each well casing was backfilled with 10/20 Colorado silica sand and Volclay coarse bentonite chips. Bentonite chips were placed in the bottom of borehole B-5 below the sand backfill and above the sand backfill in both boreholes to 0.3 m below ground surface. Steel, flush-mount well covers were set in concrete from 0.3 m below ground surface to the ground surface (see Schulz and Ellis, 2007, for further details).

B-4 and B-5 pore pressure data are not equivalent to data from the other piezometers because both are water-table observation wells and provide only water table elevation. The other piezometers are Casagrande piezometers that provide discrete measurements of groundwater pressure at a point.

In November 2006 the USGS also installed four soil moisture probes (Table 1; Figure 3). These are Decagon Devices, Inc., ECH2O model EC-5 dielectric sensors. The sensors produce an output voltage that depends on the dielectric constant of the medium surrounding the sensors. The EC-5 has a claimed resolution of 0.001 m^3/m^3 and accuracy of at least 0.003 m^3/m^3 in all soils with salinity below 8 decisiemens per meter (Schulz and Ellis, 2007). Schulz and Ellis (2007) noted that the deeper probe at the LT-1 site (WC-1D, Figure 3) appears to measure very subtle changes in water content at times when large changes are measured by the other sensors but does not appear to provide accurate absolute measurements or to detect moderate and small changes in water content.

Between December 2002 and November 2004, piezometer data were collected by two single-channel GEOKON dataloggers, one at the eastern (LT-3p) site and one at the western (LT-1p) site. Data from LT-2p and LT-3p installations were collected at the LT-3p site; data from the LT-1p piezometer flowed to the LT-1p site. Data were downloaded periodically with a laptop computer. In November 2004, the USGS Landslide Hazards Program installed new dataloggers at these two sites. Both loggers are powered by rechargeable gel cell batteries recharged by solar panels. In early 2006 the USGS incorporated cellular modems into the

data acquisition systems so that data could be accessed remotely and more frequently. Pore-water pressures were recorded every hour between January 2003 and March 8, 2006. From March 9, 2006, to April 1, 2007, data were collected every 15 minutes. See Schulz and Ellis (2007) for further details on the USGS upgrade.

Erosion

Pins. An attempt was made to measure the rate of erosion at the slide toe using survey pins installed in the face of the bluff. Thirty-five, 298-mm (117/8 in) long pins were inserted in six profiles up the face of the bluff on December 9, 2002. The amount of pin sticking out was measured at installation and again on April 10, 2003 (Appendix H). Because many of the pins were lost to erosion in the first season, steel stakes 77 cm (30 in) long were driven into the base of the sea cliff in spring 2004 to obtain additional data. Extensive loss of the 77 cm pins to erosion and talus cover caused this experiment to be abandoned.

Lidar. Owing to failure of survey pins to yield accurate erosion rates, ground-based light detection and ranging (lidar) surveys (GBL) were initially undertaken as a pilot effort to obtain estimates of mass loss along three segments of the sea cliff (south, middle, and north) and encompassed the region between the toe of the landslide and the top of the bluff face (Appendix I). The GBL point density is high enough that individual trees located at the top of the sea cliff can be tracked, providing an independent means of measuring slide movement at the toe of the slide where slide movement data are lacking. Furthermore, removing the effects of differential slide movement from the GBL data will be crucial for determining the extent of bluff erosion in response to wave runup erosion and subaerial weathering processes. Processing of the data is still at an early stage, so slide movement has not yet been estimated. The initial survey of the bluff was carried out May 14, 2004, and provided a baseline for future measurements. Following the initial GBL survey, two surveys were undertaken by staff from ODOT's Geometronics group. These latter surveys were carried out respectively on October 3-4, 2006, almost 2.5 years after the first survey in 2004, and again on April 3-4, 2007. However, in contrast to the initial survey in 2004, the latter two surveys encompassed the entire length of the toe of the Johnson Creek landslide.

Airborne lidar surveys by USGS in 1997, 1998, and 2002 were examined for erosion information, but once the data were gridded and reduced to elevation contours, errors of 1.2–2.4 m (bluff accretion or exaggerated erosion) became apparent. These errors appear to be from smoothing of relatively sparse data on steep bluff slopes, so the data were not useful.

Beach erosion. Erosion and deposition of beach and dune sand can affect slide stability owing to the buttressing effect and erosion protection afforded by thick sand accumulations. Measurements of beach sand levels were obtained using lidar and topographic surveying (Appendix K). Field surveying of topographic profiles to determine beach sand volume was suspended after spring 2003. Observations since that time are qualitative from frequent visits to the beach.

LABORATORY TESTING

Laboratory testing was performed to determine soil index properties for correlation with engineering parameters and to aid with classification. All testing was performed at the Landslide Technology soil laboratory in Portland, Oregon. Tests were performed on selected samples collected during field explorations to verify field classifications and to determine the following properties:

- soil classification
- natural moisture content
- in-place density
- residual shear strength

Soil and rock core samples obtained from the field exploration program were visually re-examined in the laboratory to confirm field classifications using American Society for Testing and Materials Document 2488 (ASTM D 2488). Together with the results of additional laboratory testing, final soil descriptions were prepared in general accordance with ASTM D 2487. Soil classifications and descriptions are presented on the boring logs of Appendix B.

Moisture contents were determined on all samples retrieved from the field explorations in general accordance with ASTM D 2216.

In-place density tests were performed on selected core samples obtained during field explorations. The tests were performed in general accordance with ASTM D 2937.

Residual shear strength tests were performed on shear zone material obtained from a drill core sample. The specimen was obtained in boring LT-2 at a depth of 18.1 m (59 ft). The zone of slide movement measured in inclinometer LT-2 is from depths of 17.4 to 18.6 m (57 to 61 ft). The tested soil is soft, slightly clayey, sandy silt; no sand- or gravel-sized fragments were in the sample.

The sample was remolded by hand and placed in the ring-shear apparatus. The ring shear sample is 0.20 in thick and has a surface area of 6.2 in^2. After the sample was placed in the ring shear apparatus, it was consolidated in a water bath for each load increment prior to shearing. The sample was tested at 490, 245, and 123 KPa (5.1, 2.6, and 1.3 tons per square foot, tsf) confining pressure to simulate the range of in-situ effective confining stress along the shear zone. In-situ confining pressures at the shear zone within LT-1, LT-2, and LT-3 were estimated to be 380, 290, and 120 KPa (4.0, 3.0, and 1.3 tsf), respectively, using groundwater levels obtained from the vibrating wire piezometers. Following consolidation of the samples, shearing was commenced at a rate of 0.024 degrees per minute until reaching residual strength. The test was repeated for each of the three loads detailed above (Appendix J).

SLOPE STABILITY ANALYSIS

Two independent suites of limit equilibrium, slope stability analyses were completed to evaluate the influence of groundwater conditions, geotechnical parameters, and toe erosion on the slide movement. Although the stability modeling was performed using conventional 2-D slope stability procedures, the analyses were performed for several cross sections of the slide; thus, the results are useful for elucidating the 3-D kinematics of the slide mass. Landslide Technology (2004) executed the first suite of analyses (Appendix M), and Christie and Dickenson in the Department of Civil, Construction, and Environmental Engineering at Oregon State University carried out the second suite (Priest and others, 2006; Appendix N). Project support was insufficient to update these analyses for data collected after spring 2003.

Both Landslide Technology and Oregon State University used the method of Spencer (1967) in the computer program XSTABL by Interactive Software Designs, Inc. (http://www.xstabl.com/). XSTABL employs rigid body mechanics in the solution of circular and wedge slip surfaces. The program searches for the critical surface exhibiting the lowest margin of stability (expressed as the factor of safety against sliding). This approach does not account for the cumulative effect of multiple water-filled tension cracks or interaction between blocks within the overall slide mass. Spencer's method is a force and moment equilibrium method that assumes the resultant slide force inclination is the same for every slice. A box search method is used for the stability analysis at the toe of the slope. The force and moment equilibrium approach generates random points within the user specified search box.

The Landslide Technology (2004) analyses were performed by back-calculating the required strength (angle of shearing resistance, ϕ') along the shear zone at the drilling transect to infer incipient failure conditions (i.e., for a factor of safety equal to 1.0). The improvements to the factor of safety (FOS) were then checked for various treatment options using the back-calculated ϕ_r'. Landslide Technology used standard engineering calculations to construct site-specific remediation options (Appendix M).

Christie and Dickenson (Priest and others, 2006; Appendix N) evaluated the influence of the following parameters on overall slide mass stability: (a) drained shear strength parameters, (b) piezometric surface and threshold pore pressure required for slope movement, (c) influence of water-filled tension cracks on toe stability, and (d) evaluation of the impact of translating pore pressure pulses, or waves, on overall stability. Their approach was similar to that of Landslide Technology but used two additional cross sections, one north and one south of the drilling transect (see Appendix N).

RESULTS

GEOLOGIC MAPPING

The geologic map, cross sections, and structure contour map shown in Figures 4–9 summarize surface and subsurface interpretations of the landslide structure. Figure 4 depicts all interpretations of slide movement direction from inclinometer logs, resurveys, marker nail monitoring, and offset roads.

Topographic Expression and Structure

Johnson Creek landslide has a maximum width of 200 m from headscarp to toe. East of Highway 101, the slide extends 240 m north-south, but west of Highway 101 the slide extends ~400 m north-south (Figures 2 and 4). Steep-sided ravines bound the slide at Johnson Creek on the south and Miner Creek on the north (Figure 2). Johnson Creek cuts through the slide mass to underlying undisturbed bedrock but Miner Creek appears to lie in slide material that extends northward out of the project area.

Surface features within the slide include a 6- to 15-m headscarp, a 7- to 23-m-wide graben, a 100- to 120-m-wide translational block, and back-rotated toe block (Figures 2 and 7). The headwall graben is only 7 to 12 m wide around most of the slide (Figure 2). Internal slide scarps trend northwest in the northern part of the slide and east-west to northeast in the southern part (Figures 2 and 7).

The back-tilted toe block is 4 to 30 m wide and forms a 17-m-high bench that lies at the base of scarps separating it from the main translational blocks to the east (Figures 2 and 7). These scarps have about 10 m of relief and change northward from multiple scarps to one scarp. The width of the toe block increases by a factor of 2 where the scarps fuse into one. Bedding in Tertiary Astoria Formation exposed at the toe dips between 15° and 45° to the east, rotated from original west dip on the order of ~17° (Figures 4 and 10). This "back-rotation" is likely due to upward movement of slide blocks. If the basal slide zone of a translational slide rises to the surface at its toe, a passive wedge is formed where material can rotate relative to the main slide mass. Local slumps can also result in back-rotation of slide blocks, but this block is relatively coherent, as demonstrated by continuity of single marker beds (Figure 11). These marker beds are offset ~2 m down to the northeast on a fault or internal shear plane striking N 66° W and dipping 60° NE (solid part of the purple line in Figure 2). This structure occurs where the toe block changes width and multiple scarps behind it change to a single scarp (Figures 2 and 4).

The large translational blocks east of the toe block are generally higher in elevation in the northern half and highest in the northeast quadrant where movement over approximately the past 10 years created a near vertical headscarp (Figures 2 and 4). East of Highway 101 the translational blocks are at an elevation of 27–33 m in the northern half and 23–26 m in the southern half of the slide. West of Highway 101 the southern half of these blocks lies at an elevation of 20–23 m while the northern half lies at 25- to 31-m elevation. The surface expression of the slide is therefore suggestive of increasing displacement west and south of the northeast corner (Landslide Technology, 2004).

Offset Roads

At the southern margin of the slide on the Old Coast Highway, offset since highway abandonment in about 1943 (Len Saltekoff, ODOT, personal communication 2005; Figure 2) is ~ 3.35 ± 0.6 m left lateral and ~0.91 ± 0.05 m vertical. These vertical and horizontal components of movement imply a slide plane dip of ~15° ± 2° west. Mean rate of movement over the 62 years was ~5.4 ± 1 cm/yr horizontal and ~1.5 ± 0.08 cm/yr vertical. These values are based on displacement of the original gravel surface at the east highway embankment inside and outside of the slide. Only a few centimeters of gravel are present, so it is likely that the road was graveled only once or twice before abandonment and has not been largely disturbed (i.e., re-graded or excavated) since then. The trend of the road embankments would seem to offer another datum for estimation of lateral offset, but there was apparently continual realignment of the road as the slide moved, creating a curving embankment now disrupted at the slide margin. Lateral offset since initial construction of the Old Coast Highway can be crudely estimated by assuming the road was originally straight, trending about N 27° W (north part in the slide) to N 38° W (south part outside the slide). Left-lateral offset determined in this fashion is ~6.4 ± 1.2 m. Vertical offset since initial construction cannot be determined easily, as it is likely that the road

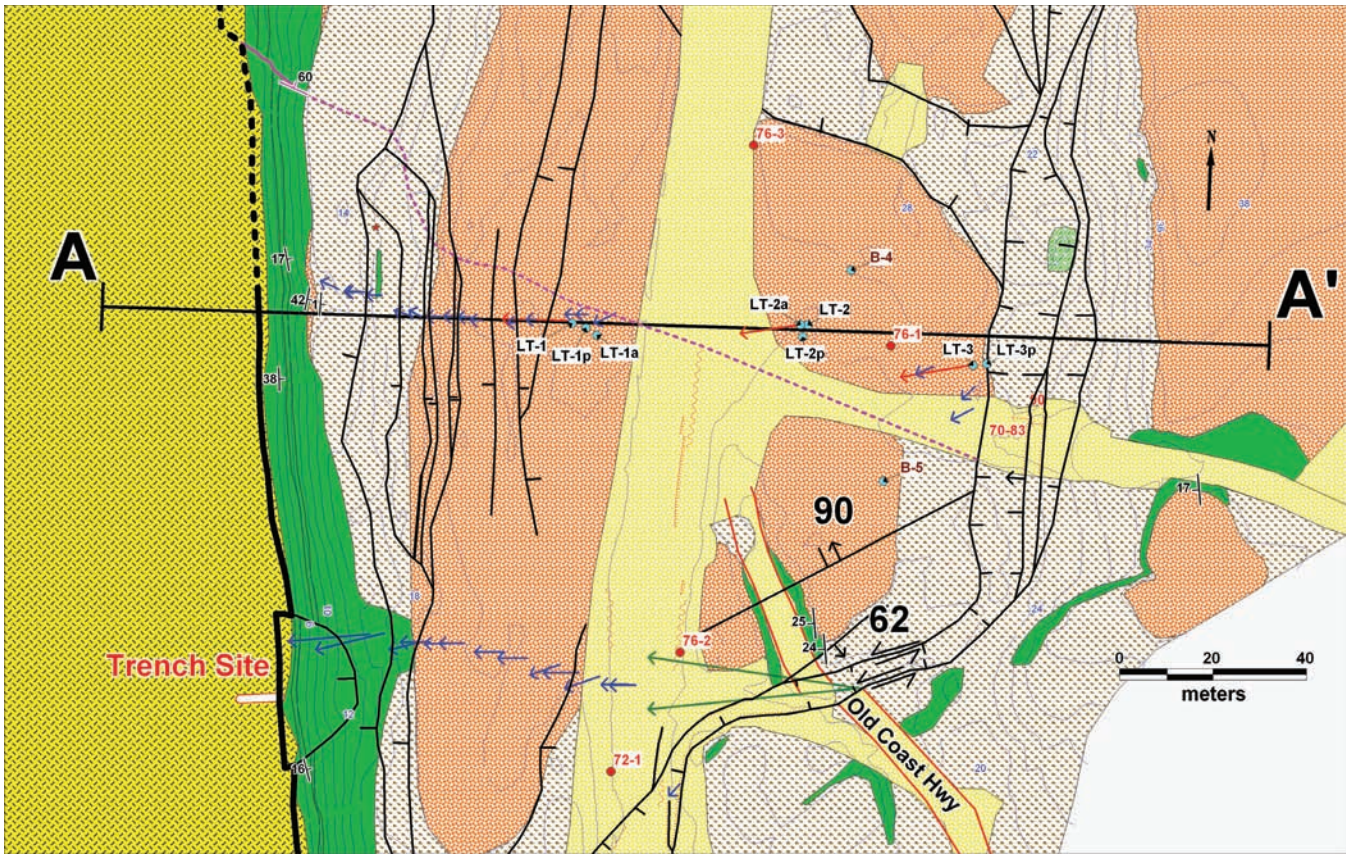

Figure 6. Geologic map in the vicinity of the boreholes (blue dots) for this project. Symbols as in Figures 4 and 5. Cross section A-A′ is shown in Figure 7.

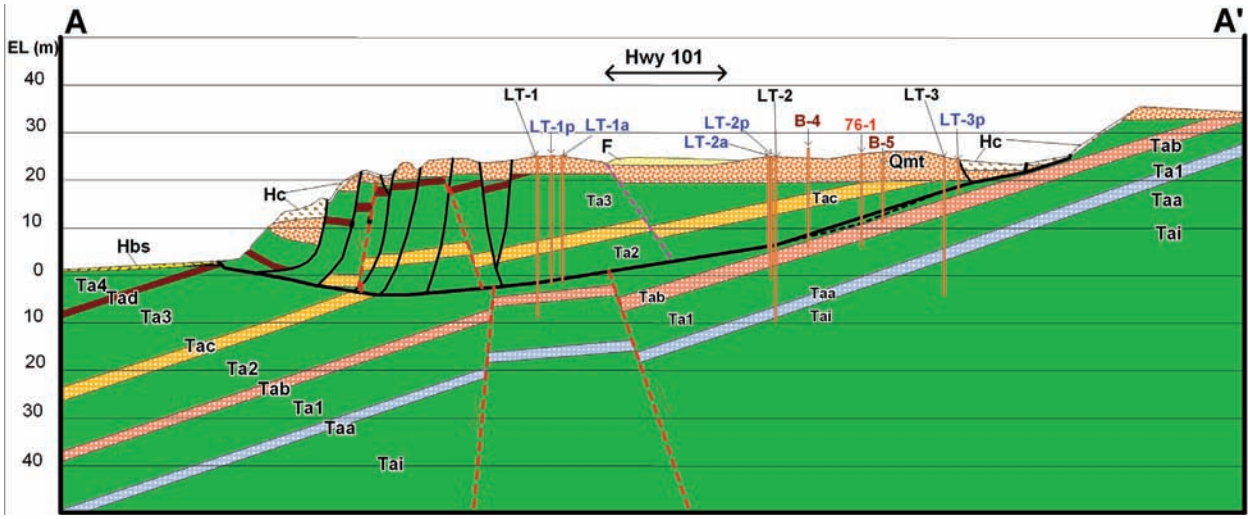

Figure 7. Generalized cross section A-A′. Strike and dip of tectonic faults (red dashed lines) are inferred faults that cannot be located more accurately than the spacing of the boreholes, so are not depicted on the geologic map. Purple dashed line is an internal slide structure with dip and offset best fitting borehole stratigraphy; lateral position between boreholes LT-1 and LT-2 is unknown. Dashed black line is the slide plane inferred from estimated depth of slide plane at inclinometer hole 76-1, but elevation and depth data for the slide plane at this hole have higher uncertainty than for inclinometer holes LT-1, LT-2, and LT-3 (solid black line labeled slide plane). Horizontal lines are isolines of elevation with labels in meters above geodetic mean sea level (NAVD 88). See Figure 5 for explanation of geologic units; vertical scale = horizontal scale.

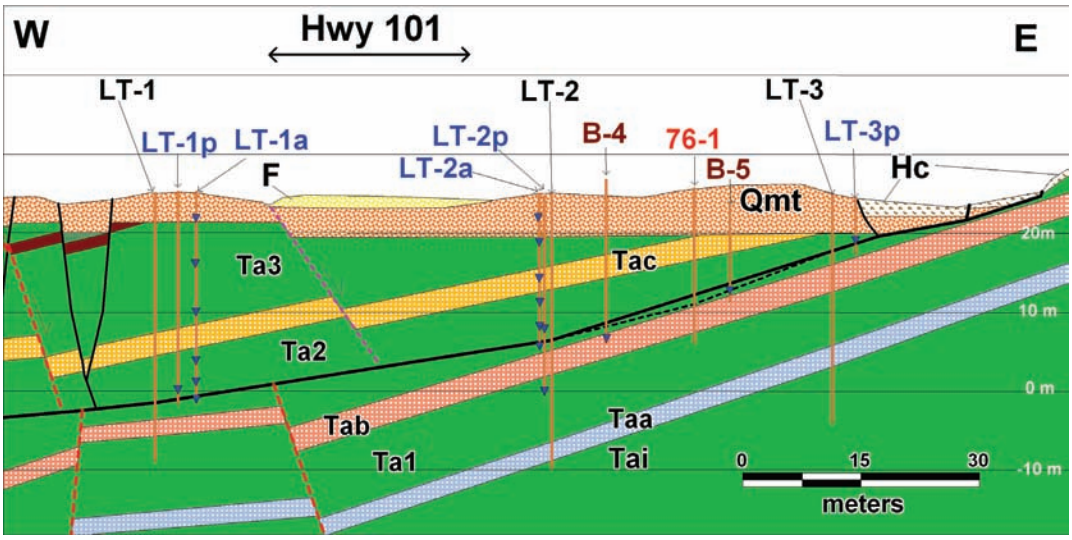

Figure 8. Cross section showing detail of geology and piezometer depths (blue triangles). See Figures 5 and 7 for explanation; vertical scale = horizontal scale.

was continuously graded as the slide moved. The age of the Old Coast Highway is not known, but construction activity was widespread in 1927–1932 (Len Saltekoff, ODOT, 2005 personal communication). Using this time frame, the average rate of lateral movement is ~8.5 ± 1.6 cm/yr, about 57 percent higher than the rate calculated from highway abandonment in 1943. There is more uncertainty in the 1927–1932 age of construction than the 1943 age of abandonment, so the ~5.4 ± 1 cm/yr horizontal and ~1.5 ± 0.08 cm/yr vertical rates are probably better estimates.

Rock Units

The Johnson Creek landslide is within the Miocene Astoria Formation (Figures 4–9; see Appendix A for detailed description). The Astoria Formation is the dominant rock exposed at the slide toe where it consists of 66 percent sandy or clayey siltstone, 27 percent moderately indurated silty fine- to medium-grained sandstone, 6 percent tuffaceous claystone or siltstone, and 1 percent calcareous claystone. The basal slip plane gouge exposed at the toe is predominantly clayey siltstone or sandy clayey siltstone overlain by ~3 m of brecciated siltstone (Figure 12; Appendix A).

The dominant surface unit in the rest of the landslide is Pleistocene marine terrace deposits that lie on a nearly flat-lying Pleistocene wavecut terrace (Figures 4 and 7). These deposits are 3 to 6 m thick and are composed of well-sorted fine- to medium-grained quartzofeldspathic sand underlain by a basal cobble layer. In some places post-depositional (Pleistocene?) erosion has removed or redistributed the original deposits. The deposits have much higher permeability than the finer grained, cemented and poorly sorted sedimentary rock of the underlying Astoria Formation (see size analyses in Appendix A). The Pleistocene sand is weakly cemented by thin films of poorly crystalline goethite (Johnson, 2003) and/or allophane with some larger voids locally filled with gibbsite (Grathoff and others, 2001; Grathoff, 2005; Johnson, 2003), but overall porosity is still quite high. As allophane dehydrates and shrinks, it loses its cementing qualities, causing the terrace sand to become friable where exposed (Grathoff, 2005); hence, most exposures of the terrace sand quickly become covered in talus. The best exposures are at the recently exposed portion of the northeast headscarp (cover page picture and Figure 13) and at the top of the sea cliff. The lower contact of the Pleistocene sand deposit is at an elevation of ~29 m in the northern half of the headscarp and at ~32 m in the southern half of the headscarp. The lower contact on the north appears to be a wave-cut platform with lag gravel, whereas the one on the south is irregular with colluvial material at the contact consistent with reworking of the original deposit in a subaerial environment, probably during Pleistocene time, as the deposit is still well consolidated.

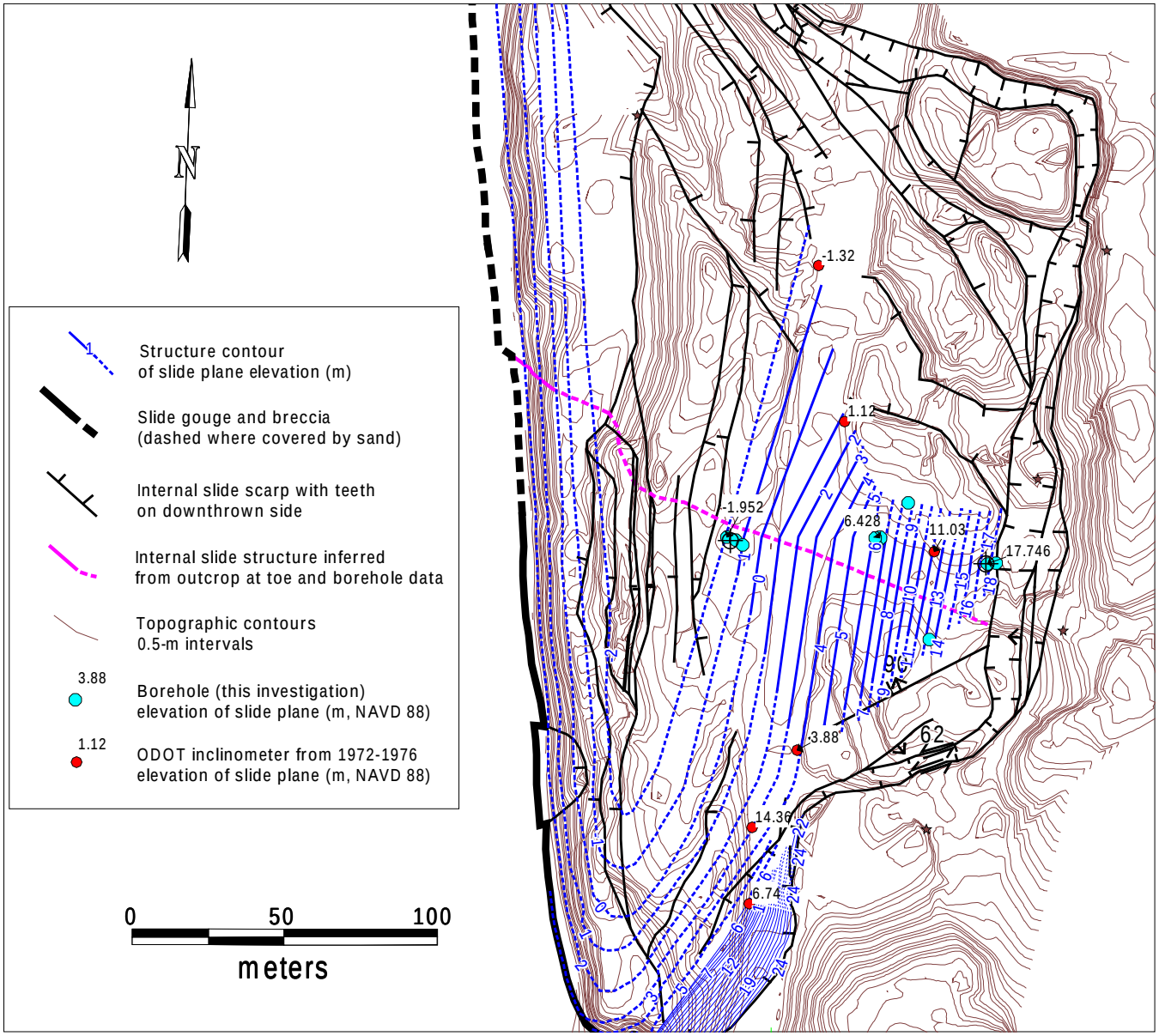

Figure 9. Structure contours (blue lines) in meters of elevation (relative to geodetic mean sea level NAVD 1988) on the slide plane. Data for the contours consist of outcrops of the slide plane, inclinometer holes from this project (blue dots) and previous work by ODOT in the 1970s (red dots). Elevations for the 1970s boreholes should be considered minimum values according to Landslide Technology (2004), as measurements could have been from casing tops rather than ground level. The zone of movement intercepted at 14.36-m elevation by the 1970s inclinometer on south margin was ignored, as this is probably a fast moving, shallow part of the slide rather than the main slide plane at depth; note the much lower elevation intercepts immediately south and northeast of this point. Dashed lines are highly speculative, whereas solid lines are inferred (assuming linear change) of slide elevation between drill holes and outcrops.

Figure 10. Looking north at Tertiary Astoria Formation at the toe of the Johnson Creek landslide. The smooth light tan unit is sandstone; sandy siltstone is the overlying dark orange gray unit. Black 0.8-m-long back pack is shown for scale. These units had an original dip of ~17˚ E, whereas in this exposure they dip 28˚–37˚ E from back rotation. See Figure 2 for location.

Figure 11. Looking north from the toe of the Johnson Creek landslide. Note light-colored marker beds that can be traced easily over the entire length of the slide toe.

Figure 12. Highly sheared dark gray sandy siltstone unit at the toe of the Johnson Creek landslide. This unit underlies the tan sandstone in Figure 3. Chuck Dennison of Dennison Surveying is pointing at the unit. Slightly reworked talus from the slide partially covers the basal shear zone.

Figure 13. Pleistocene marine terrace sand exposed in the northeast headwall of the landslide. Jonathan Allan of DOGAMI is measuring the thickness of the unit. Note the nearly flat surface of the sand sheet. The contact with underlying Tertiary Astoria Formation is ~1 m below the base of the ladder.

Colluvium of Astoria Formation and marine terrace sand covers many parts of the slide. This material is thickest at the base of slide scarps and is thicker where scarps are higher. Thickness in the headwall graben exceeded the 1-m length of a punch core.

Fractures and Joints

Erosion and road construction exposed fractures and joints in only a few places: The sea cliff and adjacent outcrops in Minor Creek and Johnson Creek, a road cut through the headscarp, and fresh scarps in the northeast part of the slide (see cover photo). Fractures within the landslide are much more closely spaced than outside the slide. Figure 2 shows localities of detailed observations.

Outside of the landslide, joints are essentially absent in the Pleistocene marine terrace deposits but common in the underlying Astoria Formation where there are generally two sets trending northwest and northeast. Within 100 m east of the landslide headscarp are two joint systems striking N 10°–30° W, dipping 62°–88° W crossing a less numerous set striking N 70° E to N 88° W and dipping 63°–73° N. A few vertical fractures striking N 45°–52° E occur locally in the same area. Johnson Creek exposes a set below the landslide striking N 17°–60° W and dipping within about 13°–17° of vertical. This set is crossed by a vertical set striking N 54°–57° E. Spacing of tectonic joints below the side plane at the toe and east of the headscarp tends to be irregular with some areas nearly devoid of joints over distances of a few meters next to areas with sets of joints spaced at a few tenths of a meter.

Joints and fractures within the landslide strike subparallel to adjacent slide block boundaries and to northwest or northeast trending tectonic joints. On the face of the sea cliff extensional high-angle fractures parallel to the cliff face have normal listric-slip of a few to several meters (Appendix A). An exposure at the sea cliff on the north side of Johnson Creek (Figure 2) has fracture systems spaced at an average of 12 cm with many only a few centimeters apart. The fractures are in three major sets, N 47° E, dipping 88° N; 32°–42° W, dipping 72°–78° E; and roughly parallel to the slide toe at N 7°–17° E, dipping within 17° of vertical. At the north end of the toe block at Miner Creek nearly vertical fractures trend roughly parallel to the block. One of these fractures near the back (east side) of the toe block is a ~1 cm fissure narrowing downward. East-facing scarps of Quaternary marine terrace sand freshly exposed in the northeast graben have fractures and sheared surfaces at N 7°–55° W, dipping 78°–90° W. The strike of most of these fractures is roughly parallel to the trend of the north-trending headwall graben. Fresh sheared surfaces at the base of the north-south headscarp in the same area strike north-south and dip 87° W (Figure 4). Other freshly sheared surfaces cutting roads at the northern, eastern, and southern edges of the landslide also strike parallel to the boundary and have inclinations toward the slide of 70°–90° (Figure 4).

Ponds, Springs, and Seeps

Surface water on the landslide locally ponds in the headwall graben, forming marshy areas. Creeks on the north and south margins of the slide flow all year long from drainage basins east of the slide. Prominent wetland features are not readily evident over most of the landslide except at the headwall graben, where a small sag pond occurs (unit Hsp, Figure 4).

Intermittent groundwater seeps were observed in the uppermost part of the sea cliff in the past five winters. These seeps issued from a perched aquifer in basal Pleistocene marine terrace sand where these deposits lie on less permeable Astoria Formation. More prominent seeps occur at the terrace contact outside the landslide where landslide fractures do not interrupt groundwater flow.

Modest seeps and a few springs of groundwater emerge from fractured Astoria Formation along the base of the landslide at the sea cliff. The toe of the slide was searched for springs and seeps on January 8, 2005, after an intense rainfall event. One spring with field-estimated flow at ~27 liters per minute (lpm) (~7 gallons per minute, gpm) issued from fractured Astoria Formation in the sea cliff 10 m south of north edge of the slide. Wave erosion of beach sand observed on April 28, 2007, exposed pervasive groundwater seeps at the slide plane (Figure 14).

Figure 14. Groundwater seeping from slide breccia and gouge of sandy siltstone at the southern toe of the Johnson Creek landslide. The mouth of Johnson Creek is in the upper right where driftwood is piled up. Note that beach sand is stripped off. Wave erosion is more efficient in this part of the slide owing to a persistent rip cell embayment that carries sand offshore. Photo was taken April 28, 2007.

SUBSURFACE EXPLORATION

Drilling

Exploratory borings encountered materials that are separated into three geotechnical engineering units identified as Pleistocene terrace sand overlying a thin layer of decomposed Astoria Formation, fractured Astoria Formation slide debris, and bedrock of Astoria Formation below the slide. Detailed descriptions of the subsurface materials are included in Appendices A and B. Correlation of rock units between boreholes is illustrated in the cross section of Figure 7 and in Appendix A.

Pleistocene marine terrace sand and decomposed Astoria Formation were encountered to depths of 5.0 to 6.9 m. Pleistocene terrace deposits consist of loose to medium dense, silty sand. Decomposed Astoria Formation lies immediately below the sand and is 1 to 2 m (3 to 6 ft) of medium stiff, silty orange clay.

The Pleistocene terrace contact with underlying Astoria Formation is 2 m lower in boreholes LT-2 and LT-3 than in LT-1 on the west side of the slide (Figure 7). The 2-m offset of the Pleistocene terrace can be explained by either a Quaternary fault or by internal deformation within the slide. Landslide Technology (2004) and Priest and others (2006) used a tectonic fault to match offset of Astoria marker beds, but the authors do not show the fault offsetting the marine terrace; Appendix A shows a cross section with this interpretation. Lacking evidence of a Quaternary fault in the area, the geologic cross section depicts an internal slide structure between LT-1 and LT-2 with apparent dip of 58˚ E, derived from a best fit for offset of both the Pleistocene terrace and the Astoria Formation. Actual strike, dip, and location of this structure are unknown. The structure was placed at a small change in direction of slide movement between LT-1 and LT-2 interpreted from the resurvey data, assuming it accommodates this

change in direction (Figure 6). In order to depict the structure on the map, it is arbitrarily connected along lineaments from this point to a structure at the slide toe with the same vertical displacement (dashed purple line in Figure 6). The structure at the slide toe strikes N 66˚ W, dips 60˚ NE, and displaces Astoria Formation 2 m down to the northeast (Figure 6). There may be no connection between the two, as simple extrapolation of this strike and dip yields a 37˚ apparent dip in the cross section and a crossing point 20 m east of the one shown.

Astoria Formation encountered in drill core consists of moderately to highly fractured sandstone, siltstone, and tuffaceous mudstone. This fractured rock is typically very soft rock (classification R1 [Sara, 2003]) with lesser soft rock (R2). In-place Astoria Formation is typically a soft rock (R2). Due to drill and sample specifications for the drilling investigation, standard penetration tests (SPT) were not taken in the drill holes except to isolate the base of the terrace sand in boring LT-3p.

Slickensides and apparent gouge zones were also encountered in the slide debris and in the rock underlying the zone of shearing recorded by the inclinometers (Figures 15–19). Slickenside orientations were typically near vertical. Vertical slickensides were also encountered on fracture surfaces in the in-place rock, which suggests that other tectonically induced strain (faults) may be present in the slide area.

Gouge material encountered in the borings is classified as very soft, slightly clayey to clayey, sandy silt. Brecciated siltstone and sandstone were commonly encountered in the slide debris but were not encountered in the rock below the slide except for a 0.15-m layer of wet, highly sheared siltstone dipping about 2° at 15.4 m depth in borehole LT-3. The gouge layer at 15.4 m depth is not described by Landslide Technology (2004) (Appendix B) but was observed by us when the core was taken.

Test Pits

The two exploratory test pits through the slide toe revealed gouge of the basal shear zone overriding beach sand and an underlying berm of rounded to subrounded cobbles and pebbles (Figure 20). Cobble and pebble lithologies appeared similar to siltstone and sandstone in the sea cliff. Location of the test pits was at the foot of a small slump block (Figure 2).

MONITORING

Automated collection of data established by the USGS in 2005 continues at the writing of this report. Data are periodically downloaded by USGS via a cell phone connection. Data may be viewed at the USGS web site, http://landslides.usgs.gov/monitoring/johnson_creek/.

Surface Displacement

Resurveys. Survey points were established on the ground surface at three east-west sections across the slide (Figure 21; Appendix E). Two sets of readings were taken, one on October 24, 2002, and one on April 17, 2003. The general trend of increasing movement to the south and southwest in the slide mass is depicted qualitatively in Figure 21 by the varying length of the blue arrows and quantitatively in Figures 22 and 23. From readings taken upslope of the headwall graben in stable ground, the survey repeatability error is large, about 11 cm to 15 cm horizontal and 1 to 130 cm vertical. The one point with 130 cm vertical error was probably a result of disturbance of the steel stake or calculation/transcription error.

Even with the relatively high error in the survey data, general trends emerged that were helpful in understanding the overall differences in ground movement across the slide during the large movement event that occurred at the end of January 2003. This event in combination with the December 2002 and March 2003 movements had enough displacement in the central and southern part of the slide to be detectable in spite of the measurement error. The error was too large to detect movement in the northern transect, so those data are not shown (see Appendix E). At the drilling transect, horizontal surface displacement was 22 to 33 cm to the west or southwest and 4–9 cm vertical. Largest movement was in the southern survey line where the slide moved 21–130 cm horizontally and 6–70 cm vertically.

The general trend of increasing displacement from the northern to the southern margin of the landslide is reflected in observations of damage immediately after the December 2002 movements. The northern margin at Highway 101 had only ~1-2 cm of vertical offset, while the highway on the southern margin had 18 cm of vertical displacement and 5-cm-wide fissures (Figures 24 and 25). As explained below, the slide at the drilling transect only had ~5 cm of movement during this

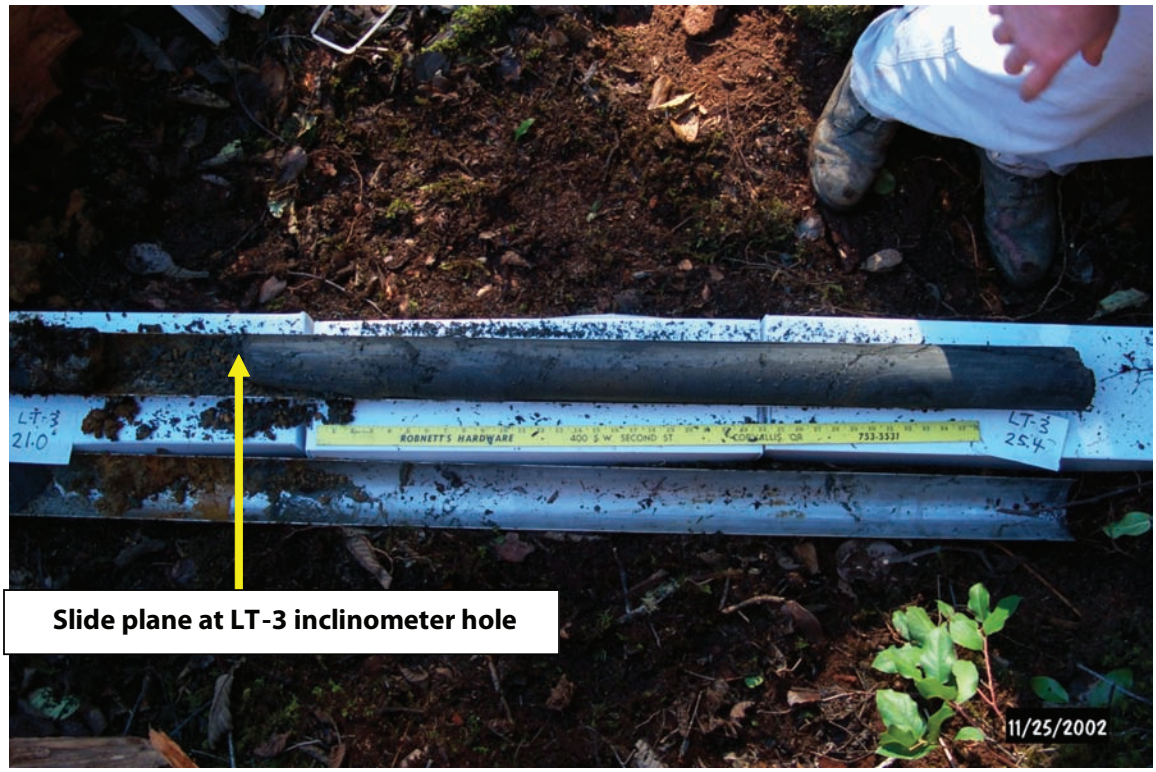

Figure 15. Core at the slide plane from the eastern (LT-3) inclinometer hole.

Figure 16. Core of slide breccia from 1.9 to 0.9 m above the base of slide from the middle (LT-2) inclinometer hole. Inclinometer data show shearing at 18.6-m (61 ft) depth. Photo of the slide plane is not available.

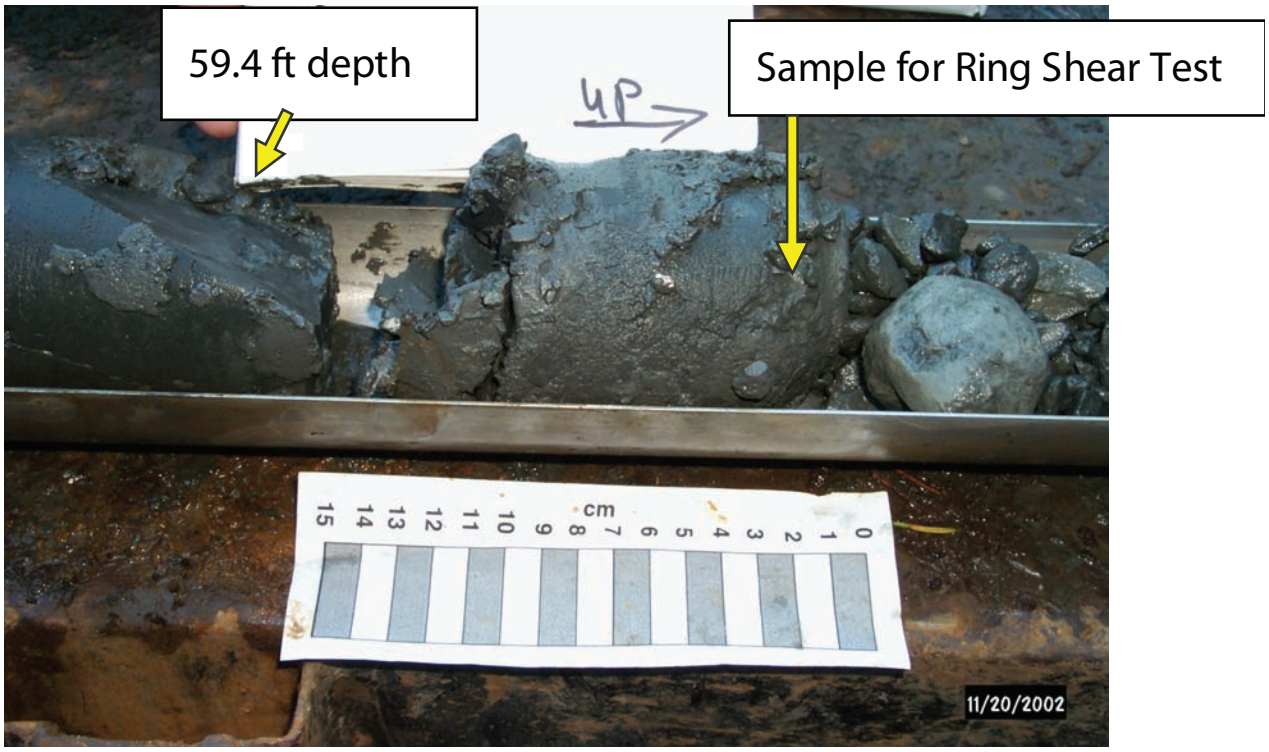

Figure 17. Sample used for ring shear test at a depth of ~18 m (59 ft) in borehole LT-2. Inclinometer data show shearing at 18.6 m (61 ft).

Figure 18. Core at the slide plane from the western (LT-1) inclinometer hole. Numerous sheared fractures occur just above the slide plane.

Figure 19. Core of altered Astoria Formation siltstone (orange) at 4.6- to 5.2-m depth immediately below the Pleistocene marine terrace sand contact at ~4.3 m (14 ft) depth in borehole LT-3. Dark gray material below 5.2-m (17 ft) depth is unaltered siltstone.

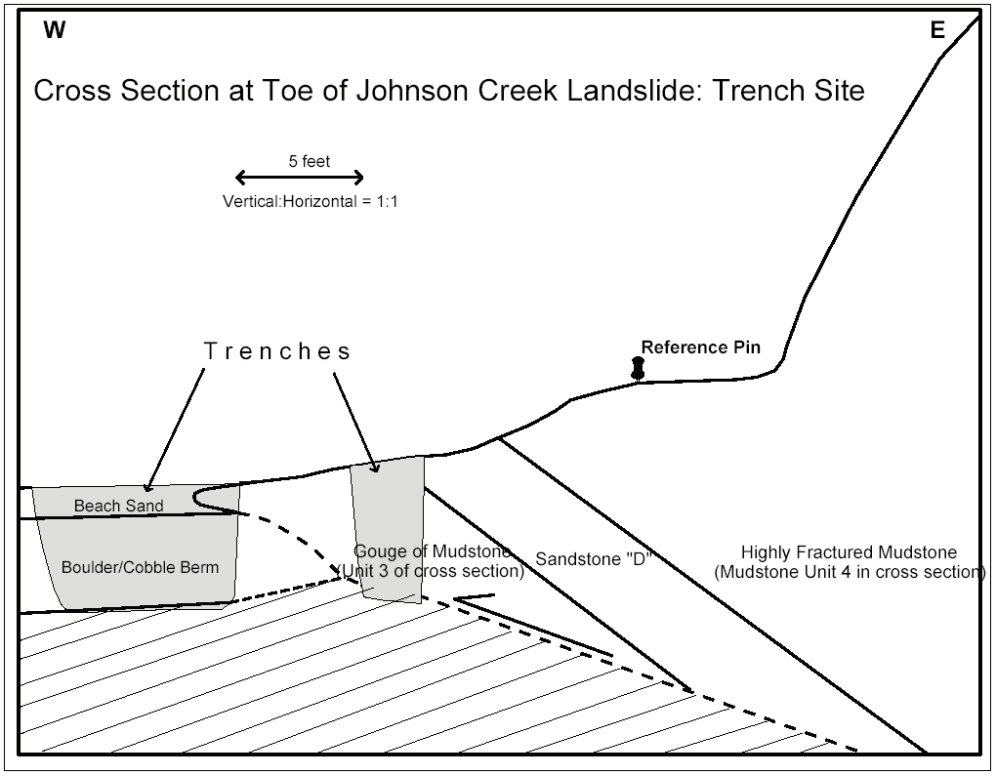

Figure 20. Cross section showing Astoria Formation mudstone and sandstone of the Johnson Creek landslide overriding an apron of beach cobbles at the toe of the landslide. Slanted line pattern indicates west-dipping, undisturbed Astoria Formation below the landslide.
See Figures 2 and 6 for location and Plate A1 for cross section units.

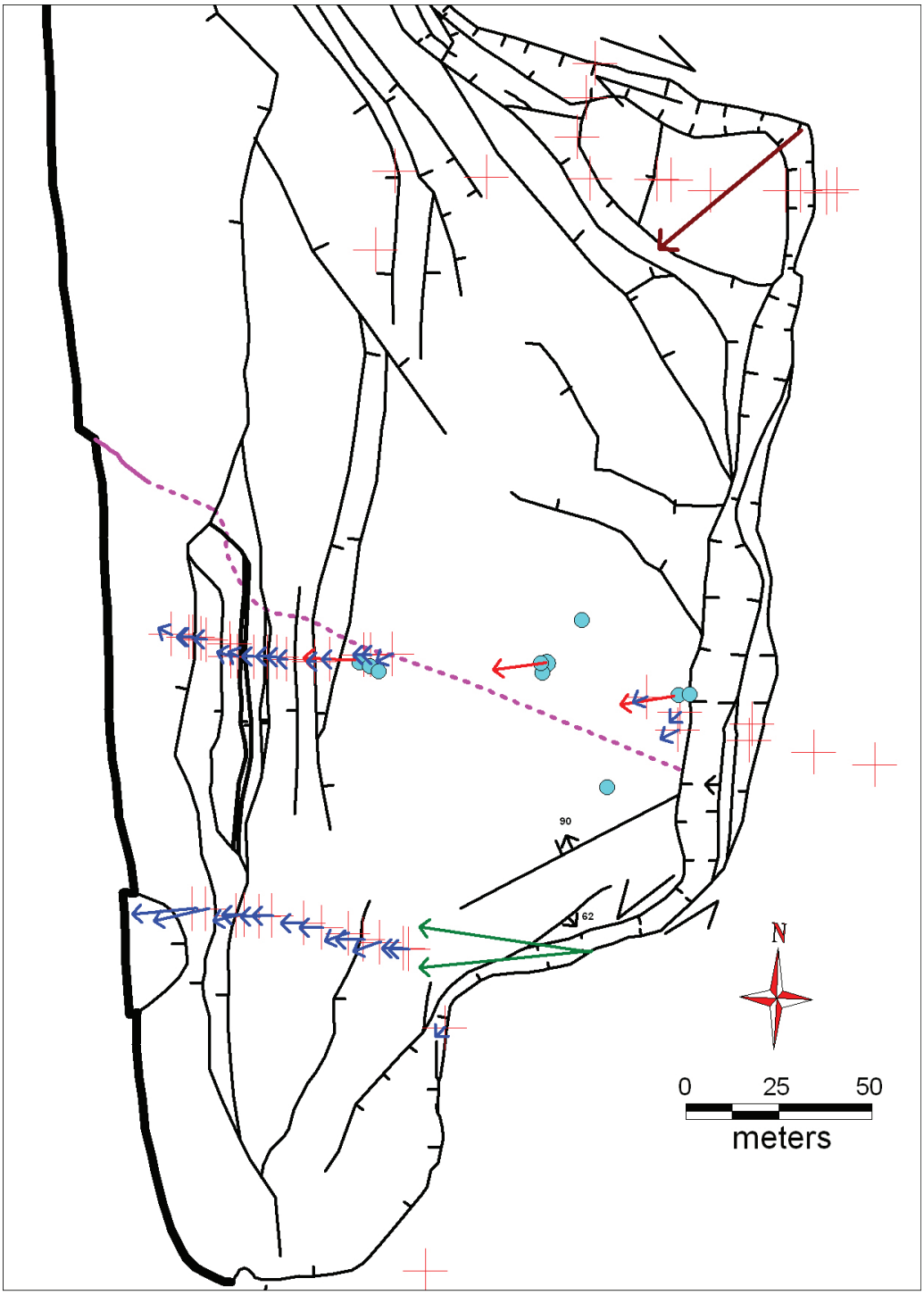

Figure 21. Qualitative vectors (blue arrows) drawn in direction of slide movement for steel stakes surveyed October 24, 2002, and April 17, 2003, and for inclinometer data (red arrows) collected between December 11 and December 31, 2002. Relative lengths of arrows correspond roughly to relative amount of movement. Red crosses without arrows are points where slide movement between surveys was less than the error in the measurement. Green arrows illustrate possible movement direction from offset of the Old Coast Highway; brown arrow illustrates general movement direction inferred from scarp trends and offset of marker nails in the northeastern part of the slide.

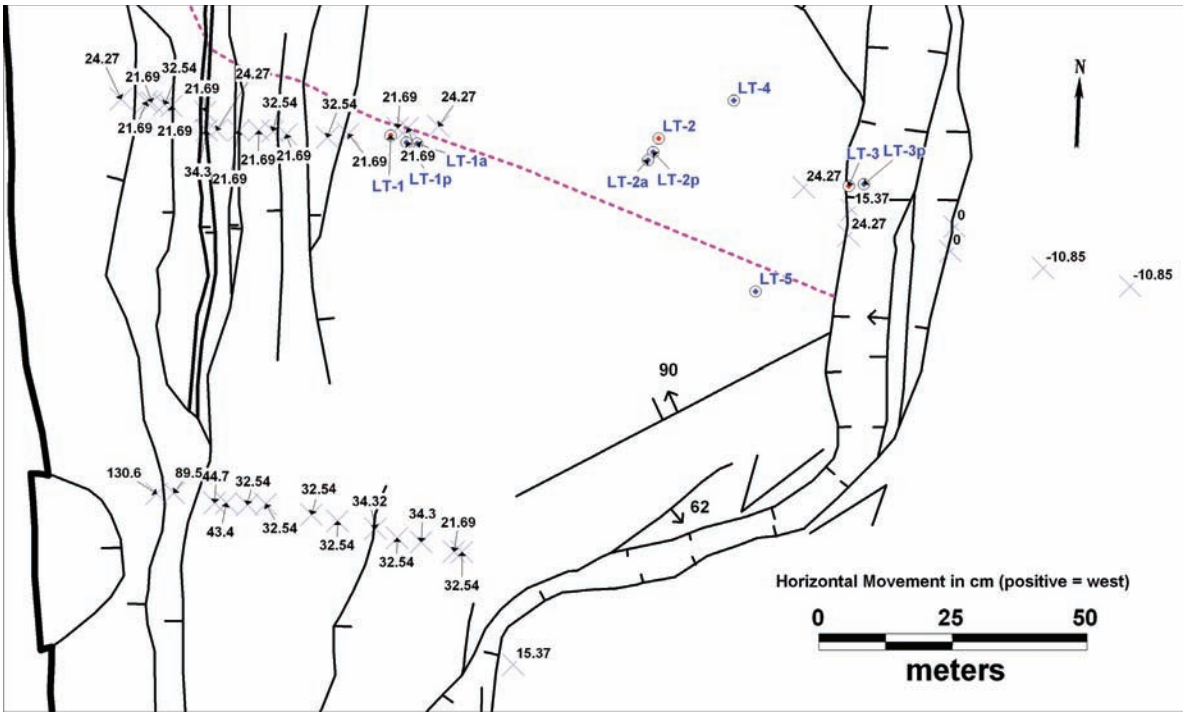

Figure 22. Horizontal movement (cm) at steel stakes (blue crosses) in the southern part of landslide from resurvey of steel survey stakes October 24, 2002, and April 17, 2003. Key boreholes are also shown (circles with diamonds and blue labels). Movement east of the headwall of –10.85 cm (eastward movement) is survey error, so this is the approximate error of the data.

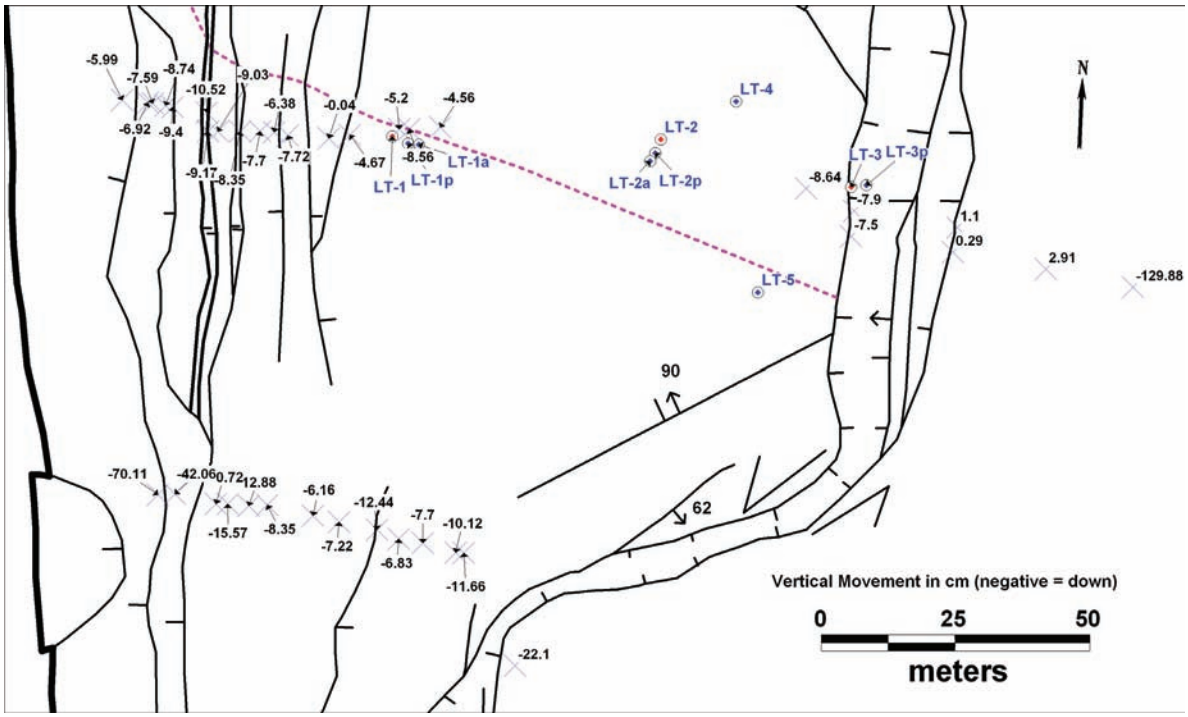

Figure 23. Vertical movement (cm) at steel stakes (blue crosses) in the southern part of landslide. Movement east of the headwall of +0.29 to +2.91 cm (upward) is typical survey error. There are two survey stakes east of the headwall with displacements of –129.88 cm and -22.1 cm, but these are probably local anomalies caused by displacement of steel stakes by causes other than slide movement (falling tree debris, survey notation errors, tampering, etc.).

Figure 24. Damage to Highway 101 on the south margin of the Johnson Creek landslide immediately after a slide movement in January 2003. Maximum vertical offset is 17.8 cm down to the northwest; fissures are as wide as 5 cm. This part of the slide is south of the resurvey lines and confirms the general trend of increasing offset to the south. Roger Hart is in the background.

Figure 25. Damage to the north slide margin on Highway 101 from the same movement as in Figure 24. Note that vertical offset is only 1-2 cm.

time. The largest slide movement during the resurvey observation interval was at the end of January 2003 and was about 24 cm at in the central part of the slide, so movement on the southern margin was probably much larger than that; unfortunately, it did so much damage to the highway that it was repaired before a measurement could be made.

The line-of-sight survey readings taken in January and February 2003 (Appendix F) also show that the southern area of the slide has moved faster than the northern area. The general trend of west-directed movement in the western part of the slide and southwest-directed movement in the northeast portion inferred from scarp trends is also reflected in the resurvey data (Figures 21 and 22).

Marker nails. On March 12, 2003, marker nails were placed across fresh scarps created from the February 2003 slide movement and then measured March 24 and April 11, 2003. A slide movement measured at ~2 cm at extensometers in March 21–28, 2003, displaced all of the nails around the slide perimeter ~2 cm (Appendix G). Direction of motion determined from the nails matched other observations, west at the headwall graben, right lateral at the north margin, and left lateral at the southern margin (brown arrows, Figure 4). Nails placed across an older, sharply defined bedrock scarp in the interior of the slide showed no movement (east-northeast trending scarp with 90˚ dip in southeast part of slide, Figure 4). The results are consistent with en masse movement of 2 cm with insignificant internal deformation.

Table 2. Interpretations of slide plane depth from Schulz and Ellis (2007) versus Landslide Technology (2004).

Borehole	Maximum Depth (m)	Minimum Depth (m)	Probable Depth (m)	Landslide Technology (2004) Depth (m)
LT-1	26.52	25.30	25.81	26.5
LT-1a	25.76	24.54	25.05	—
LT-2	18.59	17.37	17.77	18.6
LT-2a	18.62	17.34	17.74	—
LT-3	6.46	5.79	6.13	7.0

Table 3. Displacement for each movement event episode.

	West Site (LT-1)			Middle Site (LT-2)			East Site (LT-3)		
Episode	Inclin. (cm)	Extens. (cm)	Inferred (cm)	Inclin. (cm)	Extens. (cm)	Inferred (cm)	Inclin. (cm)	Extens. (cm)	Inferred (cm)
December 13–31, 2002	2.3	1	5	2.8	1	4	3.2		3.2
January 31–February 3, 2003	—	14	14	—	24	24	—	5	5
March 21–28, 2003	—	2	2	—	2	2	—	2	2
November 15–March 4, 2004	—	4	4	—	2	2	—	3	3
November 11–18, 2004	—	0	0	—	0	0	—	2	2
December 27–January 4, 2006	—	1.4	1.4	—	1.4	1.4	—	1.0	1.0
January 6–24, 2006	—	3.3	3.3	—	3.5	3.5	—	1.8	1.8
January 27–February 10, 2006	—	3.4	3.4	—	4.0	4.0	—	3.2	3.2
November 6–15, 2006	—	0.6	0.6	—	1.1	1.1	—	0.6	0.6
December 24–28, 2006	—	0.3	0.3	—	0.2	0.2	—	0.3	0.3
January 2–11, 2007	—	1.1	1.1	—	1.0	1.0	—	0.9	0.9
February 15–16, 2007	—	0.0	0.0	—	0.0	0.0	—	0.2	0.2
February 25–March 9, 2007	—	2.2	2.2	—	2.2	2.2	—	2.2	2.2
March 12–15, 2007	—	0.0	0.0	—	0.0	0.0	—	0.1	0.1
Total displacement	2.3	33	37	2.8	42	45	3.2	22	25

Inclin. = inclinometer; Extens. = extensometer. Differences of 1-2 cm in total inferred movement between this table and summary charts are caused by accumulated rounding errors in extensometer data collected before November 20, 2005; those data have measurement errors of 1 cm.

Subsurface Displacement

Data. All subsurface displacement data collected in this investigation are in the digital file Piezometer+Soil Mois+Movement_DATA.xls on the publication CD. Estimated depths to the basal shear zone at all boreholes are listed in Table 1. Table 2 lists alternative slide plane depths from Schulz and Ellis (2007). Table 3 summarizes all slide movements during the observation period. Note that some elevations and depths to the slide plane differ slightly from those reported by Schulz and Ellis (2007). These differences are from small differences in interpretation of geological and geotechnical data. For example, we used basal shear zone depths from interpretations of Landslide Technology (2004) that placed the slide plane near the bottom of the shear zone deflection in inclinometer data. Schulz and Ellis (2007) place the slide plane near the center of the deflection, ~0.3–0.8 m above our slide plane (Table 2). Appendix D summarizes all inclinometer displacement plots. Inclinometer displacement plots for ODOT boreholes drilled in 1972–1976 are in Appendix C. Figures 26 and 27 depict all slide movement data.

Data gaps. Site vandalism caused loss of data in two instances. The data gap between July 9, 2005, and September 22, 2005, is from loss of a solar panel powering the datalogger. The LT-2 extensometer wire and pulley system experienced two sudden changes over less than the 1-hr sampling interval. A decrease of 3.2 cm occurred between 13:00 and 14:00 hours on June 30, 2005, an increase of 3.4 cm occurred between 14:00 and 15:00 hours October 11, 2005 (Figure 27). The October change was from reseating the wire into the pulley from apparent vandalism on June 30, so data collected between these dates are unreliable.

Observations. Inclinometer readings began on December 11, 2002. Shear movement was first detected in the casings on December 16, 2002. Inclinometers measured 2.3 to 3.2 cm of displacement before the probe could not pass distorted casing at the slide zone. Each inclinometer was converted to an extensometer when this happened. Inclinometer readings ceased progressively from the western to the eastern inclinometers: December 23, 2002 for LT-1, December 26 for LT-2, and January 3, 2003, for LT-3. Figure 26 shows displacements for the inclinometers and extensometers during this time. Dashed lines in Figure 26 depict how extensometer data were merged with inclinometer data to determine total movement since the start of monitoring. Figure 27 shows all displacement using this merged data.

Shear movements were detected at depths of 26.5 m, 18.6 m, and 7.0 m below ground surface for LT-1, LT-2, and LT-3, respectively (Appendix D; Landslide Technology, 2004). Schulz and Ellis (2007, p. 9) noted that "all shear displacement of the inclinometer casings occurred within a 1.2-m-thick zone, indicating that the landslide basal shear zone at these locations is less than 1.2 m thick. About 64 percent and 83 percent of the shear displacement of the inclinometer casing at boreholes LT-1 and LT-2, respectively, occurred within a zone 0.6 m thick, strongly suggesting that the basal shear zone at these locations is less than 0.6 m thick and probably less than 0.3 m thick."

Inclinometers LT-1, LT-2, and LT-3 measured shear zone movement vectors in the directions 273, 258, and 247 degrees azimuth (red arrows in Figure 21), respectively. From analysis of inclinometer data by Landslide Technology (2004), apparent shear movement near the bottom of inclinometer hole LT-2 (Appendix D) is likely due to systematic error.

Six inclinometers installed by ODOT in the 1970s (Figure 2; Appendix C) provide some constraints on slide plane depth, but the data are highly uncertain. According to Landslide Technology (2004), the vertical datum and horizontal datum are not known, and the surface measurement point for the "slope meter tubes" is unknown. Depths could be from the ground surface or from casing protruding above the ground. The plots for three borings (76-2, 76-3, and 76-4) have similar appearances, which can be attributed to the depth of movement somewhat deeper than the casing (Landslide Technology, 2004).

Total displacement over the four years and four months of observation was approximately 37 cm, 45 cm, and 25 cm at the west (LT-1), middle (LT-2), and east (LT-3) sites, respectively (Table 3). Small differences in total displacement shown Table 3 and Figure 27 are from some spurious raw data from previously explained tampering with instruments and rounding errors for the less precise data collected from hand measurements prior to November 2005. All movement occurred during the five winter rainy seasons. The 24-cm displacement at LT-2 between January 31 and February 3, 2003, created 10 cm of compression between LT-1 and LT-2 and 19 cm of extension between LT-3 and LT-2 (Table 3). Twelve smaller movements over

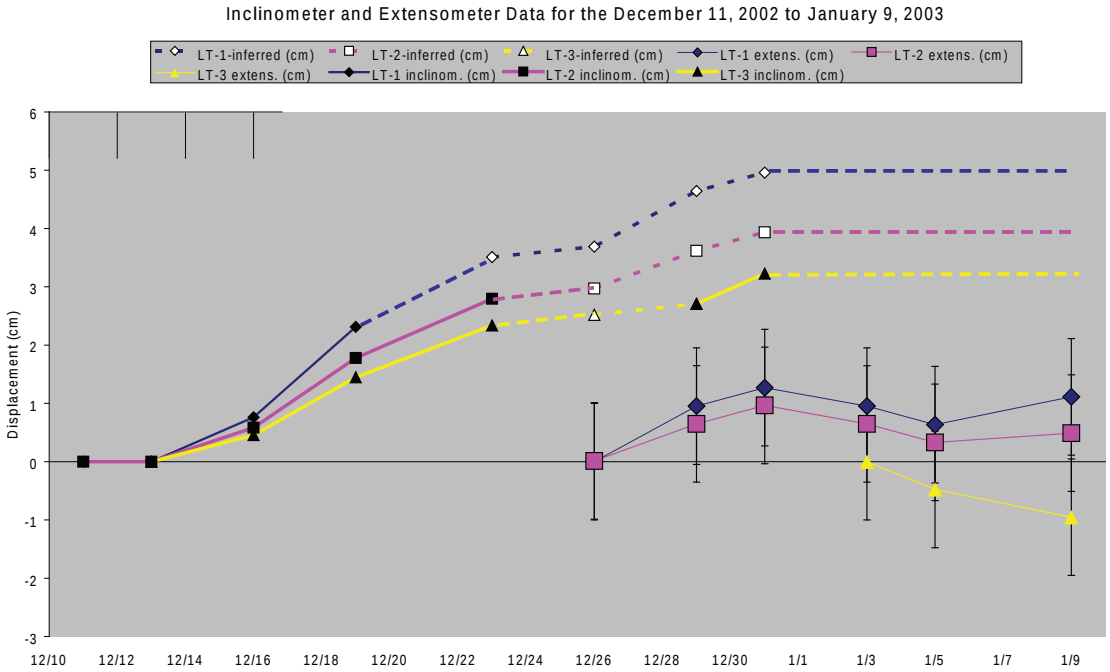

Figure 26. Inclinometer and extensometer data (solid lines) from the start of monitoring on December 11, 2002, to January 9, 2003. Dashed lines depict slide movement inferred from combined extensometer and inclinometer data; error bars on extensometer data are 1 cm; precision on inclinometer data is 0.25 mm.

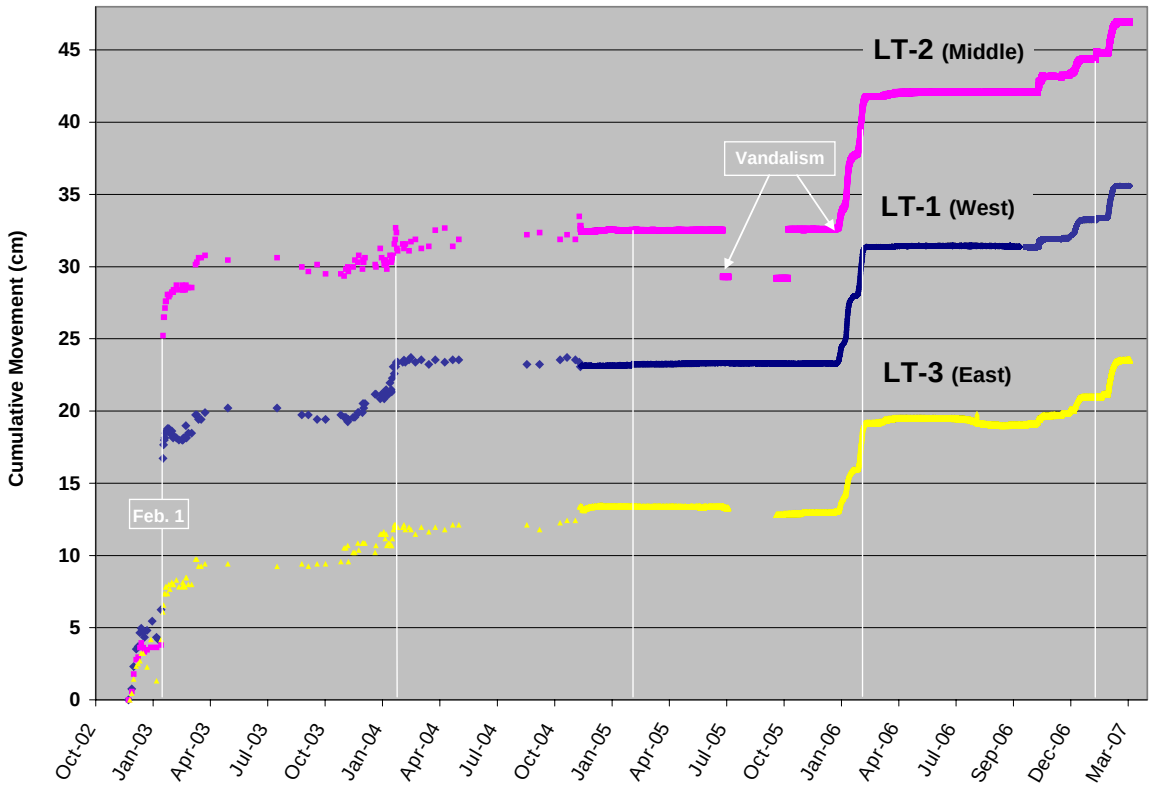

Figure 27. Cumulative movement for the observation period November 23, 2002, to April 1, 2007. Note that cumulative totals are the raw data unadjusted for error introduced by vandalism or other causes.

the subsequent four years left the 10 cm of compression unchanged and increased the 19 cm of extension to 20 cm at the head of the slide (Table 3). Given that measurement error for half of the data was 1 cm, this change in extension is not significant. Note that the terms extension and compression are used here to explain relative movement, not the stress regime of the slide; the stress regime in unknown.

Rainfall

Data. All rainfall data are in the digital file Piezometer+Soil Mois+Movement_DATA.xls on the publication CD. Data are from a recently clear-cut area above the headwall of the landslide (Figure 2).

Data gaps. Data were not recorded during two intervals in summer 2005 and 2006. The data gap between July 10, 2005, and September 21, 2005, is from vandalism. Zero rainfall recorded between July 28, 2006, and September 25, 2006, is partly due to clogging of the rain gauge with leaves. Removal of leaves on September 25 caused a spurious reading. The rain gauge 14 km south at the Hatfield Marine Science Center (HMSC) recorded a trace of rain (0.25 mm in 15 minutes) on July 31, August 9, 11, 28, 29, and 31, but the first significant precipitation missed by the rain gauge was on September 15 when the HMSC gauge recorded 2.9 mm over 3.5 hr. A larger event was missed on September 18 when HMSC recorded 10.9 mm in 6.5 hr. Therefore, the gauge was not able to collect data at least between September 15 and 25, 2006.

Observations. Most rainfall occurred between the middle of September and May in each of the five winters; the most intense precipitation was between November and February each year (Figures 28 and 29). Total rainfall was highest in 2005-2006, followed by 2002-2003, 2003-2004, 2006-2007, and 2004-2005. Cumulative rainfall to February 1 of each year is marked in Figure 28 for comparison of rainfall intensity at the point of largest slide movement in 2003. December to February 1 intensity was highest in 2002-2003, followed by 2005-2006, 2003-2004, 2006-2007, and 2004-2005 (Figure 28). Higher intensity is a steeper slope on the cumulative rainfall curve. Intensity was seldom over 10 mm/hr (Figure 29).

Groundwater

Data files. All pore pressure and soil moisture data are in the digital file Piezometer+Soil Mois+Movement_DATA.xls on the publication CD. Estimated depths of piezometers and soil moisture probes are listed in Table 1.

Soil moisture data. All but one of the soil moisture probes showed measurable variation in moisture during the December 2006 to April 2007 observation interval (Figure 30). The soil moisture probe at 2.4 m depth at the western (LT-1) site (probe WC-1d) showed little response and apparently malfunctioned (Schulz and Ellis, 2007). The probe at 1.6 m depth at the east site (probe WC-3s) had less pronounced and slower response to wetting events than the one at the 1.5 m depth at the west site (probe WC-1s) (Figure 30).

The soil moisture probe at 3.1 m depth at the east (LT-3) site responds to major rainfall events before the probe at 1.6 m depth (Figures 31–33). The probe at 3.1 m depth responds at variable times after rainfall event but always when total piezometric head at the site reaches 1 m above the probe elevation (Figures 31–33).

Piezometer data. All piezometer data are illustrated in Figure 34 for sand-packed piezometers, in Figures 35 and 36 for grouted piezometers, and in Figure 37 for piezometers in two groundwater monitoring wells. Drilling effects and data losses are noted in the illustrations. The anomalous rise in pore pressure from drilling fluids did not persist more than about three days at each site.

Grouted versus sand-packed piezometers. Sand-packed piezometer data did not match data from grouted piezometers at the same depths. Mikkelsen and Green (2003) verified the high accuracy of pore water pressures from grouted piezometers and recommended abandoning sand-packed installations. Water pressure in sand-packed piezometers near the slide plane in the LT-1p and LT-2p boreholes is consistently lower than pressure in grouted piezometers LT-1a and LT-2a at about the same depth (Figures 38 and 39). Differences are 1.7–2.0 m lower at LT-1p and 0.9–2.0 m lower at LT-2p. During peak head events, head at LT-1p is 0.9 m lower than at LT-1a, while at LT-2p it is lower by 0.9–1.4 m than LT-2a (Figures 38 and 39). Figure 40 illustrates that cemented piezometers in the vertical arrays from the LT-1a and LT-2a boreholes plot on a hydrostatic line, whereas contemporaneous water pressure from the sand-packed piezometers fall off the line.

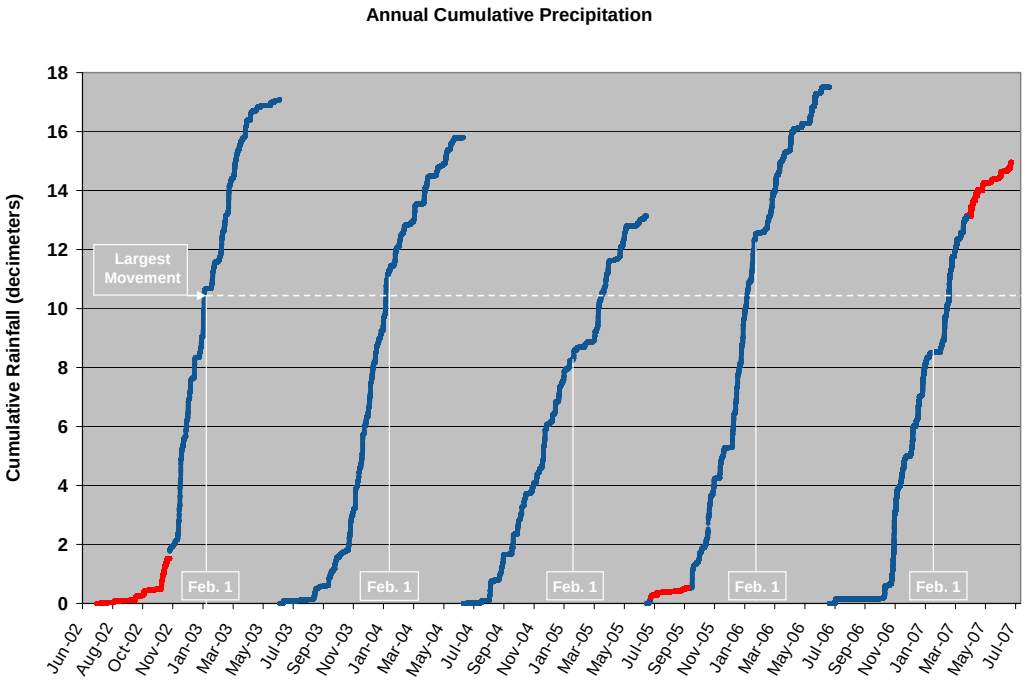

Figure 28. Cumulative rainfall by water year (July 1 to June 30) for all observations. Cumulative rainfall associated with the largest slide movement on February 1, 2002 is shown as the dashed reference line; vertical lines mark the same date in each water year. Red = data from the Hatfield Marine Science Center 12 km south of the study area. The data gap in 2005 is from vandalism.

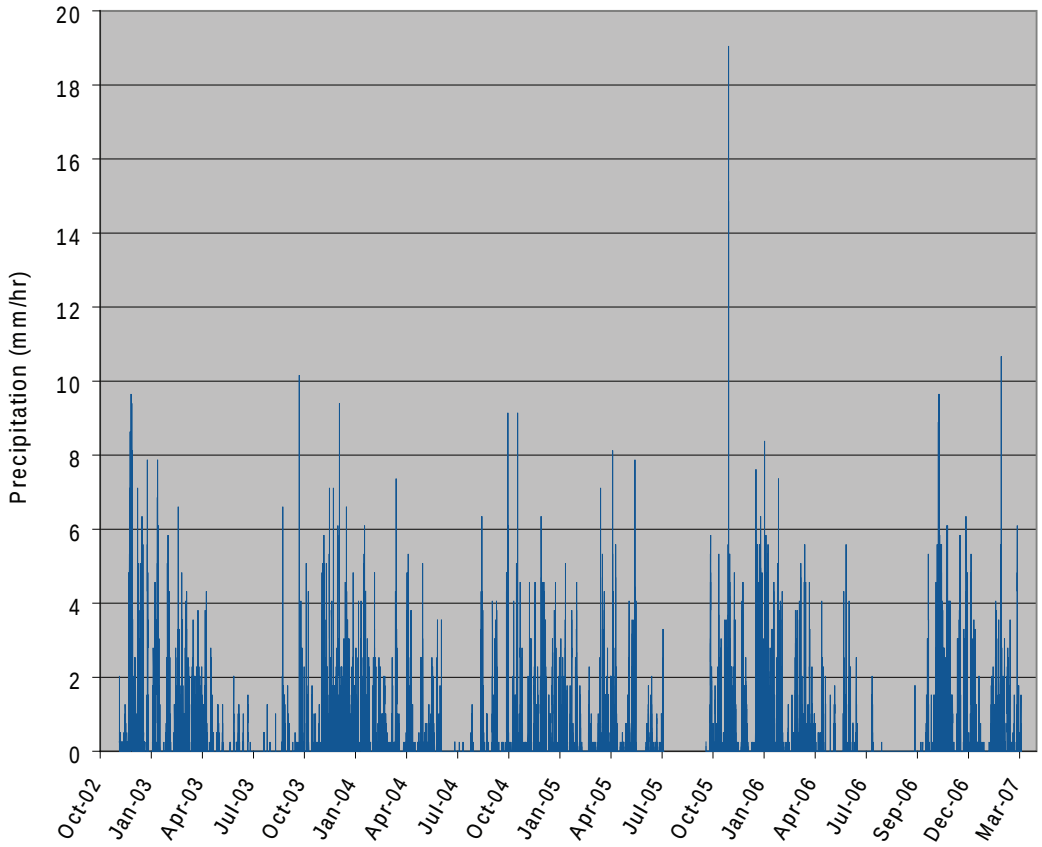

Figure 29. Hourly rainfall variation during the observation period October 2002 to March 2007.

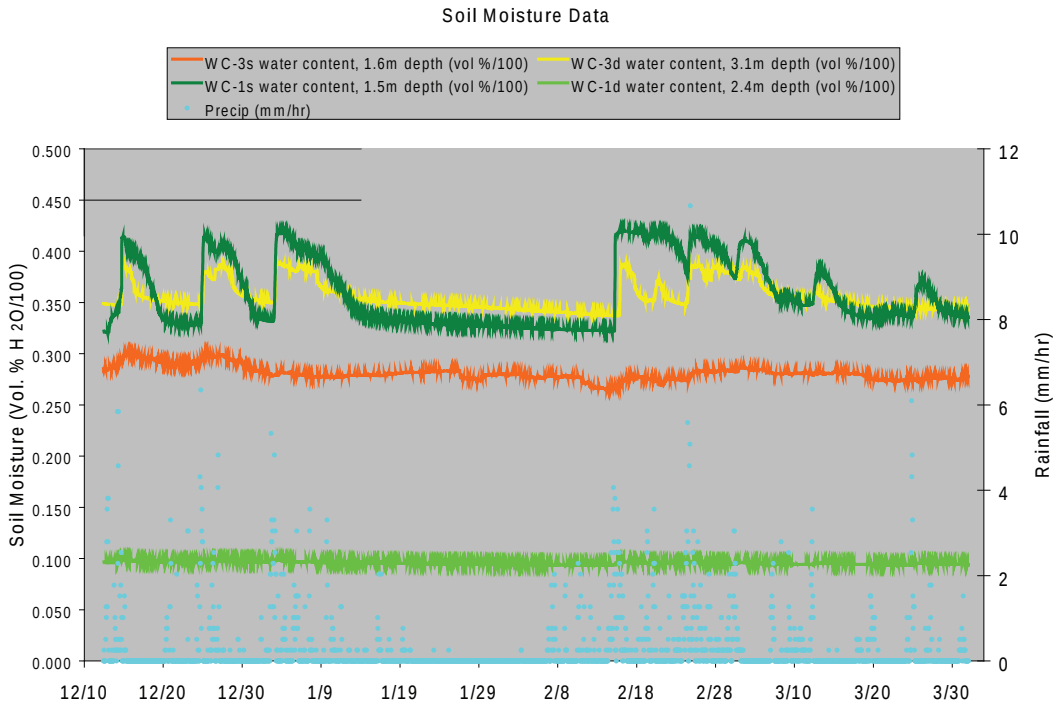

Figure 30. All soil moisture data and hourly precipitation for December 2006 to April 2007.

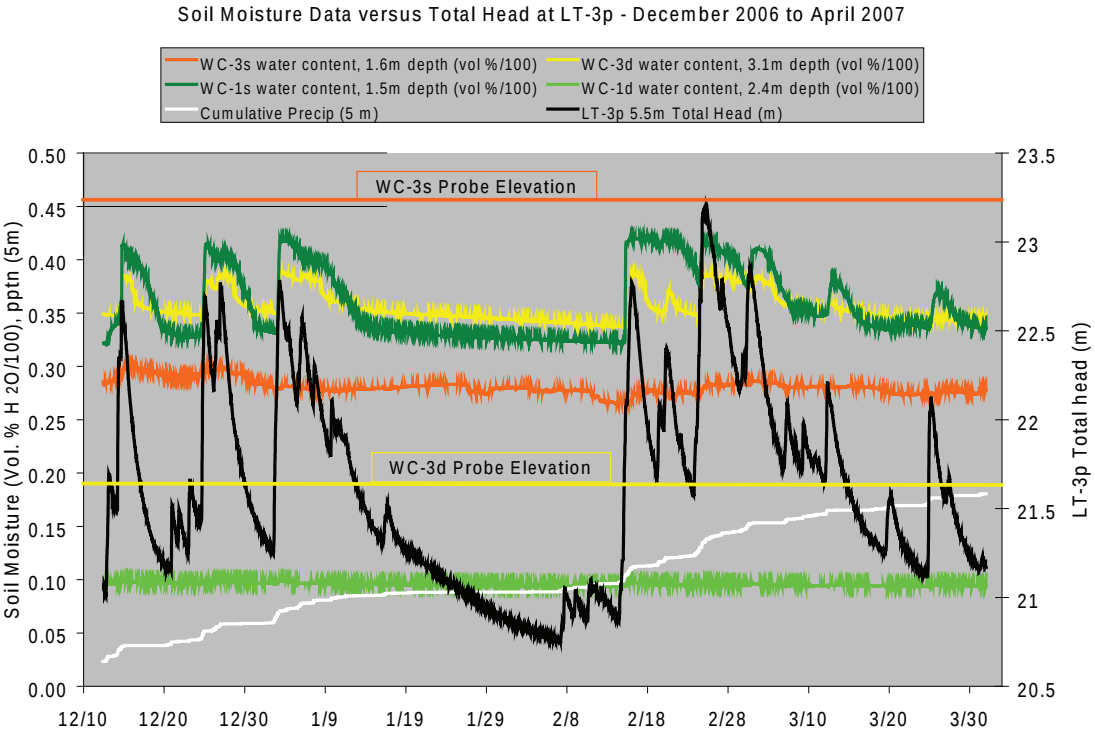

Figure 31. Soil moisture observations for the period December 2006 to April 2007 relative to cumulative precipitation and to total head at the LT-3p borehole. Note that the deeper moisture probe at the LT-3 site, WC-3d, lies below the total piezometric head at that site in some intervals. Cumulative precipitation (pptn) is in units of 5 m in order to plot on the graph.

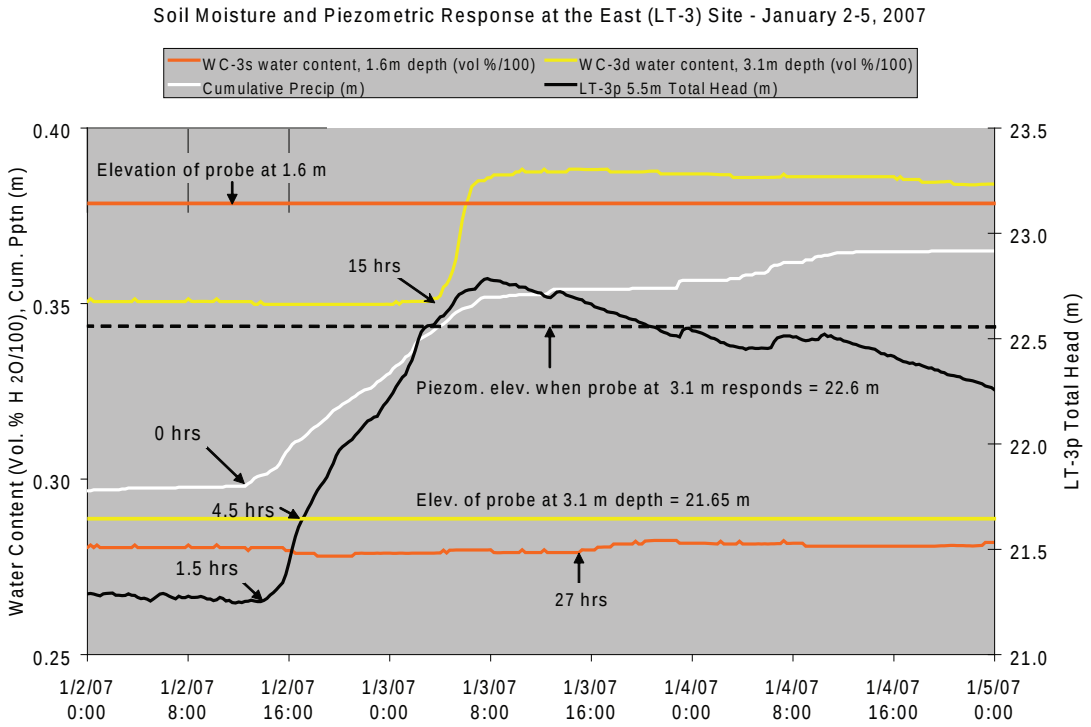

Figure 32. Soil moisture and piezometric response at the east (LT-3) observation site relative to a major rainfall event in January 2007.

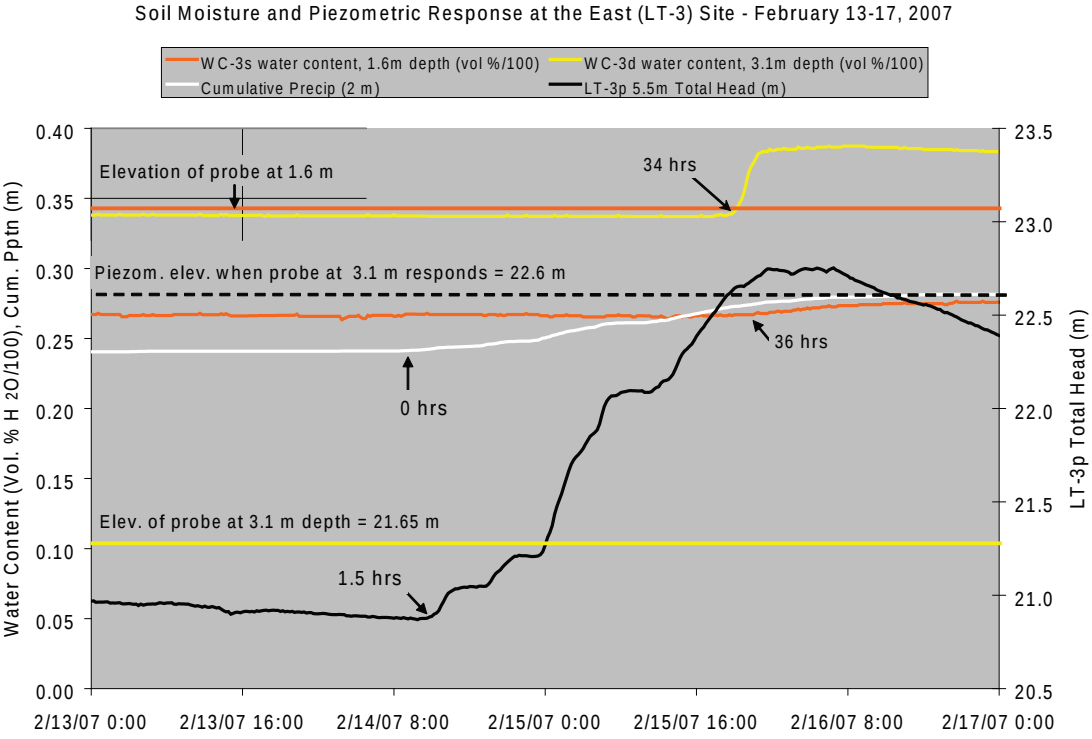

Figure 33. Soil moisture and piezometric response at the east (LT-3) observation site relative to a major rainfall event in February 2007.

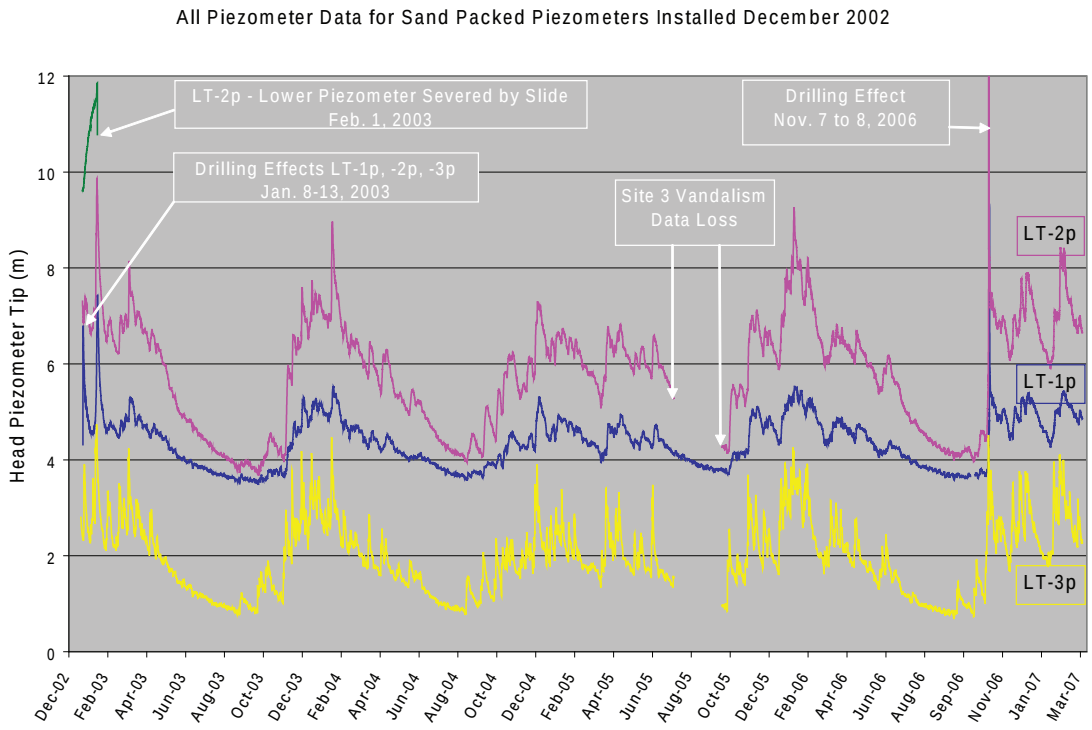

Figure 34. All piezometer data from sand-packed piezometers. Note the drilling effects when these instruments were installed and when the vertical arrays of grouted piezometers were installed adjacent to the LT-2p and LT-1p boreholes November 7 and 8, 2006.

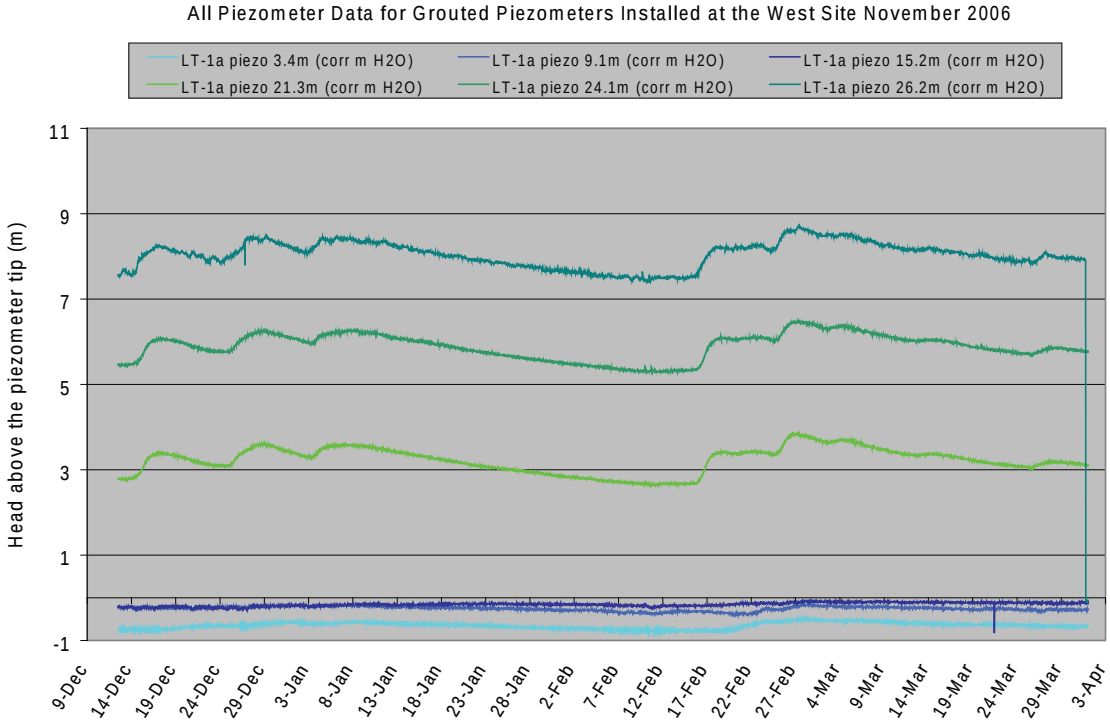

Figure 35. Water pressures in the vertical array of piezometers from the LT-1a borehole. Negative values are suction pressures in the vadose zone above the water table; numbers in the figure explanation are depths in meters to each piezometer.

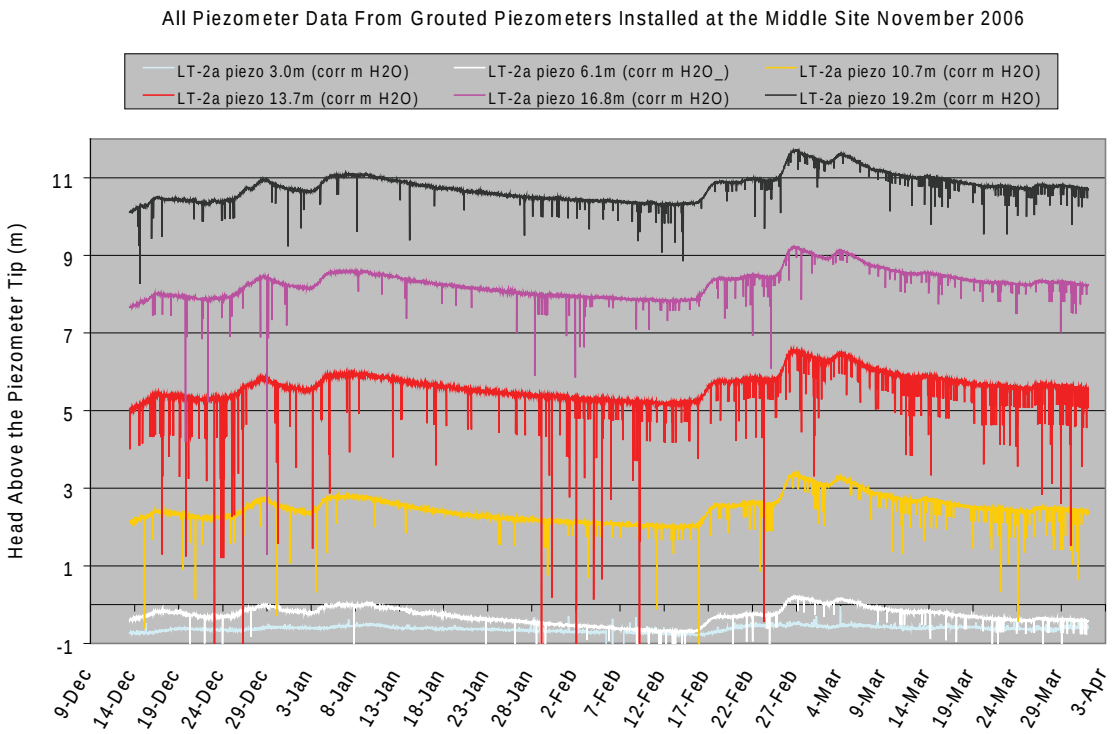

Figure 36. Water pressures (head above the piezometer tip) in the vertical array of piezometers from the LT-2a borehole; depth labels refer to depth of the piezometer tip. Negative values are suction pressures in the vadose zone above the water table; numbers in the figure explanation are depths in meters to each piezometer.

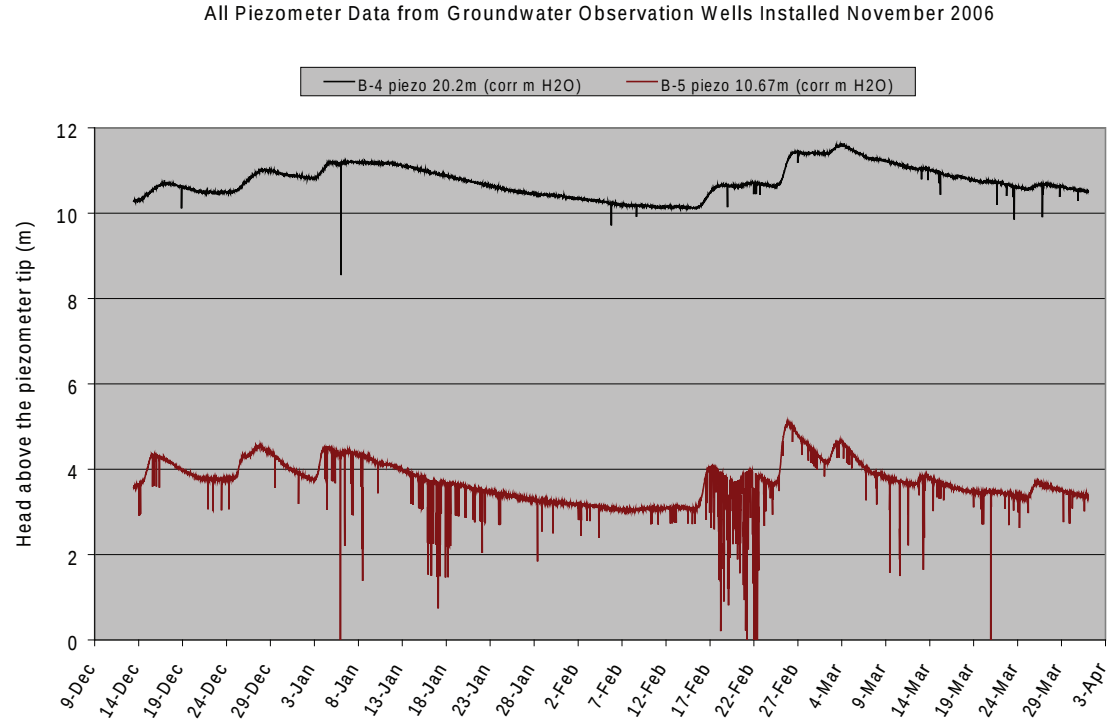

Figure 37. Water pressures (head above the piezometer tip) in piezometers from the groundwater observation wells; numbers in the figure explanation are depths in meters to each piezometer.

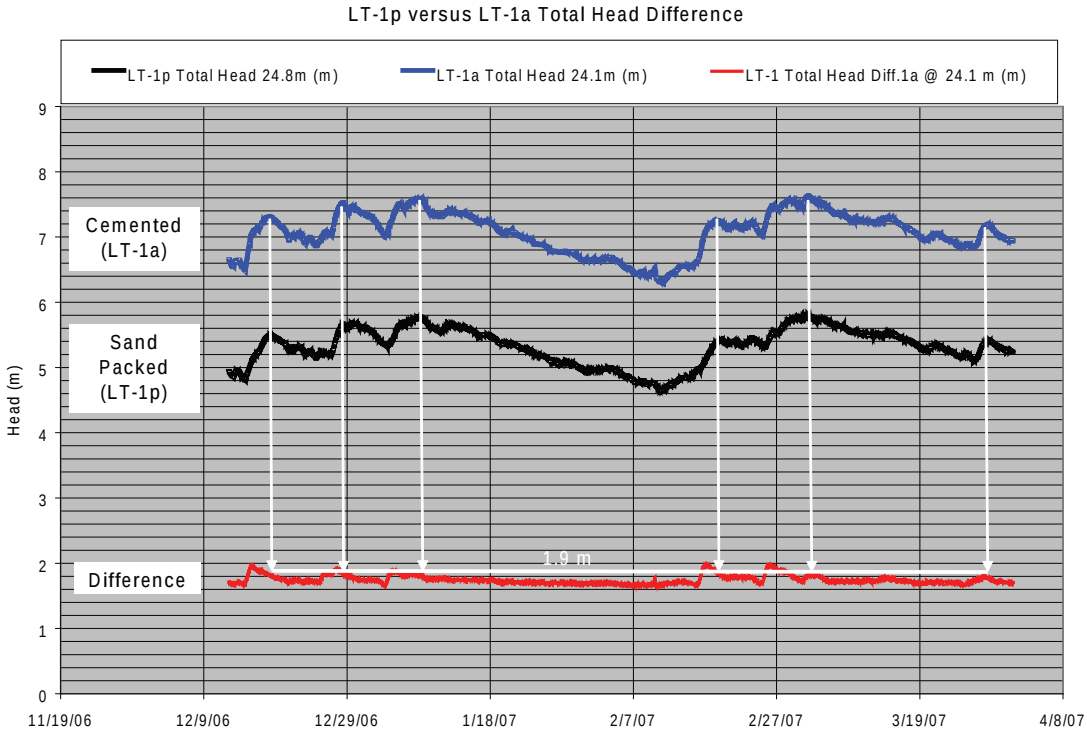

Figure 38. Difference in elevation head between sand-packed and cemented piezometers at the western (LT-1) drill site.

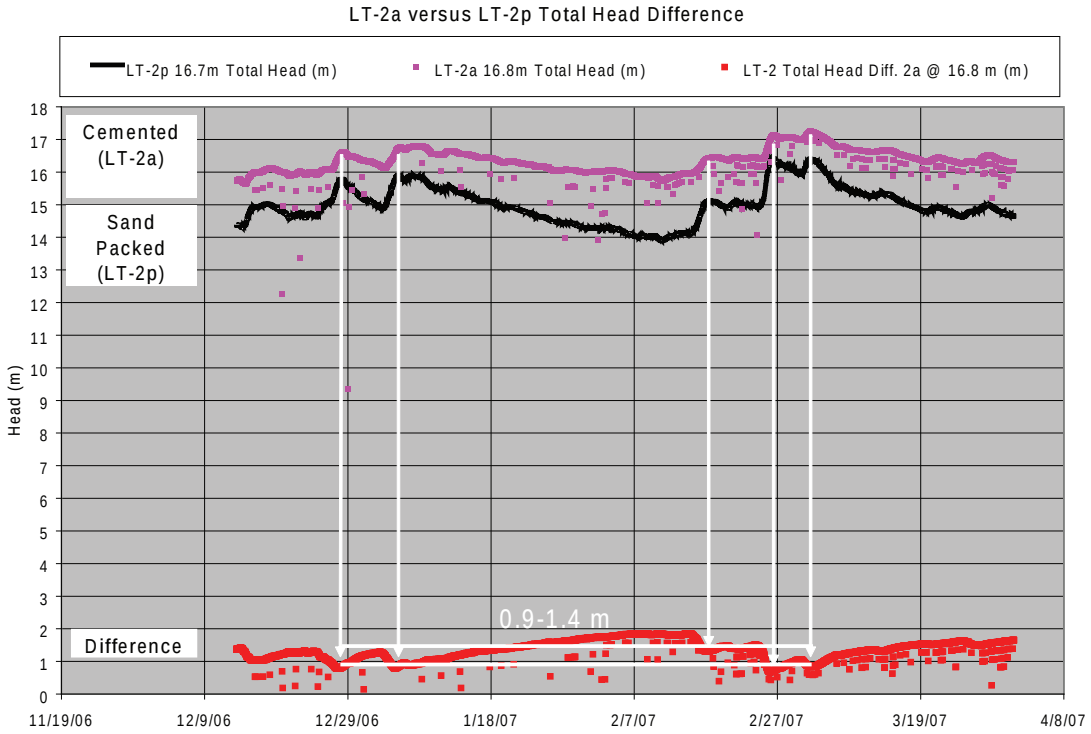

Figure 39. Difference in elevation head between sand-packed and cemented piezometers at the middle (LT-2) drill site. Difference in head during peak head events (white arrows) is between 0.9 and 1.4 m.

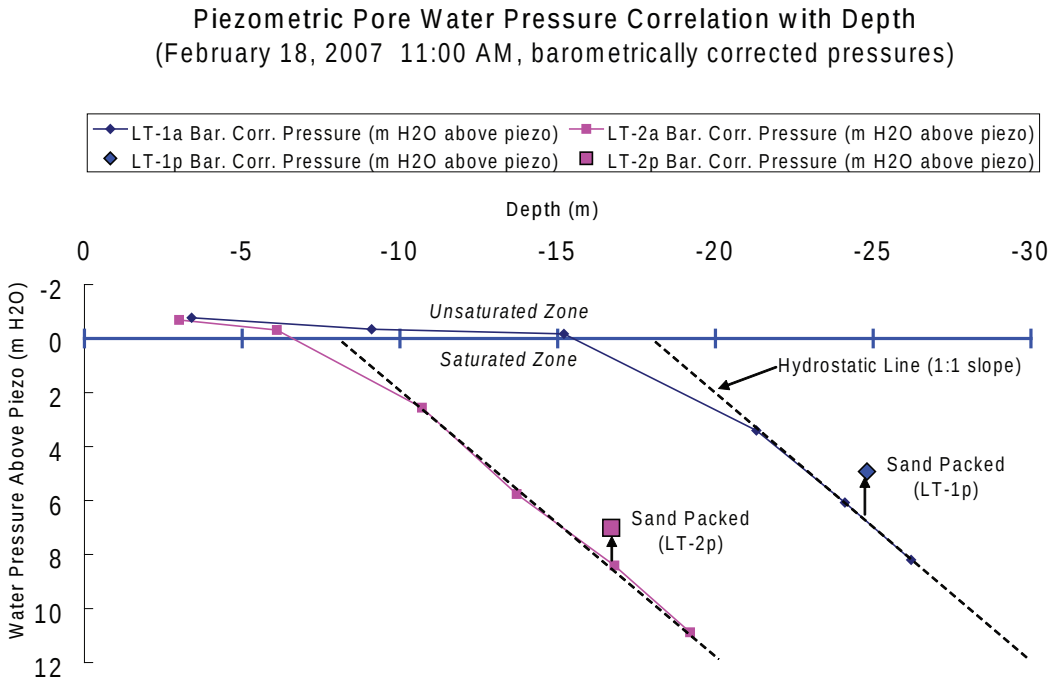

Figure 40. Variation of pressure with depth in vertical arrays of grouted piezometers (colored lines connecting small squares and diamonds) compared to two sand-packed piezometers in adjacent boreholes (larger square and diamond). Dashed lines depict ideal increase in water pressure with depth predicted by the weight of the water column in the saturated zone at each borehole. Sand packed data do not plot on the hydrostatic line.

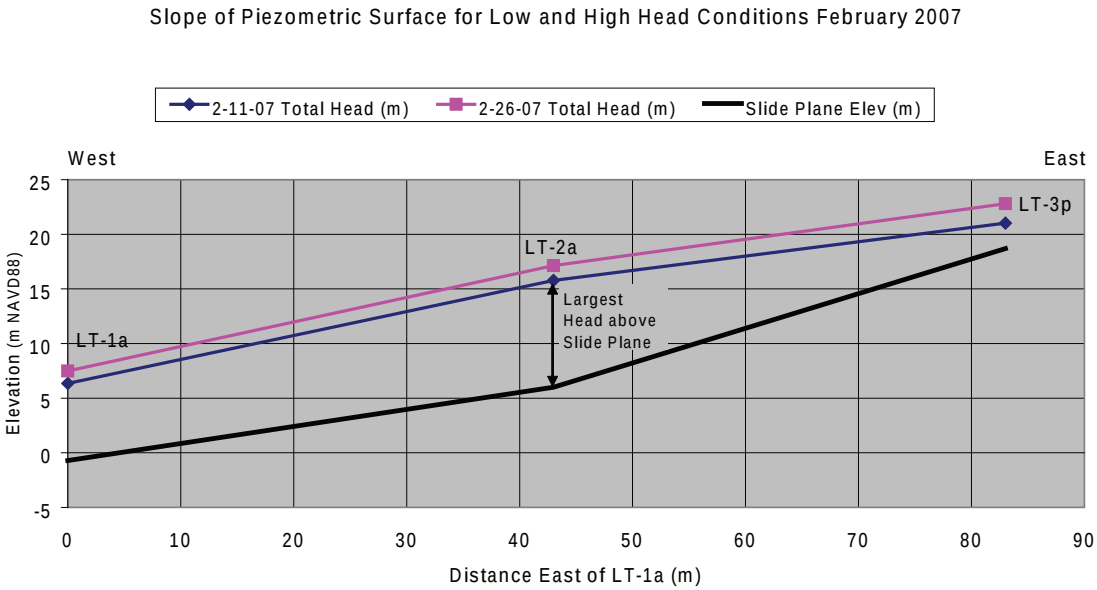

Figure 41. Slope of piezometric surface for winter and spring of 2007 relative to base of basal shear zone. Piezometric data from two grouted piezometers, LT-1a and LT-2a, are used in preference to data from sand-packed piezometers (LT-1p and LT-2p), so head elevations are not underestimated. All piezometers are installed above the base of the basal shear zone; horizontal scale = vertical scale.

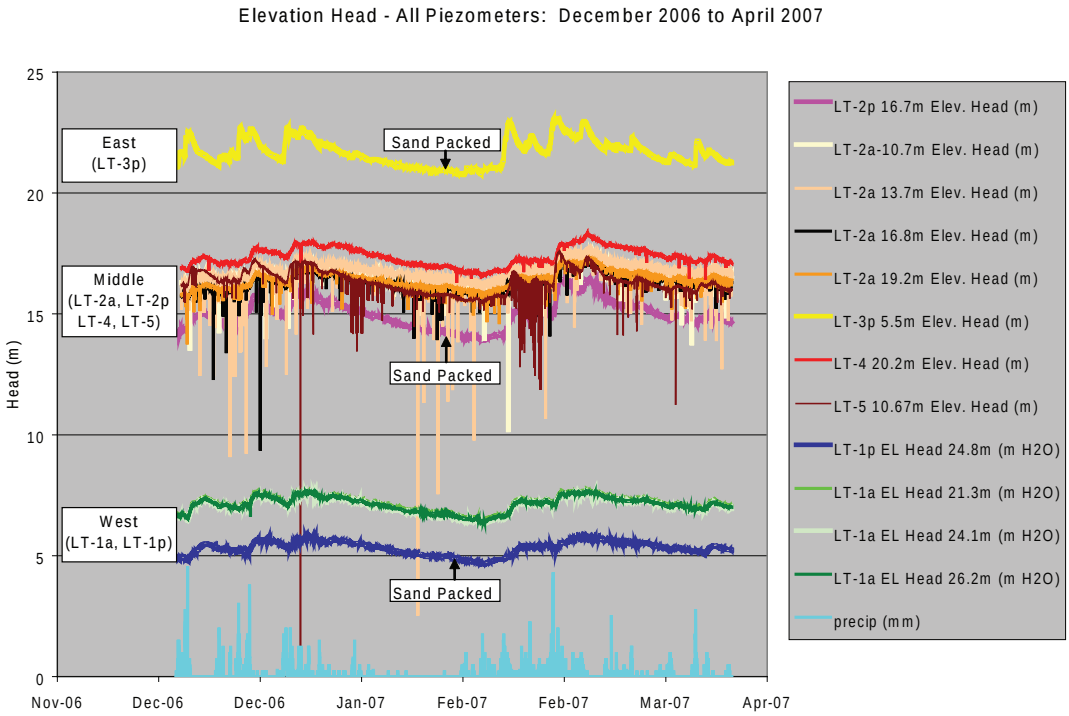

Figure 42. Elevation head for all piezometers. Vertically descending lines in the piezometer data are errors in the data most likely caused by data logger frequency mismatch to frequency of the signal from the vibrating wire piezometers (Erik Mikkelsen, 2007, personal communication).

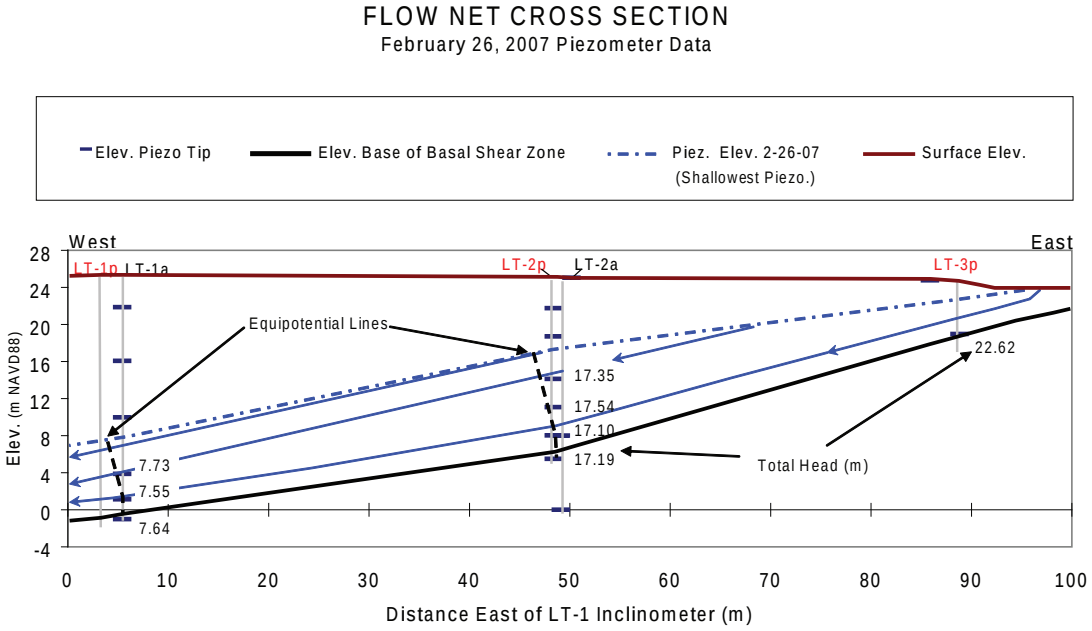

Figure 43. Groundwater flow net for February 26, 2007, a time of relatively high pore water pressure. Numbers are total head at each piezometer; dashed black lines are equipotential isolines; blue lines are estimated groundwater flow paths.

These relationships suggest that sand-packed piezometers are underestimating pore pressures for installed depths.

Hydrologic regime. The piezometric surface slopes westward from the head to the toe of the slide and is steeper on the west side (Figure 41). Head above the basal shear zone is highest in the middle of the slide (Figure 41).

Hydraulic gradient is negligible in the slide and up to 0.5 m below the basal shear zone. (Figure 42; Ellis and others, 2007b). Flow direction from construction of a flow net is roughly parallel to the slide plane (Figure 43).

A piezometer installed in a sand pack 6.3 m below the base of the basal shear zone January 9, 2003, in boring LT-2p recorded a total head lower by ~5 m than total head from a piezometer immediately above the slide plane (Figure 44). Only 24 days elapsed before the slide sheared off the cable at LT-2p, but pore water pressure steadily rose during this period. This limited amount of data is difficult to interpret, so it is not included in the flow net of Figure 43.

Lateral transmission of pore pressure front. Pore water pressure perturbations from rainfall arrive at the LT-3p site within 45 minutes to 2.75 hours of rainfall change (Figure 45), then travel at speeds of 1.4–2.5 m/hr in the upper part (between sites LT-3 and LT-2) and 3.5 m/hr to virtually instantaneous in the middle part of the slide between monitoring sites LT-2 and LT-1 (Figures 46–53). Arrival time of pressure changes varies little with depth (Figures 50 and 53). Schulz (2007) concluded that these data are consistent with nearly horizontal groundwater pressure transmission from the head of the landslide toward the toe and suggested that the landslide basal rupture surface has no effect on groundwater flow. The examples illustrated in the figures are the largest pore water pressure change in the five winter seasons of observation, January 29, 2002, to February 3, 2003, and the largest pressure changes during the 2007 season, February 14 to 19 and February 23 to 25, 2007. The largest pressure perturbations are easily identified at each monitoring site, but smaller ones are progressively more muted in deeper piezometers to the west (Figures 46 and 47; Figure 2).

Infiltration. Pore pressure perturbations in the unsaturated zone occur many hours after perturbations affect the saturated zone and the capillary fringe ~0.7 m above the saturated zone (Figures 54 and 55). Deeper parts of the unsaturated zone infiltrate somewhat more slowly than shallower parts. For example, in the west (LT-1a) borehole unsaturated piezometers responded 132 hours at 3.4 m, 199 hours at 9.1 m, and 263 hours at 15.2 m after intense rainfall (Figure 55). The piezometer in the saturated zone responded within 36 hours of this event. The unsaturated piezometer at 3.0 m depth at the middle site (LT-2a) responded nearly three times faster than the unsaturated piezometer at 3.4 m depth at the west site (LT-1a) (Figures 54 and 55). Overall vertical propagation through the unsaturated zone is ~50 mm/hr (Figure 56), 20–60 times slower than lateral propagation of pore pressures in the saturated zone.

Erosion

Pins. Loss of erosion monitoring pins in 2002–2004 made it impossible to estimate meaningful overall rates of retreat for the slide toe (Appendix H). Pins were lost from mass wasting through slope failure, gradual erosion at the toe of the slope from waves, or deposition of talus cones that covered the pins. The few pins that survived the first season were in competent sandstone beds.

Lidar. Ground-based lidar measurements provide accurate erosion estimates, but collection of these data was not in the original scope of work for the project, so only preliminary results are available at this time (Appendix I). Figure 57 shows an example of the reduced point cloud data file for a small section of the Johnson Creek bluff. Due to the dense sampling of the scanner, the resultant point cloud captures virtually every feature of the bluff face and beach (i.e., it is akin to a photo of the bluff face). For example, Figure 57 clearly shows the location of the Johnson Creek culvert, the presence of woody debris strewn about the creek and a cobble berm constructed along the toe of the landslide.

As additional surveys are undertaken, changes in the morphology of the bluff face can be documented, while analysis of static features in the image (e.g., tree trunks, specialized markers) provides a means of assessing the extent of differential landslide movement over time (i.e., erosion data are adjusted to reflect the movement of the landslide). Because of limited processing capabilities at this stage, we are unable to document the degree of landslide movement along the bluff face, an issue that we hope to resolve in the near future. Accordingly, the results presented here reflect the "unadjusted" state of the landslide face; in other words, west movement

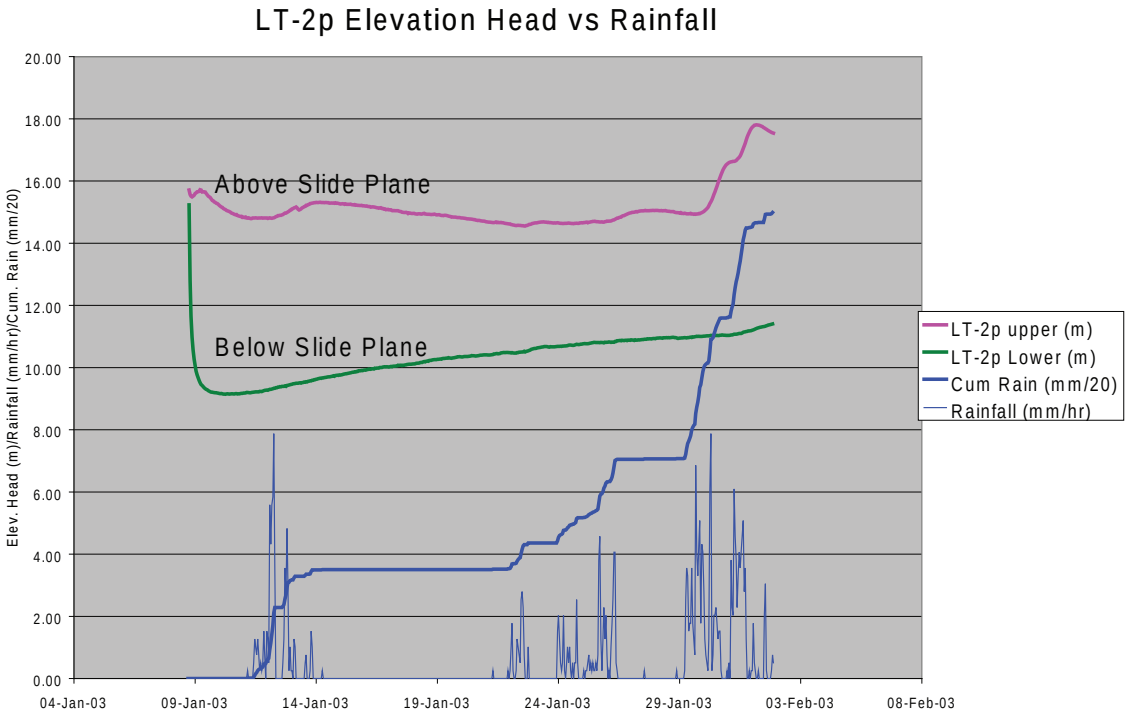

Figure 44. Piezometric head elevation above geodetic mean sea level (NAVD 1988) at the LT-2p borehole, January 2003. Data for the piezometer below the slide plane end when the piezometer cable was severed by slide movement at 9:00 PM on February 1, 2003. Cum. Rain = cumulative rainfall from January 9, 2003, to February 2003.

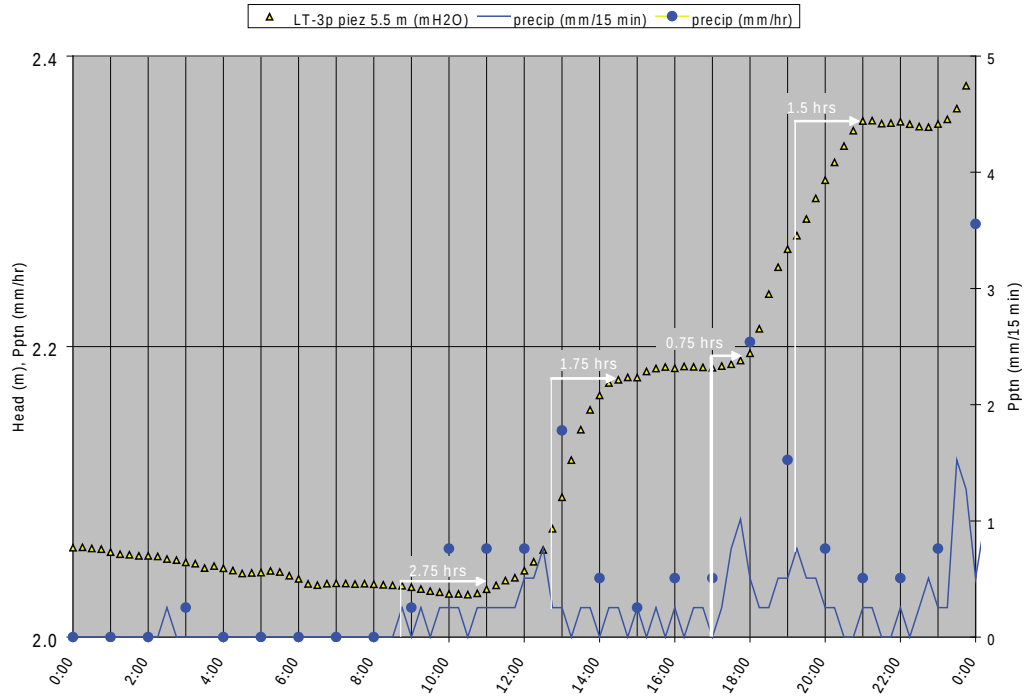

Figure 45. Response of LT-3p piezometer to rainfall; piezometer is at the western margin of the headwall graben. Water pressure response is generally within ~2 hours of a rainfall event and can be used as a proxy for pressure responses to rainfall at graben.

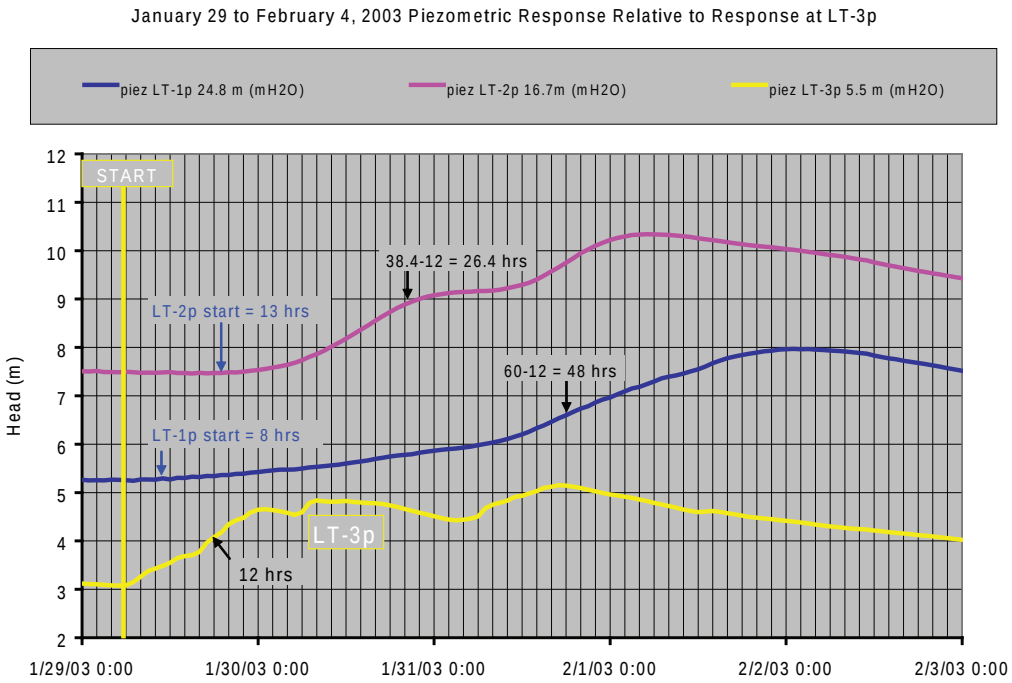

Figure 46. Timing of January 29 to February 4, 2003, piezometric response from the east site (LT-3p) on the west margin of the headwall graben to other sites to the west, northwest, and southwest (see Figure 2 location map). Data are from piezometers near the basal shear zone. Distances west refer to distance from the west margin of the headwall graben. Blue numbers are first response times after response at the LT-3p site. Black numbers are the times when pressure reached half the amplitude of the perturbation; vertical lines are in increments of 2 hrs.

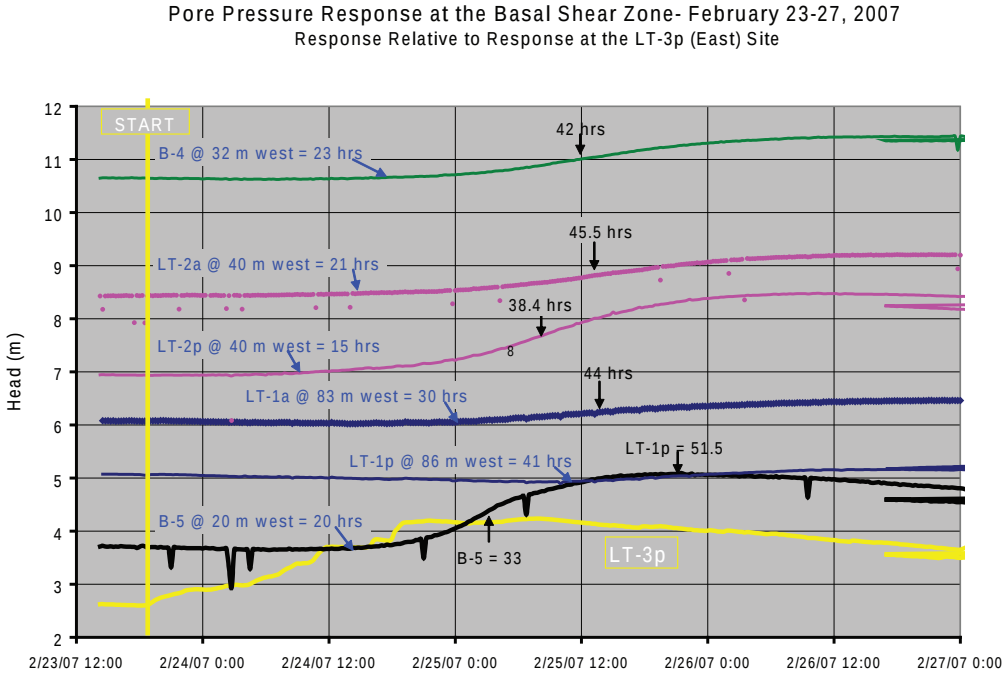

Figure 47. Timing of February 23 to 27, 2007, piezometric response from the east site (LT-3p) on the west margin of the headwall graben to other sites to the west, northwest, and southwest (see Figure 2 location map). Data are from piezometers near the basal shear zone. Distances west refer to distance from the west margin of the headwall graben. Blue numbers are first response times after response at the LT-3p site. Black numbers are the times when pressure reached half the amplitude of the perturbation. LT-2p is installed in a sand pack; B-4 and B-5 are groundwater monitoring wells; all others are grouted. Vertical lines are in increments of 2 hrs.

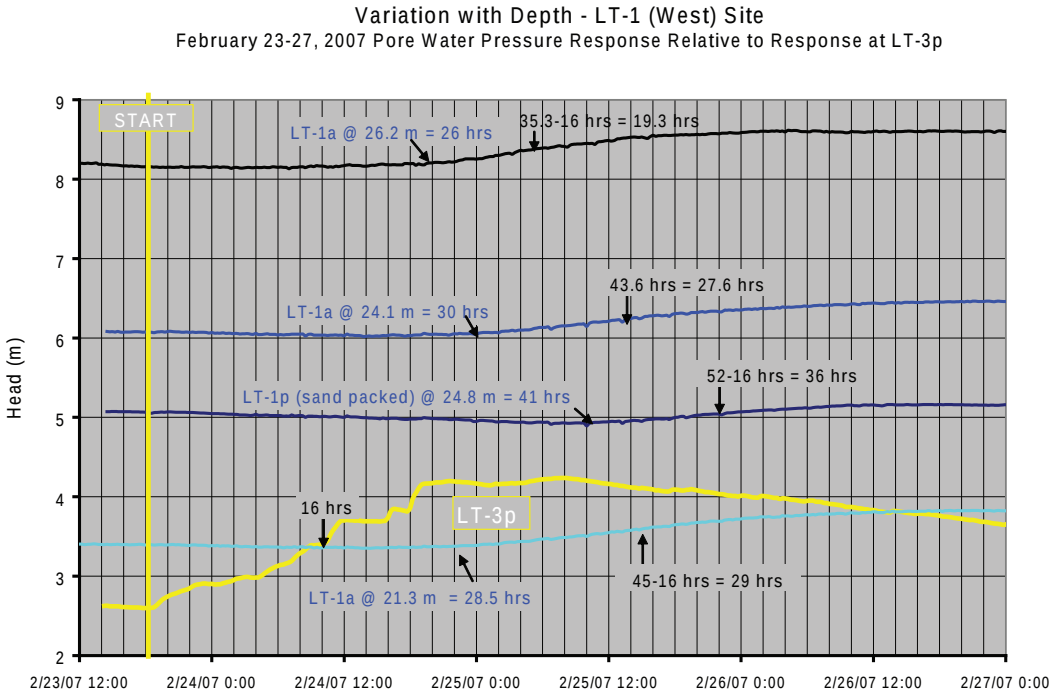

Figure 48. Variation of pressure response with depth at the LT-1 observation site February 23 to 27, 2007. Blue numbers are first response times after response at the LT-3p site. Black numbers are the times when pressure reached half the amplitude of the perturbation. Vertical lines are in increments of 2 hrs.

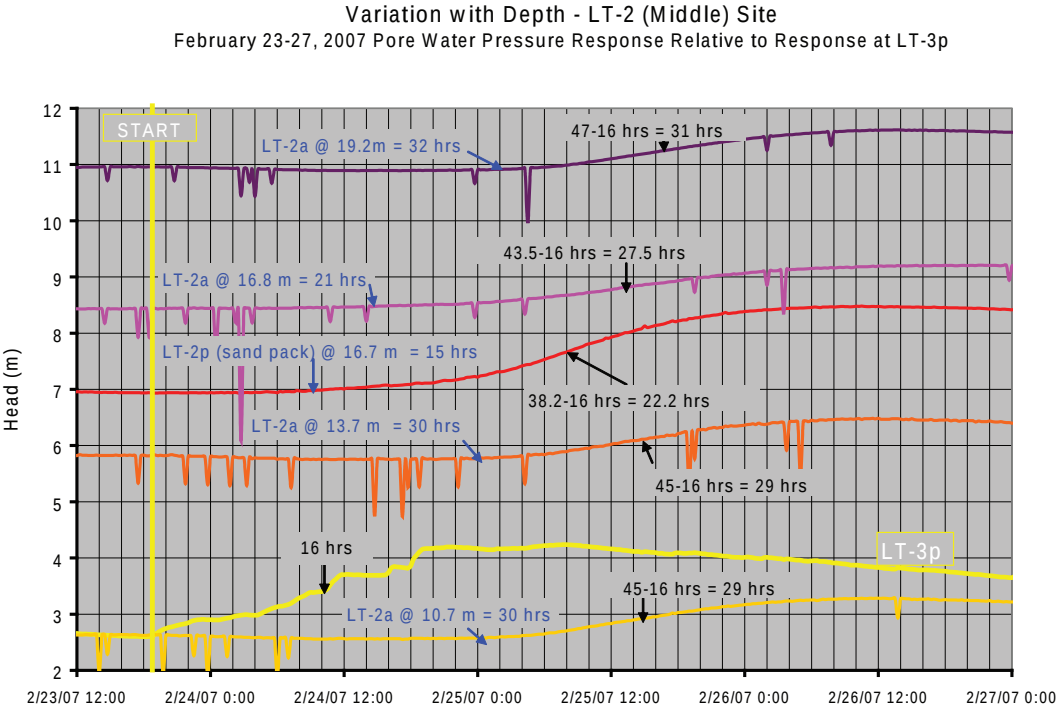

Figure 49. Variation of pressure response with depth at the LT-2 (middle) observation site February 23 to 27, 2007. Blue numbers are first response times after response at the LT-3p site. Black numbers are the times when pressure reached half the amplitude of the perturbation. Vertical lines are in increments of 2 hrs.

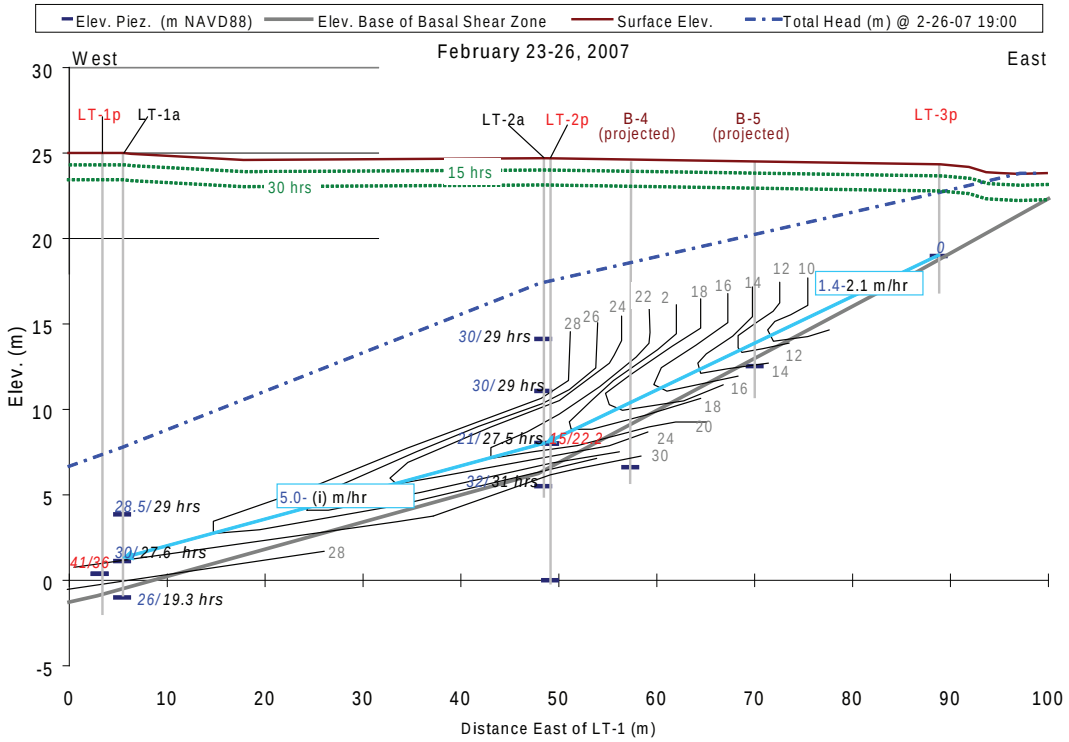

Figure 50. Isochrons (black lines) in 2-hr intervals for first response of grouted piezometers to pressure increase for February 23 to 26, 2007. Baseline is the time when the increase occurred at the LT-3p site. Blue numbers are the first response time; black numbers separated by a back slash are response time for half of the total response; red numbers are the same data for sand-packed piezometers. Blue boxes list travel velocity of pressure response; (i) = virtually instantaneous response between the two monitoring sites. Green dotted lines are isochrons for downward infiltration of groundwater, assuming a mean rate of 50 mm/hr. Vertical exaggeration is 1.6.

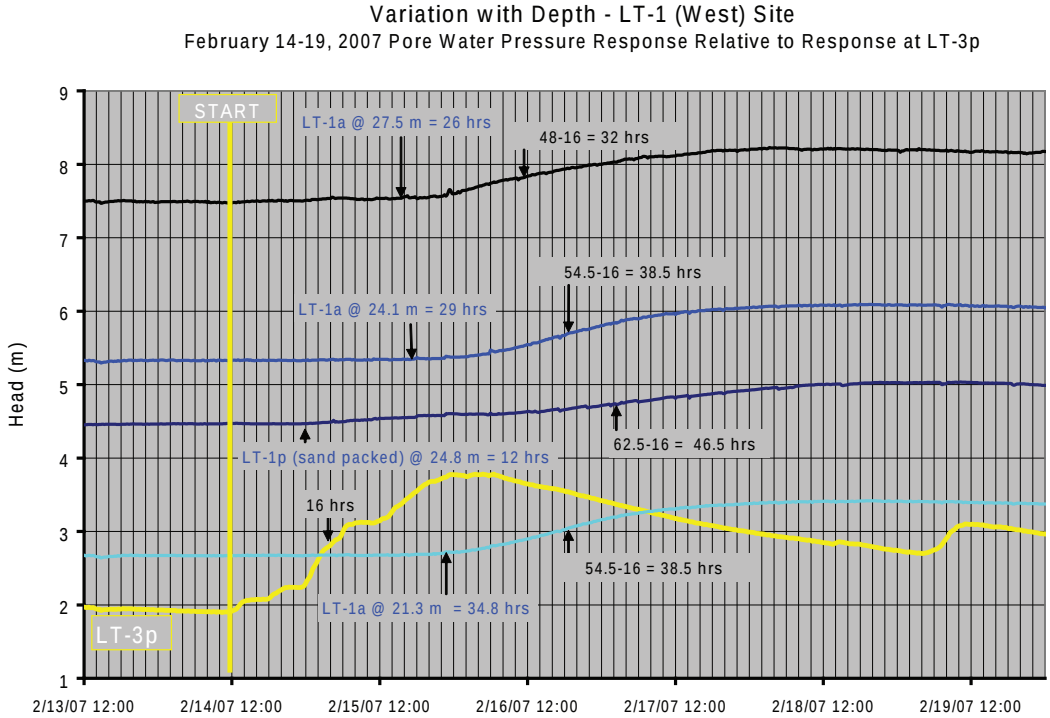

Figure 51. Variation of pressure response with depth at the LT-1 observation site for February 14 to 19, 2007. Blue numbers are first response times after response at the LT-3p site. Black numbers are the times when pressure reached half the amplitude of the perturbation; vertical lines are in increments of 2 hrs.

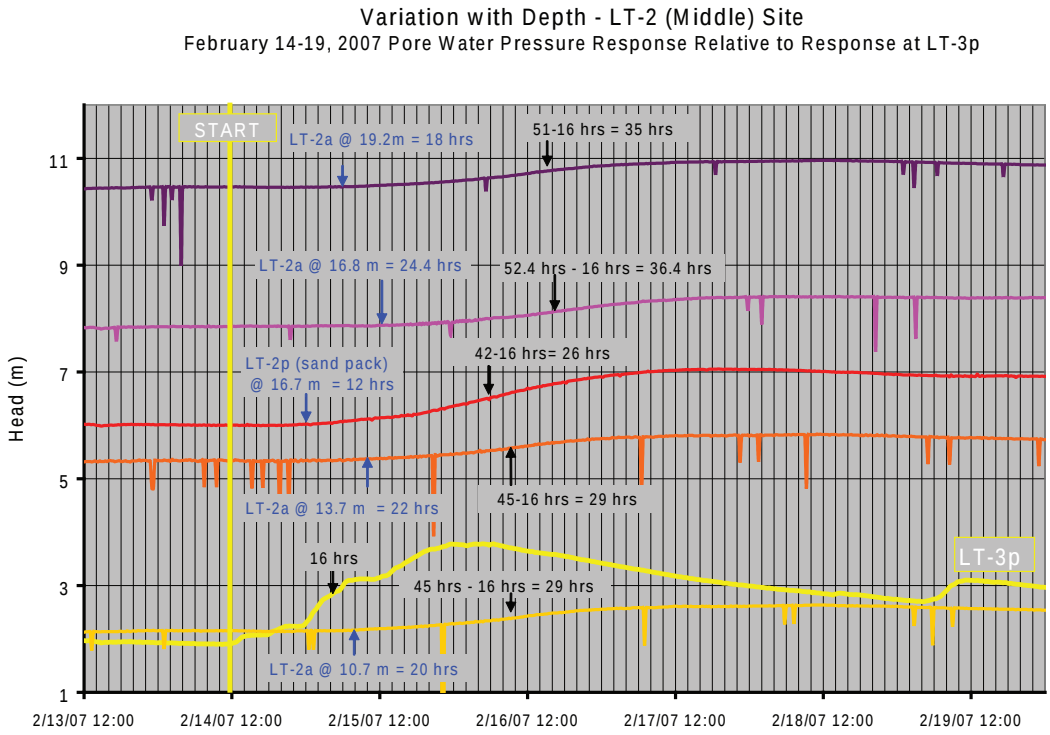

Figure 52. Variation of pressure response with depth at the LT-2 (middle) observation site February 14 to 19, 2007. Blue numbers are first response times after response at the LT-3p site. Black numbers are the times when pressure reached half the amplitude of the perturbation; vertical lines are in increments of 2 hrs.

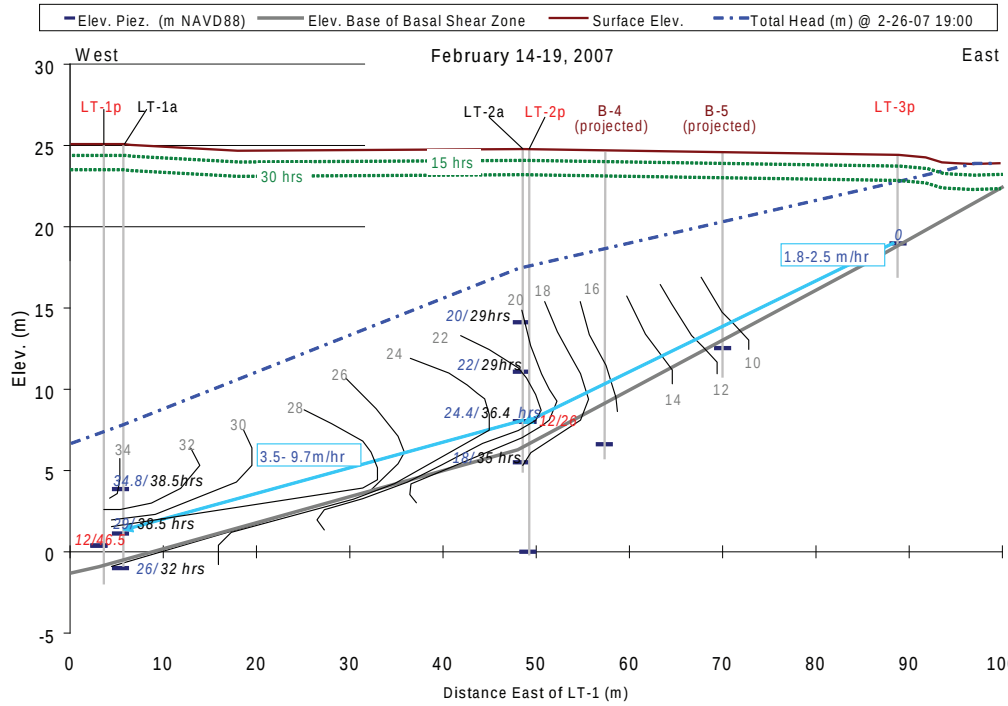

Figure 53. Isochrons (black lines) in 2-hr intervals for first response of grouted piezometers to pressure increase for February 14 to 19, 2007. Baseline is the time when the increase occurred at the LT-3p site. Blue numbers are the first response time; black numbers separated by a back slash are response time for half of the total response; red numbers are the same data for sand-packed piezometers. Blue boxes list travel velocity of pressure response; (i) = virtually instantaneous response between the two monitoring sites. Green dotted lines are isochrons for downward infiltration of groundwater assuming a mean rate of 50 mm/hr. Vertical exaggeration is 1.6.

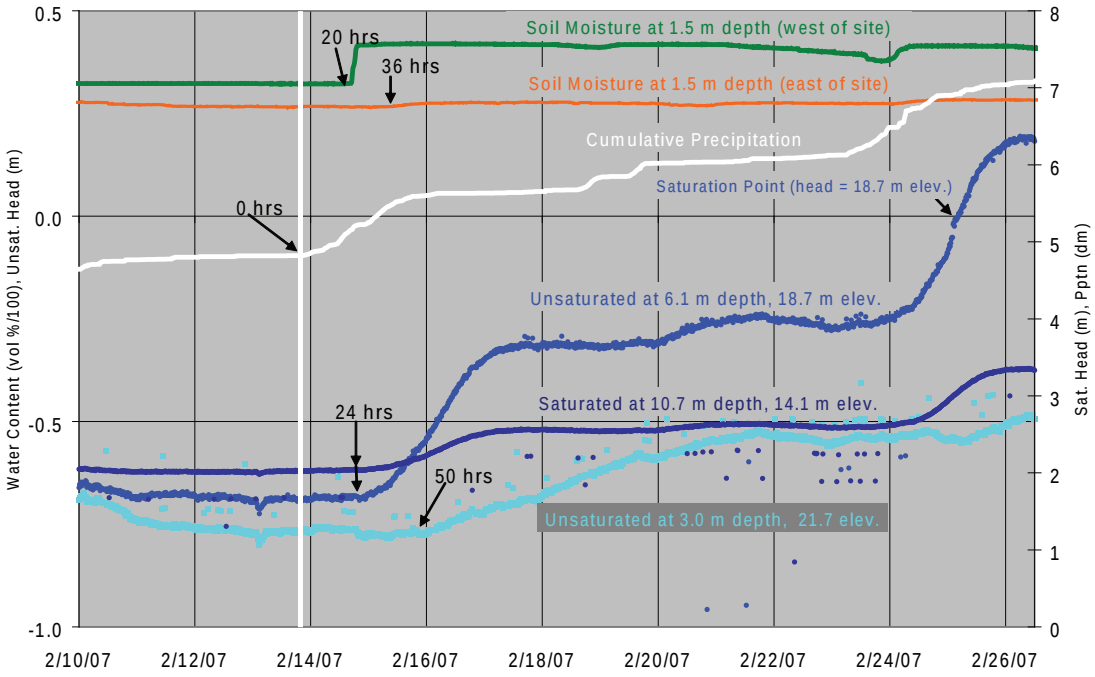

Figure 54. Delay of response of a piezometer in unsaturated zone relative to piezometers in or within 0.7 m of the saturated zone for the middle (LT-2a) borehole. Note that the piezometer at 6.1-m depth becomes saturated after February 25, 2007. The soil moisture data are from the LT-1 observation site to the west.

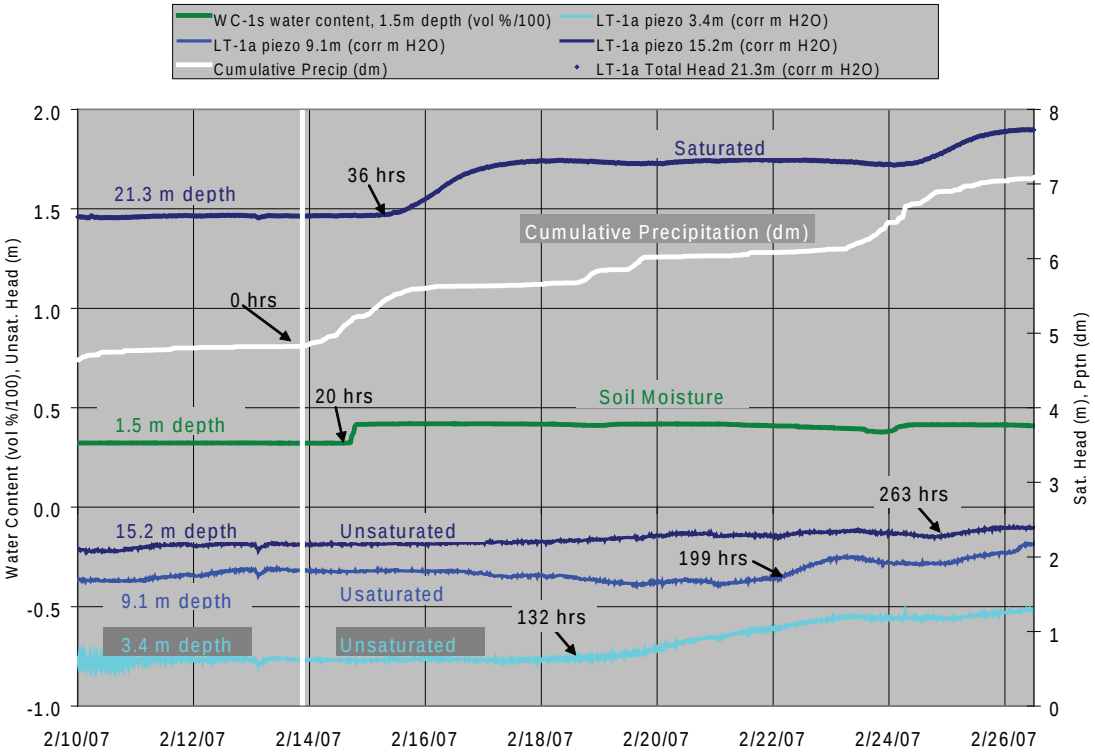

Figure 55. Delay of response of piezometers and soil moisture probe in unsaturated zone relative to a piezometer in the saturated zone for the west (LT-1a) borehole. Depths are to piezometer or soil moisture probes tips.

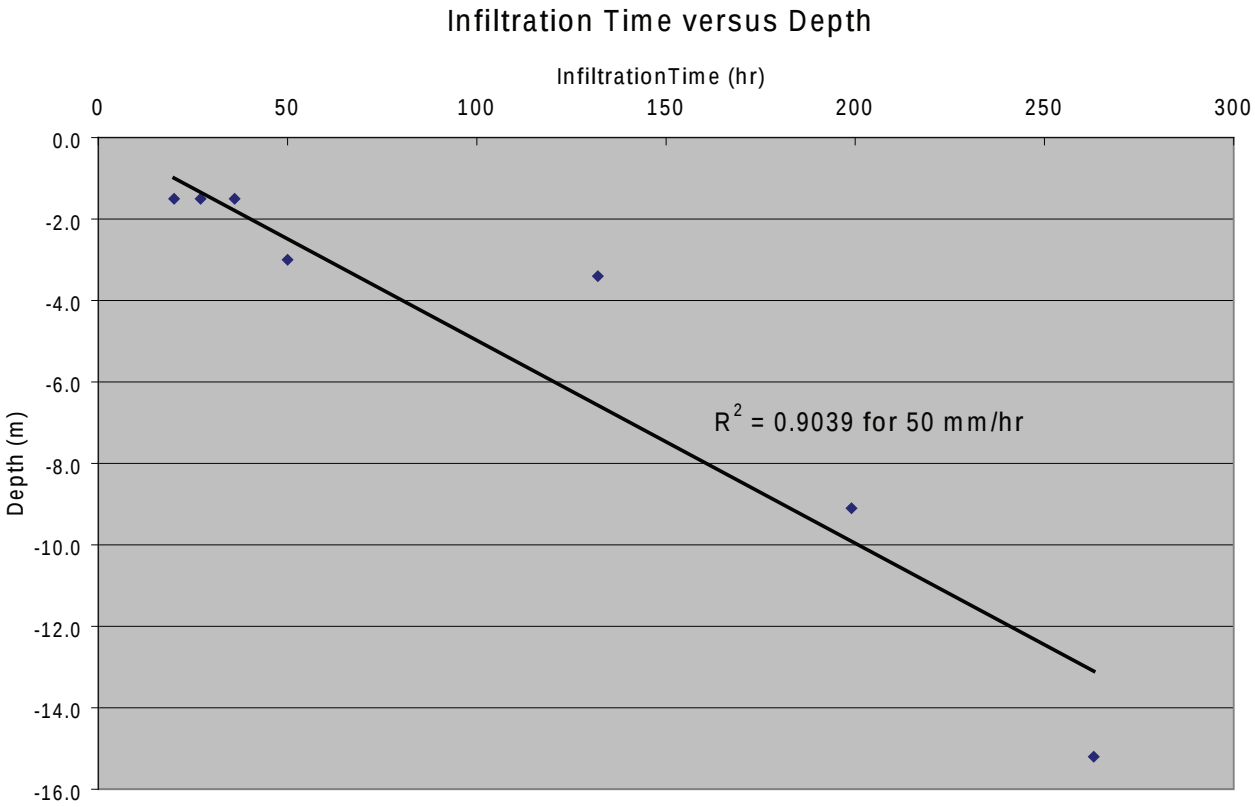

Figure 56. Infiltration time versus depth for unsaturated piezometers and soil moisture probes above the piezometric elevation. Data are from February 14 to 26, 2007, plus soil moisture data from January 3, 2007.

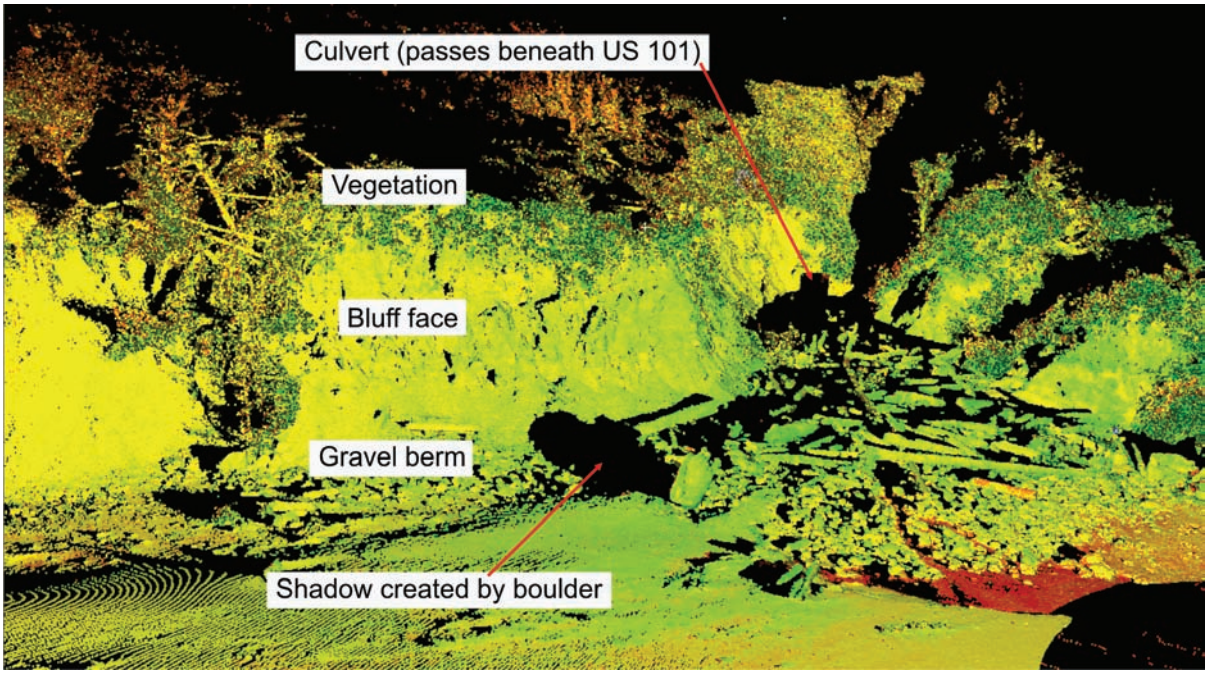

Figure 57. Point cloud example derived from a survey in October 2006 at the mouth of Johnson Creek on the southern slide margin (point density is approximately 2 per cm^2).

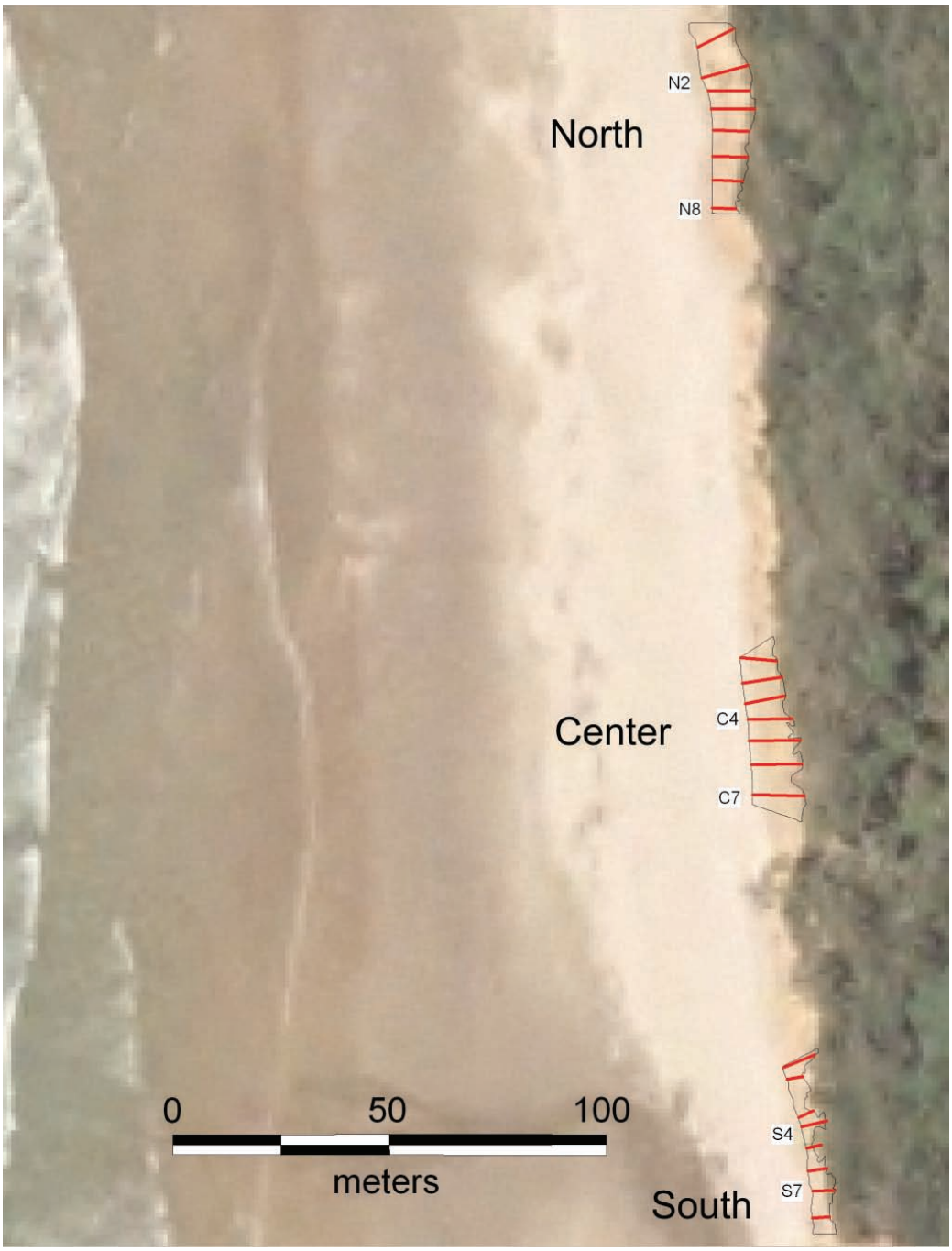

Figure 58. Map showing locations of representative bluff profile sites.

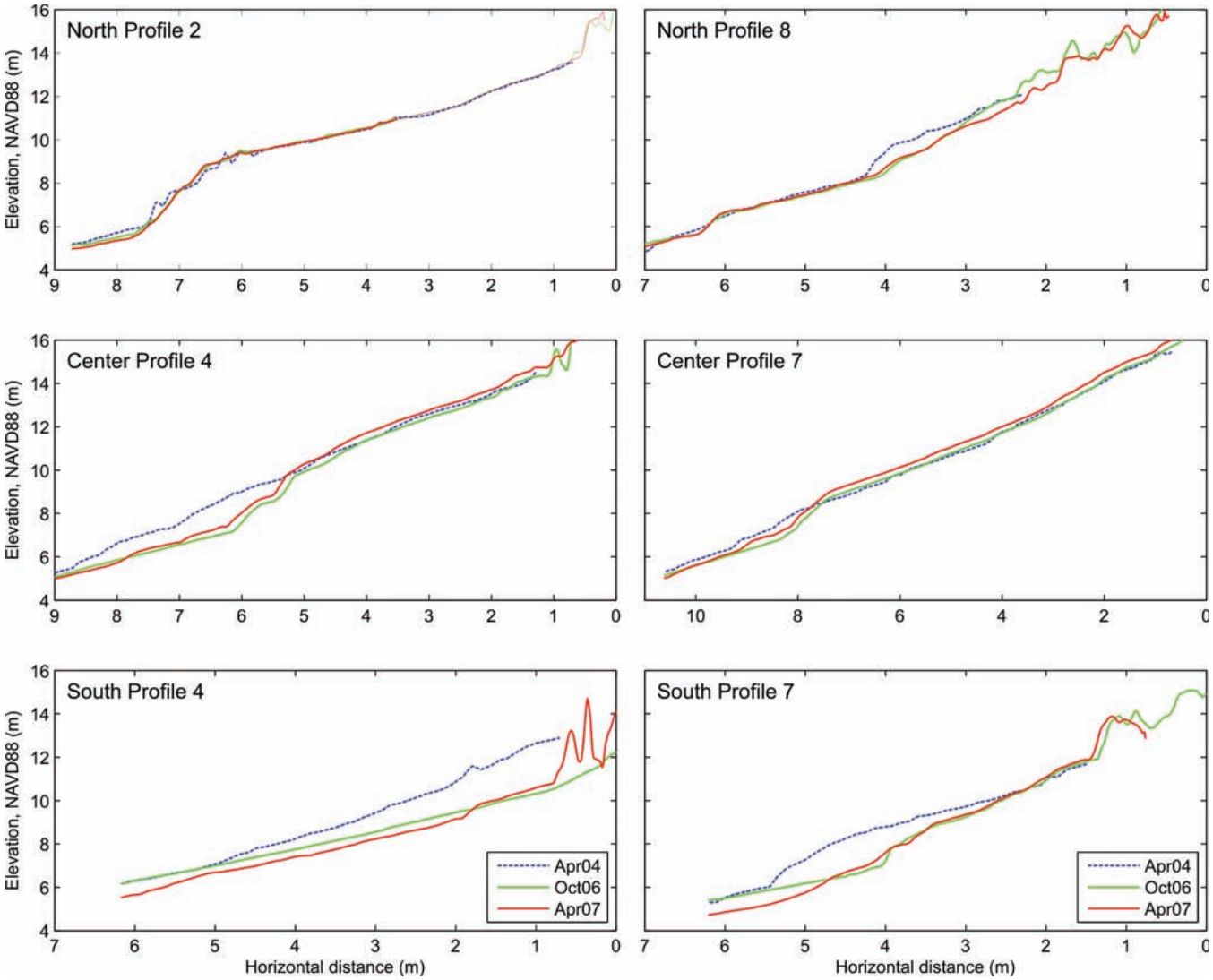

Figure 59. Six representative bluff profiles derived from the three sections along the Johnson Creek bluff face (site locations are shown in Figure 58). Note that the elevation data are relative to the North American Vertical Datum of 1988 (NAVD 1988).

of the landslide between each sampling interval has not been backed out of the data. Figure 58 is a location map showing the three sections of the slide toe where GBL data are available for all three years and locations of transect lines used to document changes across the bluff face. The degree of bluff change between 2004 and 2007 is shown in Figure 59 based on six representative transects. The amount of profile change in the north is less when compared with the central and southern portions of the bluff face. Furthermore, the cross-section data indicate generally greater erosion at lower elevations (i.e., below about 8 m), while the upper portions of the bluff showed very little change. The exception to this pattern is the response shown for the north profile 8, which experienced a small slump failure.

Aside from developing cross sections, it is also possible to determine from GBL data volumetric changes between consecutive surveys. Preliminary analysis indicates that the bluff face lost 25 m^3 (32.7 yd^3) of material along a 40-m section in the central part. Additional comparisons (not included here) indicate that erosion of the bluff is greatest between the southern and central scan regions and decreases to the north.

Beach Erosion. Monitoring of sand movement (Appendix K) was abandoned when Landslide Technology (2004) determined that the 1.5–2 m seasonal change in beach sand thickness has negligible influence

on slide stability. The 2003 survey did reveal that the central part of the slide toe is exposed to a lower beach and higher wave strike (Appendix K). Johnson Creek generally lowers the beach profile during the winter allowing free access of winter waves to the slide toe on its southern margin.

LABORATORY TESTING

Laboratory testing results of Landslide Technology (2004) are compiled here for convenience. Results of in-place density tests are summarized in Table 4. Moisture contents are listed on the borehole logs of Appendix B. Results of the ring shear test are given in Appendix J. The phi angle of the Mohr stress envelope was 13.1˚ for ring shear testing of the slide gouge.

SLOPE STABILITY ANALYSIS

Parametric Analysis by Landslide Technology

Landslide Technology (2004) did a parametric investigation to evaluate the sensitivity of landslide stability to the precipitation, groundwater levels, erosion and beach sand level. The analysis and recommendations are summarized in Appendix M. They first back-calculated the residual strength (ϕ_r') value for the slip surface analyzed in cross section A-A' (Figure 7), finding a value of 6.5˚ for initiation of movement at threshold pore water pressures (10 m above the slide plane at the middle, LT-2, site). This single-digit value is comparable with similar slides in the Astoria Formation and other large translational landslides in tuffaceous sediments and decomposed volcanic rocks in the region, all of which have been investigated by Landslide Technology utilizing similar procedures. The back-calculated ϕ_r' value is an average for the model. The difference between the back analyzed ϕ' value and the value obtained from the ring shear testing (13.1 degrees) may be attributed to the fact that (1) the sample tested may not be representative of the entire failure surface, and (2) systematic underestimation of water pressure by the sand-packed piezometers at the LT-1p and LT-2p boreholes, as previously explained.

Using the back-calculated ϕ_r' of 6.5˚, Landslide Technology performed a parametric analysis to evaluate sensitivity of the slide to three parameters: (1) precipitation and groundwater, (2) erosion, and (3) the seasonal deposition and removal of beach sand. For each parameter, incremental changes were made to determine the resulting percent change in factor of safety (FOS). A summary of the analyses is provided in Table 5.

Landslide Technology (2004) demonstrated that at the latitude of the cross section A-A' (Figures 6 and 7) the greatest reductions in FOS occur from high pore water pressure from severe storms and loss of toe support. Shifting beach sand was an insignificant factor (Table 5). They determined that the landslide is at the stability limit when head above the slide plane is 7.0 m at the west (LT-1) site, 10 m at the middle (LT-2) site, and 6.3 m at the east (LT-3) site. Factor of safety is 2 percent above the stability limit during average winter conditions when head above the slide plane is 6.6 m at the west (LT-1) site, 8.9 m at the middle (LT-2) site, and 4.4 m at the east (LT-3) site. Factor of safety was 7.2 percent below the stability limit when simulated head above the slide plane was 10.6 m, 13.3 m, and 7.1 m at the west, middle, and east sites, respectively. The latter was the "severe storm" scenario when piezometric head at the basal shear zone was assumed to be 1.5 m above the highs recorded during the 2002-2003 season. Any higher uniform increase in head would place the piezometric surface above the surface at the shallowest part of the slide at site LT-3p. Highs in piezometric head during 2002-2003 are still the largest observed in five

Table 4. Summary of in-place density testing.

Boring No.	Sample No.	Depth, m (ft)	Soil Description	Moist Unit Weight kN/m³ (pcf)	Moisture Content	Dry Unit Weight kN/m³ (pcf)
LT-1	R-4	10.5–10.8 (34.4–35.4)	soft (R2), gray, silty, fine sandstone	21.3 (135.5)	21%	17.5 (111.8)
LT-2	R-10	18.8–19.0 (61.7–62.3)	very soft (R1), gray, fine silty sandstone	21.5 (137.1)	18%	18.3 (116.5)

R2 and R1 refer to rock hardness in the classification scheme of Sera (2003).

Table 5. Summary of sensitivity analysis by Landslide Technology (2004).

Parameter	Change in Factor of Safety from Back-Analysis (– Decrease / + Increase)
Groundwater	
"Normal" 2003 winter level	+2.0 %
"Severe Storm"	–7.2 %
Erosion of Cliff Face	
0.5 m (1 ft) of Erosion	–0.8 %
1.5 m (5 ft) of Erosion	–3.6 %
3.0 m (10 ft) of Erosion	–6.8 %
Seasonal Deposition/Removal of Sand	
1.0 m (3 ft) Removal	–0.3 %
1.0 m(3 ft) Deposition	+0.3 %

winter seasons of observation, so this is an extremely conservative assumption.

FOS decreases by 2 percent for every meter of head rise at the middle (LT-2p) site, on the basis of extrapolation of the three data points listed by Landslide Technology (2004). FOS decreases by 2.3 percent for every meter of erosion of the toe, on the basis of on a similar extrapolation of their data. A meter of change in depth of sand at the toe of the slide changed FOS by only 0.3 percent.

Supplementary Stability Analysis by Christie and Dickenson

The stability analyses performed by Christie and Dickenson of Oregon State University are given by Priest and others (2006) and are reproduced in Appendix N. Christie and Dickenson verified the results of Landslide Technology (2004), examined the effect on stability of water filled cracks in the slide mass, and further evaluated the influence of parameters such as groundwater conditions and geotechnical strength parameters for three sections through the slide mass. Their analysis resulted in a residual friction angle of $\phi' = 5.9°$ for a similar cross section to the one used by Landslide Technology (i.e., at the drilling transect). They also constructed cross sections in the northern and southern parts of the slide, finding maximum residual friction angles of 9° to 11° for a southern section, and 5.7° and 8.3° for a northern cross section. These residual friction angle data are for slide geometries that most closely matched 1970s inclinometer data from ODOT (Appendix C). Their findings demonstrate that a higher assumed residual friction angle is needed in the southern part of the slide to maintain stability when that area is subjected to threshold pore pressures for instability of the northern and central parts of the slide. In other words, the southern part is inherently less stable. This observation fits with the resurvey data and observed greater movement in the southern part of the slide (Figures 22–25).

Christie and Dickenson evaluated the influence of the phreatic surface on stability (i.e., factor of safety against sliding) in order to determine the contribution to FOS of each portion of the slide in the drilling transect, using the "severe storm" case of Landslide Technology (2004). This scenario results in a 9 percent decrease in factor of safety from "normal winter" groundwater conditions. The analysis shows that 50 percent of the decrease occurs over the eastern (upslope) 25 percent of the slide plane. These findings underscore the critical importance to slide stability of pore water pressure between the LT-3 and LT-2 monitoring sites in the upper part of the slide.

The analysis of a water-filled crack near the slide toe found that water-filled cracks penetrating deeper than ~8 m can destabilize the toe. Failure of the toe in front of the crack is the source of instability to the rest of the slide.

Remediation Options

Landslide Technology (2004) examined the following remediation options based on the stability analysis (see Appendix M for details):

1. Unloading the upper part of the slide by excavation.
2. Buttressing the slide toe with a revetment at the beach:
3. Installing horizontal drains at the slide toe.
4. Installing a tied-back shear pile wall within the slide.
5. Maintaining the highway affected by the slide through periodic repaving.

Table 6 summarizes the pros and cons of each option. Landslide Technology (2004) recommended buttressing as the best long-term option. Dewatering by horizontal drains was thought impractical because drains would be severed by the back-rotated toe block.

D. Andrew Vessely of Landslide Technology (e-mail communication, April 26, 2005) detailed the reasons that dewatering is generally less effective than buttressing for this slide:

"Horizontal drains would have limited benefit in improving the stability of Johnson Creek landslide due to (i) relatively low existing groundwater levels, and (ii) the low residual shear strength at the failure zone. For our evaluation of conceptual treatment options, we assumed that horizontal drains would be drilled from the beach to obtain a suitable angle into the slide mass. Given the landslide geometry and constructability limitations, the drains could only dewater the upper portion of the slide mass (the drains would not intercept groundwater in the lower portion).

Keep in mind that our sensitivity analyses indicated that seasonal groundwater level increases of 3 to 6 feet (across the entire slide mass) would decrease the stability by approximately 2 percent." . . ."One would expect that a drop of 3 to 6 feet over the entire slide mass would improve stability only 2 percent. Even if the horizontal drains were successful in lowering the upper groundwater levels, say 5 to 10 feet, they would not act over the entire slide mass - hence the 1 percent improvement as indicated in our report.

Also, when dealing with a translational slide with a low residual friction angle of 6.5 degrees, increasing the effective stress (for example by dewatering) would have limited benefit since the available shear strength is a function of $\sigma'_n(\tan \phi')$.

As far as using well points or even deep dewatering wells, it has been our experience that any type of dewatering in a heterogeneous slide mass involves a high degree of uncertainty. Horizontal drains are relatively cheap and can often be tried on an experimental basis, but as discussed in this E-mail and in our report, horizontal drains are not well suited for this landslide. Dewatering wells can be significantly more expensive than horizontal drains, and therefore should be considered with caution as a treatment for this slide. Given the relatively shallow depth of sliding in the graben area (i.e. limited potential for significant draw downs) and the low residual friction angle, I am not an advocate of dewatering for this slide. Furthermore, and perhaps more importantly, it is my opinion that bluff erosion would over time, negate any stability improvements obtained from dewatering. Our analyses indicated that 1 foot of bluff erosion decreases the stability of the slide mass by 1 percent. As you know, this amount of bluff erosion can occur over a fairly short timeframe."

Table 6. Remediation option comparison (Landslide Technology, 2004)

	Remediation Option				
	1 Unload Upper Slide	**2 Toe Buttress**	**3 Horizontal Drains**	**4 Tied-Back Shear Pile Wall**	**5 Road Maintainance**
Effectiveness	moderate	high	low	high	low
Constructibility	good	good	moderate	difficult	not applicable
Engineering	simple	moderate	moderate	difficult	simple
Environmental long-term impact	low	high	low	low	low
Maintenance long-term	low	low	moderate	low	high
Construction costs ($ million)	0.9	1.1	0.5	11–14	0.4 (20 yrs)

DISCUSSION

LANDSLIDE MOVEMENT

The landslide moves in a more or less coherent block during small (≤2 cm), continuous movements but has increasing internal deformation among blocks as single-event displacement exceeds 2 cm. The largest movement occurred between January 31 and February 10, 2006, and produced net extension in the eastern part of the slide and compression in the western part as the middle part moved ~24 cm (Figure 27; Table 3). This movement was preceded by a 4-5 cm movement in December of 2002 that involved the western part of the slide moving ~1 cm more than the middle of the slide. Marker nails were placed across fresh scarps from this and the December 2002 episode and then measured after a March 21–28, 2003, movement. All nails around the slide perimeter were displaced ~2 cm (Appendix G), matching extensometer displacement (Table 3). Nails across an interior scarp had no relative movement (Appendix G), so the slide moved en masse during the March event.

Resurveying in April 2003 of steel stakes placed on the slide in fall 2002 (Appendix E) revealed that the northern part of the slide moved less than the survey measurement error. Surface displacements in the central part matched the December 2002 to March 2003 cumulative totals of 10–28 cm for the extensometers (Table 1), but 21–130 cm horizontal and 6–70 cm vertical displacement occurred in the southwestern part of the slide. Survey error was as high as 11 cm to 15 cm horizontal and 1 to 130 cm vertical, so no firm conclusions can be drawn. Nevertheless, the general finding of more movement to the south matched the greater highway damage there (Figure 24).

All displacements after the big 2003 storm event were ≤ 4 cm and produced only small differential movement between the extensometers (Table 3). Movements between 2 and 4 cm appear to have the same general pattern as large 2003 movement, the middle borehole, LT-2, moving somewhat faster than the other two, the west borehole moving faster than the east one (Table 3).

Movement direction estimated from the resurvey data, marker nails, and inclinometers is generally down the axis of the slide away from headscarps. Directions were southwest in the northeast part of the slide, west in the central part, and west-northwest in the southeast corner of the slide (Figure 4).

The slide plane in the drilling transect appears to follow siltstone beds in the Astoria Formation, crossing the bedding dip at low angles but staying above competent sandstone beds (Figure 7). The slide must curve upward to meet its outcrop at the beach and flatten somewhat at the mouth of Johnson Creek where it has a near-zero measured dip (Figure 60). Back rotation on the toe block is further evidence of upward curving geometry. Astoria Formation in the headwall of the slide dips ~17˚ W, but the same rocks in the toe block dip at angles of 16˚–42˚ E, hence rotation was 33–59˚. Numerous small listric displacements occur in the outer part of the toe block, so rotation probably decreases rapidly toward the back (east side) of the block. Johnson Creek creates a cross section exposure at the south end of the block revealing rapid change of dip from east inclination to west over distance of only 20 m (Figure 60). The structure contour map (Figure 9) summarizes the probable geometry of the slide based on available inclinometer and outcrop data.

GROUNDWATER AND PRECIPITATION

Recharge and Discharge

Water enters the slide mainly from rainfall. Groundwater is discharged as subsurface flow into beach sediment or as seeps and springs observed at the surface during the wet season.

There are perennial creeks on the northern and southern margins of the slide but only the northern creek, Minor Creek, flows in significant slide material (Figure 2). Groundwater may be exchanged with Minor Creek in or out of the slide, depending on local hydraulic gradients. Johnson Creek on the south margin flows through a concrete conduit where it intersects the head of the slide. The mouth of the creek flows on bedrock underlying the slide, although large discharge events may make intermittent contact with the toe of the slide.

Flow Patterns

The vertical piezometer arrays at the middle and west observation sites provided detailed measurements of hydraulic gradient. A flow net cross section illustrates

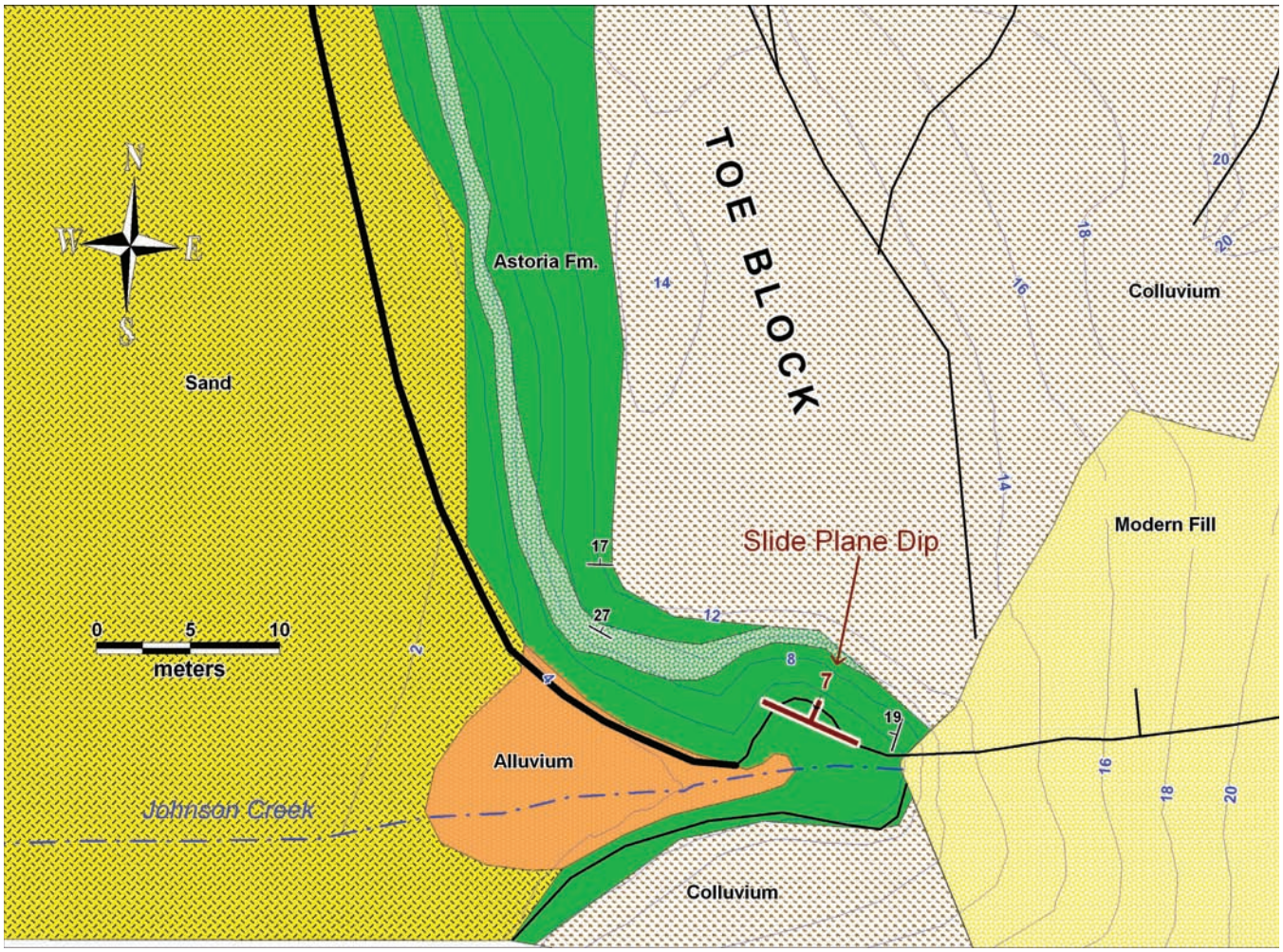

Figure 60. Detailed geologic map of the southwest end of the Johnson Creek landslide. Blue numbers are elevations in meters above geodetic mean sea level (NAVD 1988); black numbers are bedding dip in Astoria Formation. Black lines are slide scarps. Note the prominent sandstone marker bed (light green unit).

the west sloping piezometric surface, low hydraulic gradient, and flow directions roughly parallel to the slide plane (Figure 43; Ellis and others, 2007b). The low hydraulic gradient is consistent with high effective hydraulic conductivity within the slide mass (Ellis and others, 2007b). The steeper slope of the piezometric surface toward the toe of the slide could be from better drainage of the lower part. Astoria Formation and the Pleistocene marine terrace are offset ~2 m down to the east between the west and middle observation sites (Figure 7), so this structure may create a barrier to lateral flow or pressure transmission. West inclination of the piezometric surface between the LT-3 and LT-2 sites is lower than the west dip of the basal shear zone, so head above the slide plane rises rapidly from the LT-3 to the LT-2 site (Figure 43). Head above the slide plane is highest at LT-2 at all times of the year, contributing the main driving force for the landslide (Landslide Technology, 2004; Ellis and others, 2007a, 2007b).

Total head measured 6.3 m below the base of the basal shear zone in Astoria Formation was ~5 m lower than total head immediately above the slide plane (Figure 44) and may indicate some limited downward flow below the slide. Data could be gathered from the piezometer below the slide for only 24 days before it was severed by the December 2002 slide movement, so it is difficult to draw firm conclusions. It may be possible that with greater elapsed time after a major, prolonged period of rainfall that the pore pressures beneath the

slide increase due to the lag in rise of phreatic surface beneath the slide plane. This could be in response to deeper recharge and change in the local hydraulic gradient following the storms. There was no significant hydraulic gradient between the slide and piezometers installed in 2006 below the base of the basal shear zone (Ellis and others, 2007b; Figure 42), but these were only 0.35 m below the base of the shear zone at the western (LT-1a) borehole and 0.52 m below at the middle (LT-2a) borehole (Table 1). According to well records from the Oregon Department of Water Resources, two wells within the landslide at its northern end yielded ~ 45–64 lpm (12–17 gpm) below a static water level of ~9 m (28–30 ft) depth (in Astoria Formation), while a well ~200 m south of the landslide in Astoria Formation bedrock yielded of 2 lpm (0.5 gpm) below the static water level of 14.6 m (48 ft) depth. These data and previously discussed lower fracture density below the slide are suggestive of lower hydraulic conductivity and permeability, but there is not enough quantitative information to draw firm conclusions.

Response to Rainfall

Correlation of pressure rise to small rainfall events is progressively more difficult from piezometers further down the axis of the slide. Whereas every fluctuation in rainfall is obvious in the pressure data at the LT-3 site (Figure 45), the response is more muted at the LT-2 site and even more subdued at the LT-1 site (Figures 46 and 47).

The rapid rise in head at the headwall graben in response to rainfall events is transmitted laterally down the slide axis at varying speeds in different rainfall events (Ellis and others, 2007a). Ellis and others (2007a) gave two examples: A September 2005 rainfall event caused pressure rise at the LT-3 site 16 hours after start of rain, at the LT-2 site after 84 hours, and at the LT-1 site after 90 hours. A mid-December storm produced pressure rise at LT-3 three hours after rain began, after 31 hours at LT-2, and after 79 hours at the LT-1 site. Two additional examples are the beginning of two of the largest rainfall events in the observation period, January 29, 2003, and January 5, 2006. Pressure rose 1 hour after rainfall in both of the January events at LT-3p, but response in the LT-2p and LT-1p sites was completely different. In January 2003 the western (LT-1p) site responded in only 10 hours while the middle (LT-2p) site responded 15 hours after rainfall (Figure 61). In 2006, the western site responded 37 after the rain while the middle site responded after 9 hours (Figure 62). The January 2003 rainfall caused the largest rise in head recorded during the investigation and was the only time that the rise in pressure at the LT-1p site rivaled response of the LT-2p site (Figure 34). Ellis and others (2007a) concluded that, "The reason for this variability in pore pressure response is not clear, but could be related in part to possible increases in hydraulic conductivity with increased ground saturation in the winter months. Landslide movements could also alter the pore pressure response by causing changes in hydraulic conductivity along the basal slip plane and/or in fractures from the surface. Such changes in timing of pore pressure increases could have implications for the use of rainfall thresholds as predictors of possible movement on such landslides because they suggest that antecedent conditions can significantly affect the timing of pore-pressure response." We agree with this assessment. Extended dry periods appear to correlate with slower pore pressure response at the head of the slide.

For the February 2007 rainfall events the vertical arrays of piezometers in grouted boreholes allowed detailed calculation of the vertical infiltration and rate of lateral translation of the "front" of pore pressure rise from the headscarp to the toe of the slide mass. The front of pore pressure rise moved laterally at a rate of 1.4–2.5 m/hr in the upper part of the slide (between sites LT-3 and LT-2), and varied from 3.5 m/hr to a very high rate (i.e., pore pressure increases measured almost instantaneously) in the middle part of the slide between monitoring sites LT-2 and LT-1. Because vertical infiltration is 50 mm/hr (Figure 56), water takes ~40–360 hours to infiltrate to the saturated zone ~2–18 m below the three monitoring sites (Figure 53). Pressure pulses take 1.5–50 hours to travel the 2–90 m from the headwall graben to the three sites (Figures 50–53); hence, pressure pulses always arrive at the monitoring sites before water can infiltrate through the unsaturated zone. The initial rise in pore water pressure from a rainfall event is transmitted somewhat more quickly down the basal shear zone but by the time half of the peak response has occurred, pressure arrives at about the same time at all depths in the saturated zone (Figures 50 and 53). The higher speed of transmission between LT-2 and LT-1 relative to LT-2 and LT-3 may be caused by higher effective hydraulic conductivity in the western part of

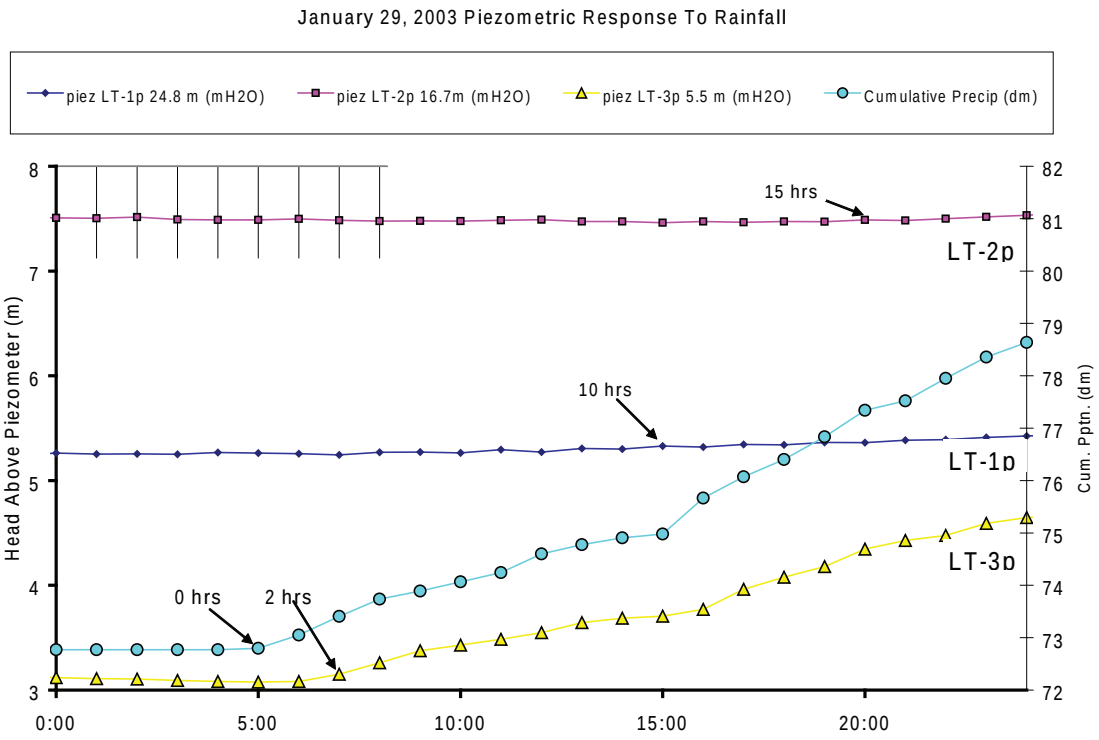

Figure 61. Piezometric response to rainfall from the January 29, 2003, rainfall event that triggered the largest increase in piezometric head during the observation period; vertical lines are 1-hr intervals.

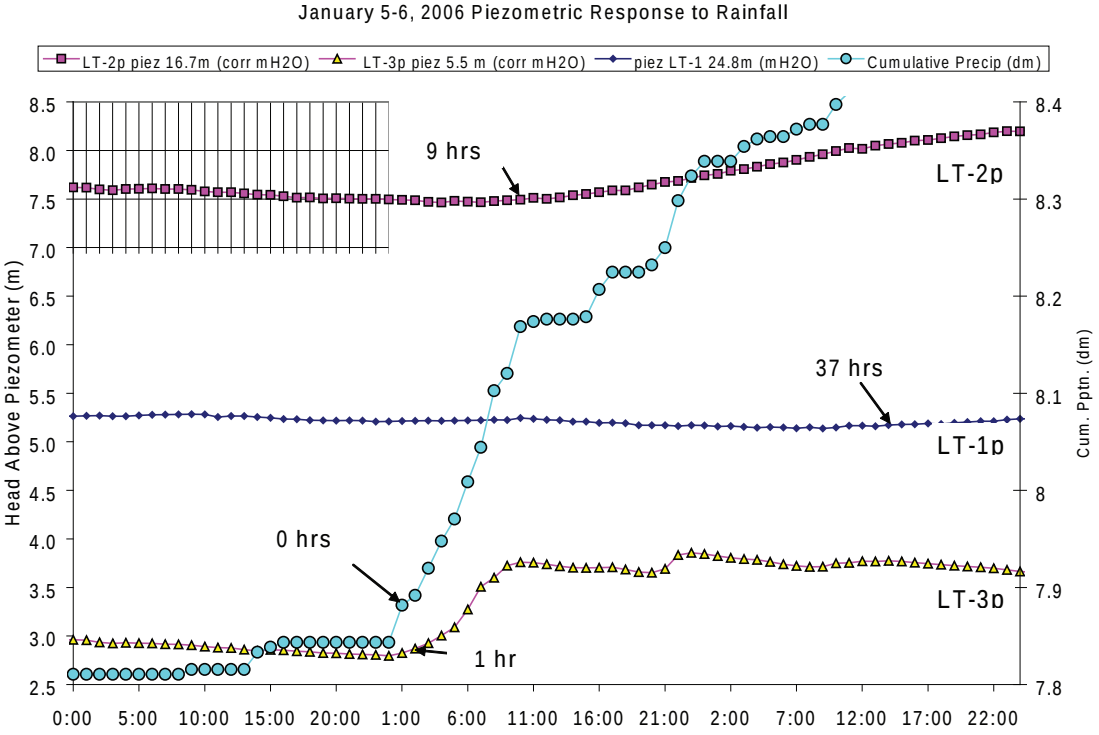

Figure 62. Piezometric response to rainfall from the January 5, 2006, rainfall event that triggered the second largest increase in piezometric head during the observation period; vertical lines are 1-hr intervals.

the slide. Perhaps better groundwater drainage through a more highly fractured rock in the western part of the slide keeps the piezometric surface lower there as well.

TRIGGERING MECHANISMS

Rainfall Thresholds

There is general correlation between slide movement, annual precipitation, antecedent precipitation before each event, and rainfall intensity (Figure 63; Table 7). The largest movement on January 31, 2002, to February 3, 2003, was preceded by 62 hours of precipitation at 2.1 mm/hr after antecedent rain since July 1 of 0.927 m; 0.84 m of this rain was concentrated in the previous two months (Figure 63). None of the later movement events were more than 17 percent of this large movement even though intensities and durations of associated rain events were in many cases similar (Figure 64). The maximum 60-day cumulative rainfall for all other slide movements was 0.64 m; this rainfall occurred prior to the second largest displacement, January 27, 2006 (Figure 64). Variation in 60-day cumulative rain prior to each movement event resembles variation in total movement per event, but there are many differences (Figure 64). Both large amounts of antecedent rain and a burst of intense rainfall appear to be necessary to trigger movements that can displace the slide tens of centimeters in less than three days.

Groundwater Pore Pressure Thresholds

Thresholds for the entire data set. Threshold head above the slide plane for start and stop of movement are compiled in Table 8; only data from LT-1p, LT-2p, and LT-3p piezometers are used (1) because they were installed for the entire observation period and (2) to eliminate any previously discussed differences between data from grouted and sand-packed instruments. Head is referenced to the base of the basal shear zone. Appendix L contains all of the charts used to compile Table 8. Figures 65 and 66 illustrate the correlation of head above the piezometers with movement during the five winters of observation. For eight small movements recorded after detailed, hourly movement data became available, threshold head above the slide plane for start and stop of movement at the LT-1p, LT-2p, and LT-3p were ~ 6.4 ± 0.2 m, 9.1 ± 0.6 m, and 3.4 ± 0.5 m, respectively, equivalent to 5.0 m, 7.4 m, and 3.2 m head above piezometer tips (Table 8; Figure 65). Standard deviation from mean values increases from the west to the east site, ~4 percent for LT-1p data, ~8 percent for LT-2p data, and ~16 percent for LT-3p data (Figure 46; Table 8). This variance is probably related to antecedent conditions such as degree of saturation of the slide mass from rainfall events and forces within the slide created by differential movement of neighboring blocks (Ellis and others, 2007a, 2007b).

Detailed observations of three movement events. Three examples demonstrate the complex behavior of the slide; Table 7 summarizes key attributes of all movement events, including these three. The base of the basal shear zone is the reference for hydraulic head in the following descriptions.

December 2002 to February 2003 (Figure 67). This movement occurred in two episodes (December 13 to 31, 2002, and January 31 to February 3, 2003; Table 7) and was in response to the largest displacement and head rise during the observation period. Rain fell at a mean rate of 1.6 mm/hr for 46 hours between December 14 and 16, 2002. Movement started sometime between the December 13 and 16 measurements, reaching by December 23, 5 cm at the west site, 4 cm at the middle site and 3 cm at the east site. The larger displacement at the west site relative to the middle and east sites was the pattern in inclinometer data before conversion to the less precise extensometers (Figure 26), so it is not simply a function of the ±1 cm error in extensometer measurement. This movement created relative extension between the middle and western boreholes. Mean rates of movement were 0.15 mm/hr, 0.12 mm/hr, and 0.1 mm/hr at the west, middle and east sites, respectively. Shear zone depths determined from this movement informed installation of piezometers at each site. Rain continued at a mean rate of 0.9 mm/hr through January 4, 2003. Rain was intermittent over the next several days, then no rain fell from 9:00 AM January 26 to 5:00 AM, January 29. Intense rain started at 6:00 AM and by 7:00 AM, January 29, pressure at the LT-3p piezometer began to rise sharply (Figure 61). Total rainfall over the next 62 hours was 0.13 m (2.1 mm/hr). This intense rain coupled with the previous rain event caused a unique response in pore water pressure not repeated since. Head began to rise at the western borehole 5 hours before it did in the middle borehole. Peak head reached 2.7 m over starting pressures in the middle and west piezometers, while the east site increased 2 m. Head above the base of the basal shear zone reached

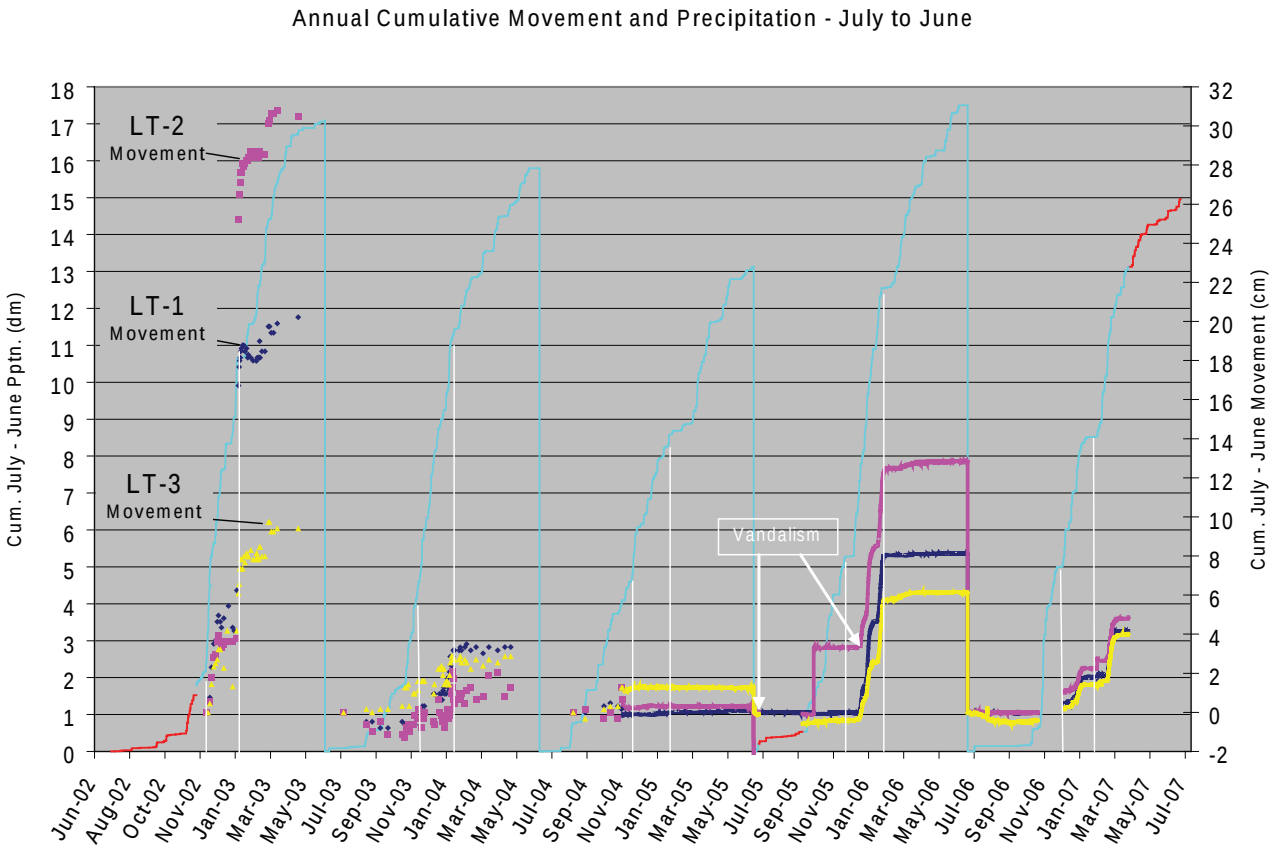

Figure 63. Annual movement and precipitation. Vertical white lines illustrate cumulative rain at December 1 and February 1 each year. Note that only in the first year is there ~1 m of rain in this interval.

the highest values recorded, 8.8, 11.4, and 4.8 m at the west, middle, and east sites, respectively. All rainfall events after this caused the west piezometer to rise no more than one third of the response at the middle site, and head generally rose in the middle borehole before the western one (Figure 65). An extensometer reading January 31 registered negligible movement but by the next reading, February 3, the middle site had moved 21 cm, the west site 13 cm, and the east site 1 cm. Over the following four days the west site moved 2 cm, the middle 3 cm, and the east 2 cm. The rate of movement at the east site extrapolated through these four days of readings projects linearly to the reading on January 31, 0.3 mm/hr. Rate of movement at the middle and west sites between the January 31 and February 3 readings was at least 6 mm/hr and 3 mm/hr, respectively. Movement was thus relatively rapid and nonlinear at the middle and west sites but constant and of an order of magnitude slower at the east site.

December 2005 to February 2006 (Figure 68). This movement occurred in three episodes and was the second largest slide movement and pore pressure rise during the five winter seasons. The second episode, January 6 to 24, 2006, had peak head values at the middle site approaching the 2003 event. The pore pressure increase was triggered by 2 days of rain at an average rate of 1.6 mm/hr. Pore water pressure increase started 1 hour after start of rain at the eastern borehole, 9 hours later at the middle borehole, and 37 hours later at the western site (Figure 62). Head reached a maximum of 7.0, 10.9, and 4.5 m at the west, middle, and east sites, respectively. Total movement occurred in three episodes over ~40 days and was 8, 9, and 6 cm at the west, middle, and east sites, respectively. The

Table 7. Summary of rainfall intensity, movement, movement velocity, and maximum head above the base of the basal shear zone for all movement events at all monitoring sites.

	Episode													
	Dec. 13–31, 2002	**Jan. 31-Feb. 3, 2003**	**Mar. 21–28, 2003**	**Nov. 15-Mar. 4, 2004**	**Nov. 11–18, 2004**	**Dec. 27-Jan. 4, 2006**	**Jan. 6–24, 2006**	**Jan. 27-Feb. 10, 2006**	**Nov. 6–15, 2006**	**Dec. 24–28, 2006**	**Jan. 2–11-2007**	**Feb. 15–16, 2007**	**Feb. 25-Mar. 9, 2007**	**Mar. 12–15, 2007**
Pptn. prior 60 days (dm)	3.2	6.4	2.3	5.7	-1.7	3.4	4.3	4.0	3.2	6.4	2.3	5.7	-1.7	3.4
Start cum. pptn. (mm)	342.00	927.00	1342.00	188.70	376.60	700.00	887	1108.00	70.60	644.00	713.00	905.00	1031.30	1222.5
Stop cum. pptn. (mm)	490.00	1057.40	1414.00	1092.00	394.00	732.00	963	1231.39	301.75	669	764	973.00	1104.00	1235.0
Pptn. (mm)	74.44	130.40	72.00	903.30	17.40	32.00	76.00	123.39	231.15	25.00	51.00	68.00	72.70	12.5
Date and time start	12/14/ 2002 3:00	1/29/ 2003 15:00	3/21/ 2003 3:00	11/15/ 2003 6:00	11/12/ 2004 20:00	12/27/ 2005 20:00	1/9/ 2006 4:00	1/26/ 2006 0:00	11/1/ 2006 20:45	12/24/ 2006 17:30	1/2/ 2007 16:00	2/14/ 2007 19:45	2/24/ 2007 0:30	3/12/ 2007 4:45
Date and time stop	12/16/ 2002 1:00	2/1/ 2003 5:00	3/22/ 2003 12:00	1/30/ 2004 1:00	11/16/ 2004 10:00	12/28/ 2005 11:00	1/10/ 2006 23:00	2/1/ 2006 7:00	11/7/ 2006 20:30	12/25/ 2006 11:00	1/3/ 2007 21:15	2/16/ 2007 16:45	2/25/ 2007 17:30	3/12/ 2007 15:00
Duration (hrs)	46.0	62.0	33.0	1819.0	86.0	15.0	43.0	151.0	143.7	17.5	29.3	45.0	41.0	10.3
Intensity (mm/hr)	1.6	2.1	2.2	0.5	0.2	2.1	1.8	0.8	1.6	1.4	1.7	1.5	1.8	1.2
Max. head LT-1p (m)	nd	8.805	6.73	6.961	5.767	6.7	7	6.7	nd	6.69	6.8	6.0	6.9	6.5
Max. head LT-1a (m)	nd	nd	nd	nd	nd	nd	nd	nd	nd	nd	7.14	7.1	8.2	7.8
Max. head LT-2p (m)	nd	11.4163	9.8	10.5769	7.1	9.6	10.933	9.88	10.19	9.4	9.57	8.5	10.1	8.9
Max. head LT-2a (m)	nd	nd	nd	nd	nd	nd	nd	nd	nd	nd	10.56	10.0	11.2	10.5
Max. head LT-3p (m)	nd	4.8	4.4	4.7	2.1	4.0	4.4	4.1	4.7	3.9	3.939	4.2	4.3	3.5
LT-1 movement (mm)	49.6	138.2	20	40	0	14	33	33.9	6	2.54	10.57	0	22	0
Date and time start	12/16/ 2002 12:00	1/31/ 2003 12:00	3/22/ 2003 8:00	12/14/ 2003 7:00	—	12/27/ 2005 23:00	1/6/ 2006 1:00	1/29/ 2006 4:00	11/8/ 2006 8:45	12/24/ 2006 0:00	1/3/ 2007 1:15	—	2/25/ 2007 4:15	—
Date and time stop	12/23/ 2002 12:00	2/3/ 2003 12:00	3/29/ 2003 3:00	2/4/ 2004 17:00	—	1/4/ 2006 16:00	1/15/ 2006 23:00	2/6/ 2006 19:00	11/15/ 2006 15:30	12/29/ 2006 18:45	1/10/ 2007 16:00	—	3/5/ 2007 17:00	—
Duration (hrs)	168.0	117.0	163.0	1258.0	—	185.0	238.0	207.0	174.8	138.8	182.7	—	204.8	—
Slide velocity @ 90% movement (mm/hr)	0.27	1.06	0.11	0.03	—	0.07	0.12	0.15	0.03	0.02	0.05	—	0.10	—
LT-2 movement (mm)	39.4	241.4	20	20	0	14	35.46	39.88	11	1.75	9.94	0	22	0
Date and time start	12/16/ 2002 12:00	1/31/ 2003 12:00	3/22/ 2003 8:00	12/14/ 2003 7:00	—	12/27/ 2005 23:00	1/6/ 2006 1:00	1/29/ 2006 4:00	11/7/ 2006 8:15	12/24/ 2006 0:00	1/3/ 2007 1:15	—	2/26/ 2007 3:45	—
Date and time stop	12/23/ 2002 12:00	2/3/ 2003 12:00	3/29/ 2003 3:00	2/4/ 2004 17:00	—	1/4/ 2006 16:00	1/15/ 2006 23:00	2/6/ 2006 19:00	11/14/ 2006 11:45	12/28/ 2006 22:30	1/10/ 2007 16:00	—	3/5/ 2007 17:00	—
Duration (hrs)	168	72	163	1258	—	185	238	207	172	119	183	—	181	—
Slide velocity @ 90% movement (mm/hr)	0.21	3.02	0.11	0.01	—	0.07	0.13	0.17	0.06	0.01	0.05	—	0.11	—
LT-3 movement (mm)	32.3	46.1	20.0	30.0	16.0	10.0	18.3	31.9	6.0	3.3	8.9	2.0	22.0	1.0
Date and time start	12/16/ 2002 12:00	1/31/ 2003 12:00	3/22/ 2003 8:00	12/14/ 2003 7:00	11/11/ 2004 13:00	12/27/ 2005 23:00	1/6/ 2006 1:00	1/29/ 2006 4:00	11/4/ 2006 21:00	12/24/ 2006 0:00	1/3/ 2007 1:15	2/14/ 2007 14:15	2/24/ 2007 14:00	3/12/ 2007 10:00
Date and time stop	12/23/ 2002 12:00	2/5/ 2003 9:00	3/29/ 2003 3:00	2/4/ 2004 17:00	11/17/ 2004 18:00	1/4/ 2006 16:00	1/15/ 2006 23:00	2/6/ 2006 19:00	11/14/ 2006 11:45	12/27/ 2006 10:00	1/10/ 2007 16:00	2/16/ 2007 13:15	3/5/ 2007 17:00	3/14/ 2007 12:00
Duration (hrs)	168	117	163	1258	149	185	238	207	231	82	183	47	219	50
Slide velocity @ 90% movement (mm/hr)	0.17	0.35	0.11	0.02	0.10	0.05	0.07	0.14	0.02	0.04	0.04	0.04	0.09	0.02

Pptn. is precipitation; cum. is cumulative; max. is maximum; nd is no data (no sensor recording); dash means no (0 mm) movement. LT-1, LT-2, and LT-3 are boreholes.

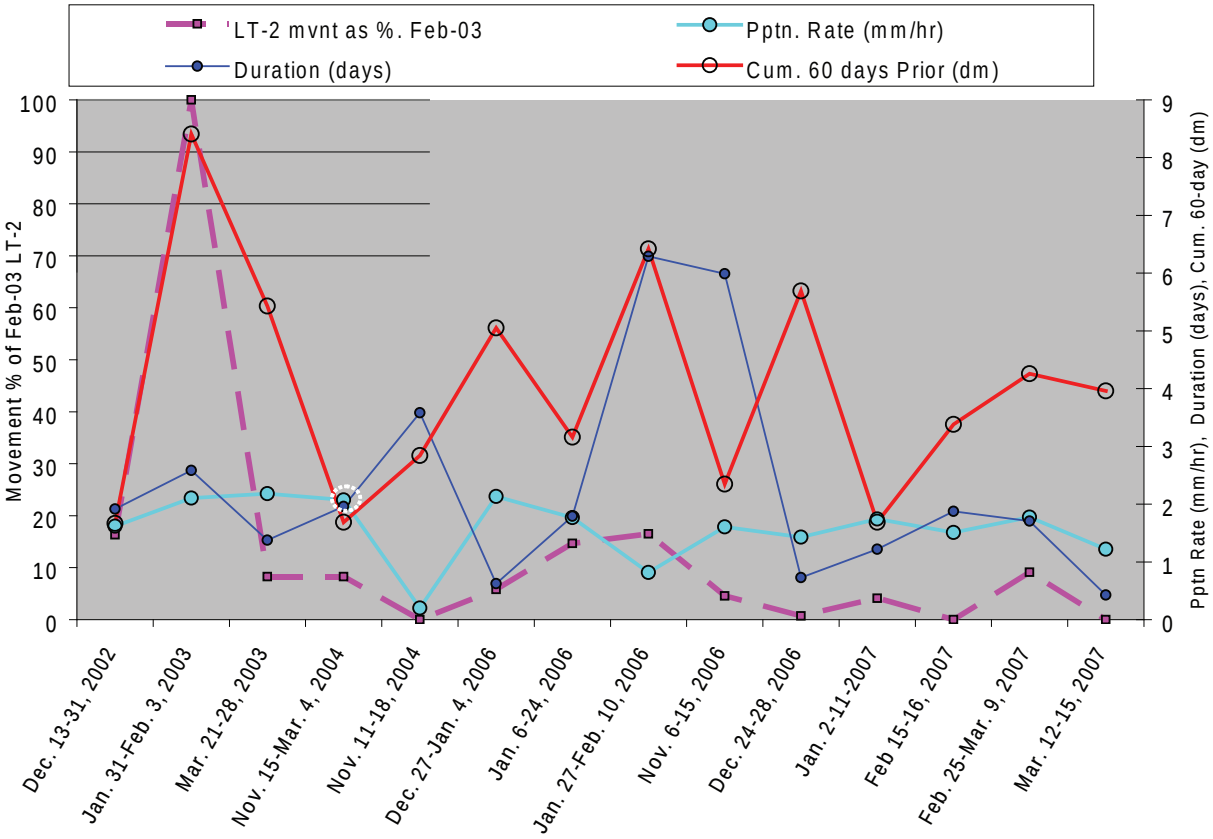

Figure 64. Movement as a percent of the largest movement versus duration and rate of intense precipitation that triggered movements. Dotted circle highlights the November 15, 2003, to March 4, 2004, rainfall data because the plotted data do not match rainfall data for this event in Table 7. The plotted data point shows the most intense rainfall episode within a series of small events that created the November 15 to March 4 movement. Table 7 lists rate and duration of rainfall for the entire November 15 to March 4 interval instead of the most intense episode. Movement data for November 15 to March 4 were too imprecise to separate small movement episodes that probably occurred in response to many rainfall events.

highest rates of movement occurred when head at the middle site reached 10.2–10.9 m January 10 to 12 and 9.4–9.8 m January 31 to February 2. In both instances the middle site accelerated to a 0.24–0.27 mm/hr, outpacing the other two sites in each case. The middle site and west sites started and stopped movement in a very narrow range of threshold pressure compared to the east site. The east site at times started movement during falling pressure or stopped movement during rising pressure. The east site appeared to be reacting to other factors than local pore pressure, perhaps interaction with the middle block. When pore pressures fell below threshold values, movement stopped February 7 at the east site, February 9 at the middle site, and February 10 at the west site. Throughout the series of movements, rise of head from rainfall events at the west site were small, ~20–25 percent of the change at the middle and east sites.

February to March 2007 (Figure 69). Only a few centimeters of movement occurred at the three sites between February 14 and March 23, 2007. This episode is good example of small (<4 cm) movements that affect the slide, but it is also unique in that the east site moved somewhat more than the other two. There were two episodes of movement in response to two intense rainfall events, February 14 to 16 for 48 hours at 1.6 mm/hr and February 23 to 25 for ~43 hours at 2.1 mm/hr. The first rainstorm caused movement only at the east site, the second at all three sites.

East site: Within an hour and half of rain starting, pressure began to rise at the east site, rising 1.8 m in 24 hours. At about 1 m of rise in head (3 m above the slide plane) the east site began to move. It continued moving through a peak in head of 4.2 m and then stopped when head decreased to 4 m. Movement stopped for the next few days as head fluctuated between 3 and 3.6 m at

Table 8. Threshold head above the base of the basal shear zone for movement at the west (LT-1), middle (LT-2), and east (LT-3) sites from sand-packed piezometers in the LT-1p, LT-2p, and LT-3p boreholes.

	LT-1p		LT-2p		LT-3p	
Episode	Start Pressure Head (m)	Stop Pressure Head (m)	Start Pressure Head (m)	Stop Pressure Head (m)	Start Pressure Head (m)	Stop Pressure Head (m)
December 2002	no data	no data	no data	no data	no data	no data
January to February 2003	>5.7; <6.8	>6.1; <6.4	>10.1; <11	>8.5; <9.2	>4.8; <5.0	>3.2; <3.4
March 2003	>6.0; <6.4	6.4	>8.2; <9.4	>8.7; <9.4	>2.9 ; <4.4	>3.3: <4.4
November 2003 to March 2004	>5.2; <6.3	>6.9; <7.1	>6.8; <8.7	>9.5; <10.6	>2.8; <3.7	>3.9; <4.5
November 2004	no data	no data	no data	no data	>1.9; <2.1	2.1
December 2005	**6.1**	**6.3**	**8.1**	**9.0**	**3.9**	**3.3**
January 2006	**6.3**	**6.5**	**9.0**	**8.7**	**3.3**	**3.9**
February 2006	**6.1**	**6.1**	**8.6**	**8.5**	**3.4**	**2.9**
November 2006	**5.9**	**6.2**	**8.1**	**8.6**	**3.1**	**3.1**
January 2007	**5.9**	**6.3**	**9.0**	**8.6**	**3.6**	**2.9**
February 2007	no data	no data	no data	no data	**3.5**	**4.1**
March 2007	**6.1**	**6.35**	**9.5**	**8.6**	**3.9**	**3**
March 2007 creep	no data	no data	no data	no data	**3.5**	**3**
Mean hourly data	**6.1**	**6.3**	**8.7**	**8.7**	**3.5**	**3.3**
Standard deviation hourly data	**0.2**	**0.1**	**0.6**	**0.2**	**0.3**	**0.5**
Mean start and stop	**6.2**		**8.7**		**3.4**	
Range	**0.4**	**0.4**	**1.4**	**0.5**	**0.8**	**1.2**

Bold numbers are from hourly movement data; other numbers are from movement data collected by hand at intervals of one or more days.

the east site, but movement started again when head reached 3.7 m. The east site stopped movement when head was at 3.3 m but moved immediately before that when head was only 3 m. The east site had one more small movement when head rose to 3.5 m. Total movement was 2.6 cm. Maximum velocity of movement was 0.15 mm/hr, but velocity varied little.

West and middle sites: Peak head above the slide plane was below threshold for movement at the middle and west sites during the first movement at the east site, remaining at or below 8.8 m and 6.5 m, respectively. A day after the east site started its second episode of movement, the west site began moving, followed within a few hours by the middle site. The middle site did not start movement until head was at nearly the peak for the entire episode, 10 m above the basal shear zone. Movement continued at the middle site until pressure fell to 9 m. Movement at the west site occurred between ~6.6 and 7 m head above the slide. The west site started movement when the sand-packed piezometer was experiencing falling pressure, but the grouted piezometer at the same elevation registered rising pressure. It was earlier noted that pressure changes arrive at different times at the two types of installations, so this may be evidence that the grouted piezometers are registering more reliable pressure changes. The sand-packed piezometer registered 6.4 m when movement started and 6.7 m when it stopped; the grouted piezometer at the west site registered ~7.9 m at both the start and stop. The narrower range of threshold values for the grouted piezometer also suggests better quality data. The middle site moved 2 cm and the west site 2.2 cm at the end of this event. Maximum velocity at both sites was ~0.4 mm/hr and was reached when the middle site had head above the slide of 9.8–10.1 m; the west site, 6.3–6.8 m. Below these pressures, the two sites moved at similar speed to the east site.

Head response comparisons. Figures 70 and 71 illustrate how the head response in 2006 and 2007 compares to the 2003 event temporally and spatially across the landslide. Head response is calculated by subtracting the starting (background) total head at each site at

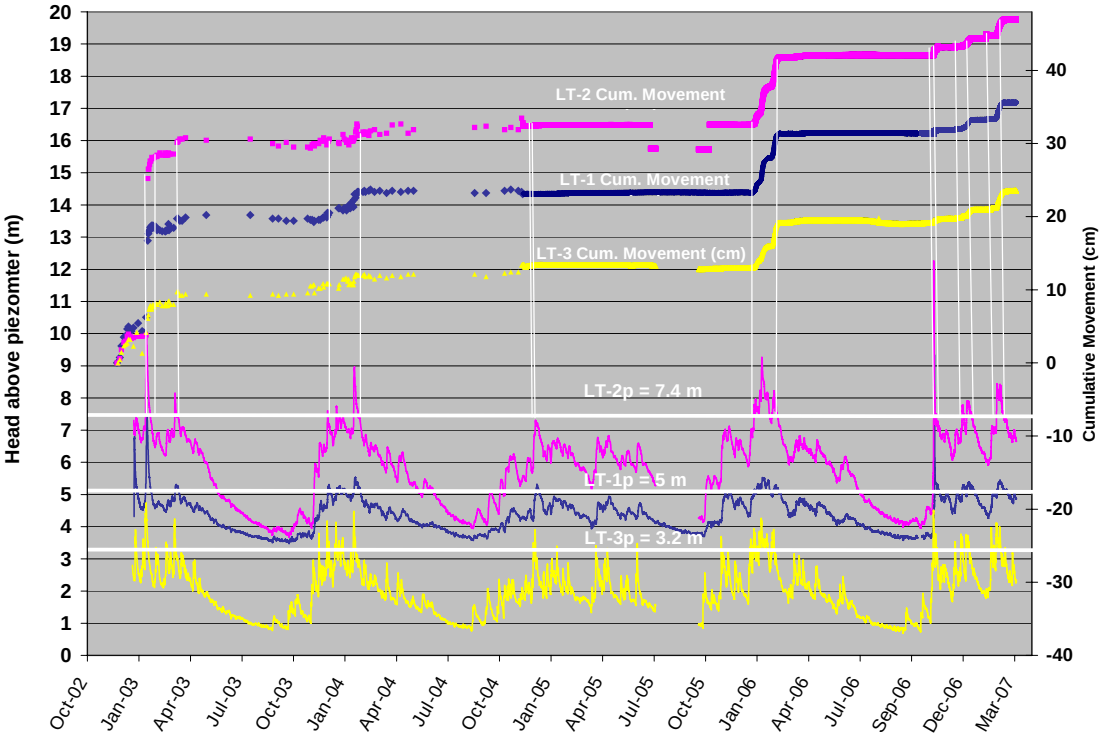

Figure 65. Summary of threshold piezometric pressure above piezometer tips for movement. Vertical white lines mark movement episodes.

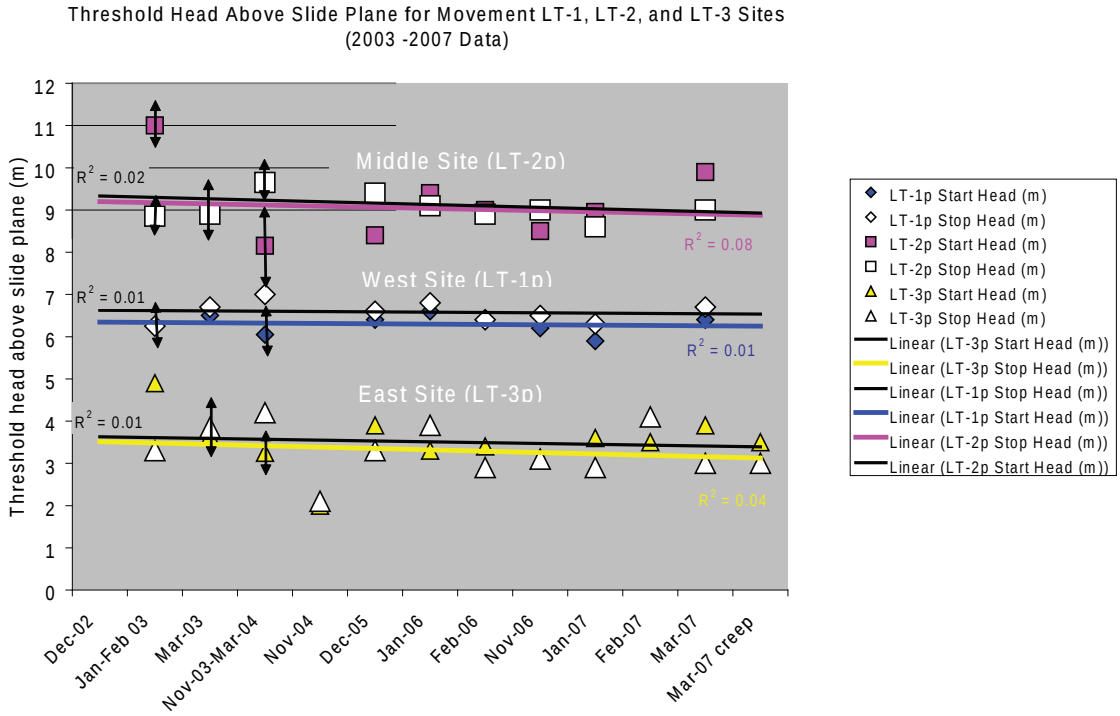

Figure 66. Variance of threshold pressure head for start and stop of movement for all movement events. Arrows indicate uncertainty introduced because of large (1–4 day) sampling intervals and ±1 cm precision of extensometer data before automated recording of movement was available. Sizes of symbols without arrows are roughly proportional to uncertainty.

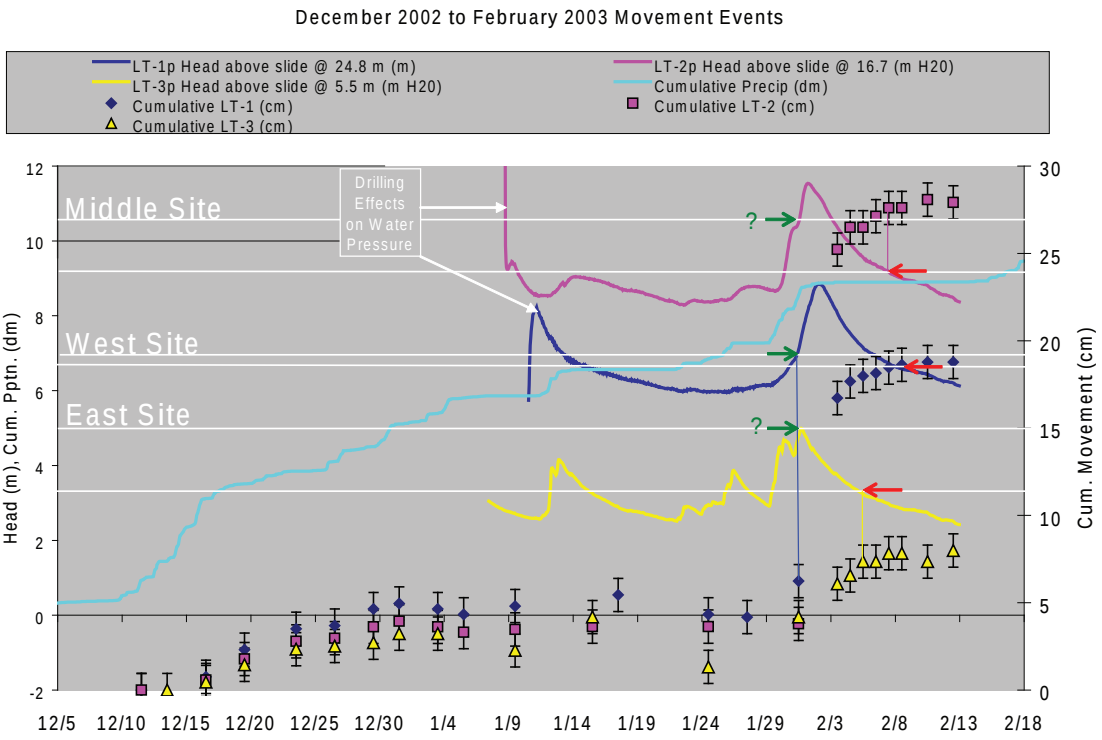

Figure 67. Correlation of movement to head above the base of the basal shear zone for a December 2002 to February 2003 movement. The February event was the largest single movement during the five years of observation. Colored arrows and lines mark head at stop or start of movement: Green arrow = start; red arrow = stop; white lines = range of threshold pressure. Data are for sand-packed piezometers in the basal shear zone. Only manually measured extensometer data were available during these observations.

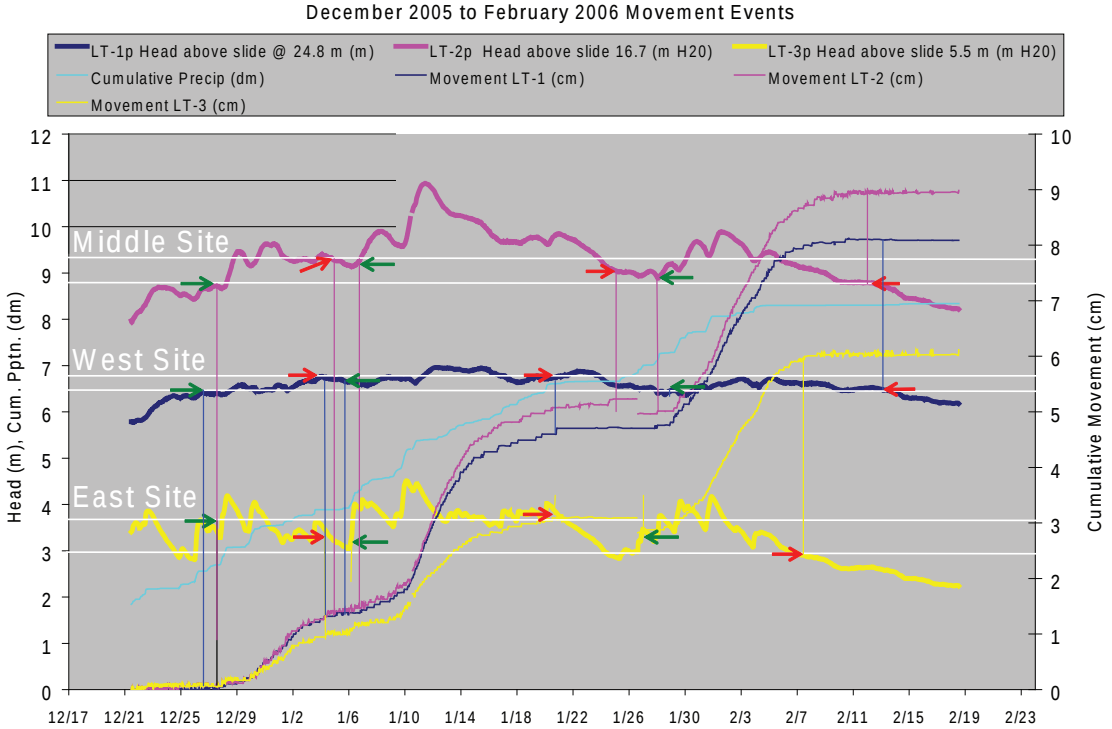

Figure 68. Correlation of movement to head above the base of the basal shear zone for a December 2005 to February 2006 movement. Colored arrows and lines mark head at stop or start of movement: Green arrow = start; red arrow = stop; white lines = range of threshold pressure. Data are for sand-packed piezometers in the basal shear zone. Extensometer data from automated data retrieval were available during these observations.

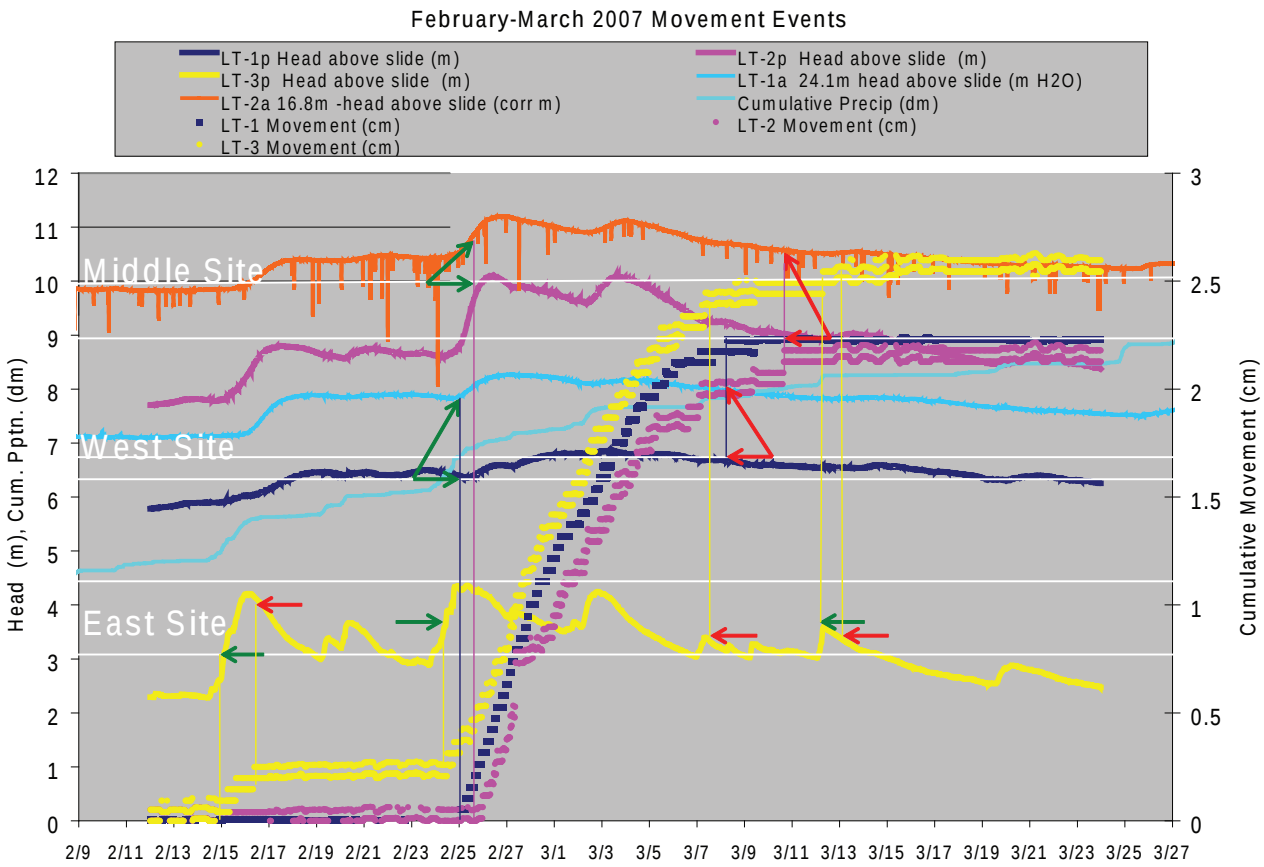

Figure 69. Correlation of movement to head above the base of the basal shear zone for a February to March, 2007, small creeping movement. Colored arrows and lines mark head at stop or start of movement: Green arrow = start; red arrow = stop; white lines = range of threshold pressure for sand-packed piezometers (angled red and green arrows point to equivalent data from grouted piezometers). Data are for sand-packed (LT-1p, LT-2p, and LT-3p) and grouted (LT-1a and LT-2a) piezometers in the basal shear zone. Extensometer data from automated data retrieval were available during these observations; the small vertical scale reveals the 0.05-cm oscillations in the data.

the start of the January 2007 movement, the minimum value for all of the comparative data. This effectively takes out the westward slope of the piezometric surface. For the 2006 sequence of three movements, only the second episode (January 6 to 24, 2006) is plotted, as it has the highest head values and shows an acceleration of the middle site (Figure 68). The 2003 event is unique in several ways but also shows some similarities to later events:

- Peak head in 2003 far exceeded the two later events.
- In 2003 movement began to slow when head at the middle site decreased 0.5 m from its peak, even though the west site had just reached its peak value for the observation period (orange line on the figures). Hence, pore water pressure at the west site was apparently not as important in controlling the end of movement as at the middle site.
- In contrast to large variation in head at the west site in 2003, head at the west site in 2006 and 2007 stayed within a narrower range. This is true in general for the entire observation period after 2003 (Figure 65).
- In 2006, larger movement at the middle site relative to the west site appears to be from increased speed of the middle site in response to the large head increase rather than decreased speed at the west site. In 2003, the speed of movement was faster at the middle site relative to the western site even though head increase was about the same at both.

- Starting (background) head was higher for the 2003 event than for the small creeping event in 2007 but similar to the moderate 2006 event.
- In January 2003 head rose earlier at the west site than the middle site; head rose first at the middle site in the 2006 and 2007 events.
- Head at cessation of movement was higher in the 2003 event at the west and middle sites but lower at the east site compared to the 2006 event. By 2007, the east site ceased moving at a lower head than in 2003.
- Threshold head at start and cessation of movement was larger at the middle site in 2007 than in 2006; the opposite is true for the west site
- At the east and middle sites, threshold for start of movement in 2003 was substantially higher than needed to start movement in the two later events (brown line in Figures 70 and 71). In 2003, the west site showed a small amount of movement at a head higher than the two later events (brown line in figures), but the previous reading showed no movement and ~1 m lower head, so the threshold could be similar to the two later events within this large uncertainty.
- In all three events, the middle site started moving at a higher threshold head than it stopped.
- In all three events, the west site started at a lower threshold head than it stopped.
- In the 2006 and 2007 events, the east site started moving at a lower threshold head than it stopped; the opposite occurred in 2003.

Conclusions from the three events. These observations appear consistent with the middle (LT-2) site being a controlling factor in slide movement (Landslide Technology, 2004; Ellis and others, 2007b). Head above the slide plane is always highest there, and the slide mass at the middle site tends to move faster than at other sites, especially the east site which seems to move at a more or less constant velocity, even when the middle site accelerates. It appears that the east site reaches some threshold rate of movement ≤ 0.3 mm/hr and is essentially "left behind" by the middle site. When the east site moved on its own in February 2007, it did not trigger movement at the sites to the west. The middle site accelerated relative to the other two when head rose above 9.4 m in one instance and 10.2 m in another, but once the site started moving it generally stopped at a lower head than it started. The west site had the opposite behavior, suggesting that the middle site was pushing the west site as each pulse of pressure affected the middle site sooner. On two occasions this pattern did not hold. In the December 16 to 23, 2003, episode, 62 hours of rain at 2.1 mm/hr preceded movement at the west site. During the February 2007 movement, the west site started moving before the middle site. In fact, the threshold head for movement and acceleration of movement varied at all three sites from movement to movement even though the middle site had a somewhat more consistent pattern than the others. One caveat to this observation is the apparent lack of precision of the sand-packed piezometers relative to the grouted piezometers in specifying both timing and magnitude of head response at the base of the slide. Data for grouted piezometers are available only for the 2007 movement and appear to show much less variation in threshold head for start and stop of movement at all sites (Figure 69). As more of these data become available, some of the apparent lack of consistency of movement with head changes may go away.

There appears to be a general tendency for movement to start and stop at decreasing threshold head from 2003 to 2007, but the decrease is only ~0.7-0.8 m of head at the key middle (LT-2p) site. Precision of the 2003 movement data is ±1 cm, whereas precision of 2006 and 2007 data is ±0.05 cm. The 2006 and 2007 observations demonstrate that large changes in head can occur within a ±1 cm range of movement, so while the observations are worth noting, the data do not support any firm conclusion about a trend of decreasing head.

A remaining question is why on February 2, 2003, the west site experienced the same large rise in head as the middle site. This unique response and the attendant large movement occurred as a result of 2.6 days of rain at 2.1 mm/hr but was absent in the later movement events that responded to rain at about this intensity for two-day periods. The response did not occur when the middle site maintained a head of 10.9 m for 8 hours in 2006 but did occur when head at the middle site reached 10.9–11.4 m above the slide plane for two days. Possibilities for raising pore water pressure in the lower part of the slide are:

- Breaching of a groundwater barrier such as the fault or internal structure that offsets the geologic section down 2 m to the east.

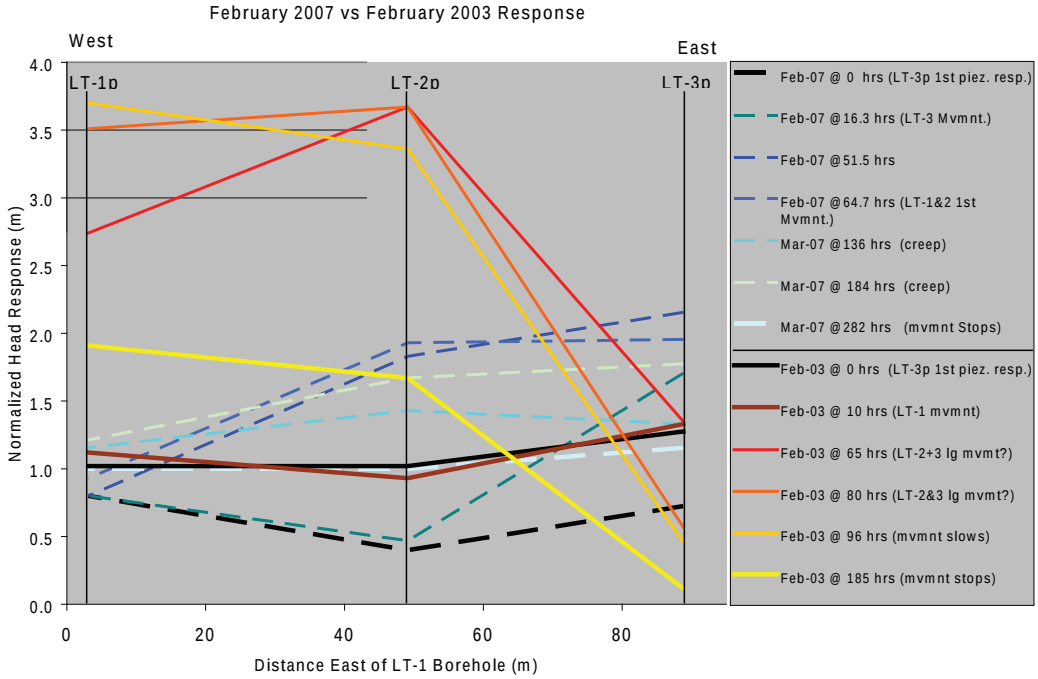

Figure 70. Comparison of piezometric head change across the landslide at sand-packed piezometers for the January 29 to February 6, 2003, large displacement to small creeping movement of February 23 to March 7, 2007. Diagram shows quantitative differences between head in the two events by normalizing to the mean piezometric gradient across the slide at the start of the two movements minus 1 meter [((starting total head 2003 + starting total head 2007)/2) – 1 meter]. Hrs = hours after first piezometric response at the LT-3p piezometer at the headwall graben; Mvmnt. = slide displacement measured at extensometers; piez. resp. = piezometric response.

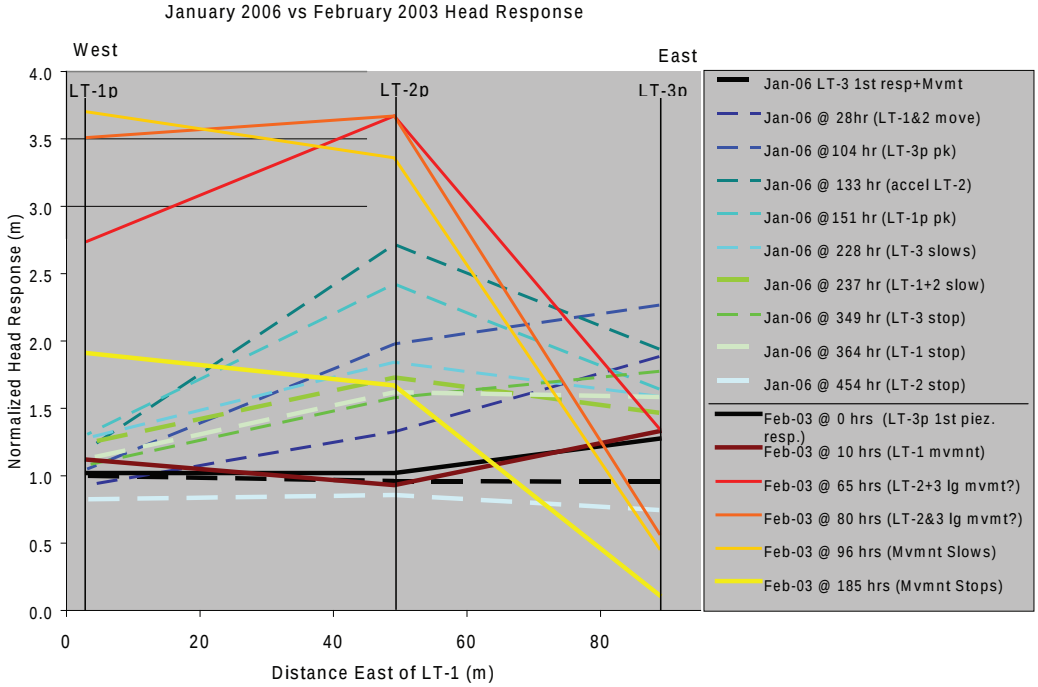

Figure 71. Comparison of piezometric head change across the landslide at sand-packed piezometers for the January 29 to February 6, 2003, large displacement to moderate slow movement of January 6 to 24, 2006. Diagram shows quantitative differences between head in the two events by normalizing to the mean piezometric gradient across the slide at the start of the two movements minus 1 meter [((starting total head 2003 + starting total head 2006)/2) – 1 meter]. Hrs = hours after first piezometric response at the LT-3p piezometer at the headwall graben; Mvmnt. = slide displacement measured at extensometers; piez. resp. = piezometric response; pk = peak piezometric head.

- Opening hydraulic conduits such as fracture systems in response to slide movement.
- Compressing the fracture system from movement at the middle site "ramming" the west site.
- Combined effect of infiltration and lateral pressure transmission. For example, the saturated zone lies ~18 m below the surface at the west site, so after 15 days of continuous rain at infiltration of 0.05 m/hr, the entire unsaturated zone is full of infiltrating water. What effect does this have on pressure response? Does continuous intense rainfall reach the saturated zone more and more quickly as time goes on?

Perhaps the 1 cm of extension created by the December 2002 movement opened up fractures, causing better pressure transmission and flow of water both vertically and horizontally between the west and middle sites. Unusually high hydraulic conductivity between the middle and west sites immediately prior to the January 2003 movement is consistent with arrival of pressure response at the western site 5 hours before the middle site.

Erosion Thresholds

Stability analysis by Landslide Technology (2004) clearly demonstrated that erosion of the slide toe could trigger movement regardless of pore water pressures. Continued wave erosion will decrease the factor of safety, so a decrease in threshold pore pressures would be expected. The slight negative slopes of the threshold data in Figure 66 are suggestive of this trend, but the uncertainty in these data is much too large to draw any conclusions. The detailed analysis of the three events above is also suggestive that erosion may be decreasing threshold pore pressures relative to the large February 2003 event, but, again, uncertainty in the data is too large to make any firm interpretation.

Preliminary erosion estimates from the ground-based lidar experiment at the Johnson Creek landslide are over too short of an interval to offer definitive estimates of erosion, but the data clearly demonstrate that both wave erosion at the base of the sea cliff and mass wasting at the top are occurring at significant rates. Erosion estimates by Priest and others (2004) for coastal bluffs in the Astoria Formation are 15–24 cm per year for the beaches around Johnson Creek and 6.1 cm for other beaches in this county. The Jumpoff Joe landslide at Nye Beach 11 km south of the study area is geologically similar to the Johnson Creek slide: It is a translational slide in seaward dipping Tertiary siltstone. In the 1940s at Jumpoff Joe, erosion through a competent sandstone buttress caused failure of a block penetrating 100 m into the coastal bluff (Priest and others, 2004). The block then eroded at ~90 cm/yr over the next 54 years (Priest and others, 2004). Assuming that (1) the range 6.1–90 cm/yr brackets possible erosion rates at the Johnson Creek slide blocks, (2) factor of safety decreases by 2.3 percent for each meter of bluff retreat (Landslide Technology, 2004), and (3) pore water pressure in the stable slide at "normal winter" pore pressure keeps the factor of safety at 2 percent above the threshold for movement (Landslide Technology, 2004), then 1–15 years of erosion at 90–6.1 cm/yr (0.9 m, 2 percent decrease of factor of safety) would bring the slide to its stability threshold for most of the winter season. Erosion for 4 to 150 years (3.9 m) would reduce the factor of safety by 9 percent, creating severe instability during the winter season ("severe storm" scenario of Landslide Technology [2004]). According to the stability analysis of Landslide Technology (2004), the latter scenario would be equivalent to an increase in head at the monitoring sites of 3.6 m for the west (LT-1p) piezometer, 3.3 m at the middle piezometer (LT-2p), and 0.8 m at the east piezometer (LT-3p). The slide currently appears to have stability similar to when the observations started within the uncertainty of the data, so is seems unlikely that the worst-case erosion scenarios have occurred during the observation period.

SLOPE STABILITY ANALYSIS

Uncertainties

Limit equilibrium slope stability analyses demonstrated that pore water pressures and erosion of the toe control stability and that either can trigger movement. The limit equilibrium back analysis of Landslide Technology (2004) assumed threshold pressures above the slide plane of 7.0 m at the west (LT-1p) piezometer, 10 m at the middle (LT-2p) piezometer, and 6.3 m at the east (LT-3p) piezometer. As previously explained, observed thresholds from five winters of observation are, 6.4 ± 0.2 m, 9.1 ± 0.6 m, and 3.4 ± 0.5 m, for LT-1p, LT-2p, and LT-3p, respectively. The modeled head is within the uncertainty of observational data for all but the eastern (LT-3p) site, which is 46 percent higher than observed. The reason for this is that the Landslide Technology (2004) site map had the piezometer site mislabeled as the inclinometer site, leading them

to assume that the piezometer was down the slide dip from the inclinometer instead of up dip. Because the inclinometer and piezometer are within a few meters of each another and the piezometric surface has a gentle inclination in the eastern part of the slide (Figure 53), the total head at the modeled position (and thus head above the slide plane) is probably very close to the value assumed. There is probably no significant error in the model from this source.

Another potential problem with the analysis is use of data from sand-packed piezometers. As previously discussed, the sand-packed piezometric head is lower and apparently less accurate than head measured from grouted piezometers. The difference is 0.9 m at LT-1p site and 0.9–1.4 m at LT-2p; these values are for peak head events like those used in the stability analysis. Observed thresholds are based on sand-packed piezometer data, so equivalent grouted data for the LT-1p site should be approximately 7.3± 0.2 m and 10–10.5 ± 0.6 for LT-2p. These values are essentially identical to those used by Landslide Technology, so there is no significant error.

Remediation Options

The stability analyses, calibrated with field monitoring and observational data, are useful tools for evaluating the effectiveness of various remedial options for this slide. The input parameters in the numerical models have been refined with the observational data to provide results that are consistent with control of slide movement by pore water pressures in the upper part. The stability analysis found that factor of safety (FOS) decreased more in the upper part of the slide than in the lower part for a given rise in pore pressure (Appendix N). The percent decrease in FOS cumulatively for each monitoring site was 21 percent from the head of the slide to piezometer LT-3p, 52 percent to piezometer LT-2p, and 73 percent to piezometer LT-1p (Appendix N). Monitoring of surface movement by resurveying and observation of highway damage found much larger movement and instability in the southern part of the slide. Using threshold head determined at the drilling transect, the southern part of the slide required a higher back-calculated residual shear angle to remain stable (Appendix N).

The stability analysis of Landslide Technology (2004) underscored the importance of erosion in triggering movement, a finding not obvious from any of the observational data. A 2.3 percent decrease in FOS from erosion of 1 m at the toe is a major component in choosing remediation options for any coastal landslide of this type. The same analysis found that a 1-m rise in head at the middle monitoring site caused a 2 percent decline in FOS and that the slide reaches instability when head rise at the middle site reaches 1.1 m above normal winter levels. Removal of 3 m from the toe could thus destabilize the slide during most of the winter season. In general, buttressing all or part of the toe is the most effective option, as it achieves slope stability while eliminating erosion and mass wasting. The first priority for a buttress of this landslide is the southern, least stable part where most highway damage has been concentrated and where resurvey data indicate highest deformation. Mitigating the large increases in pore water pressure in the critical upper 25 percent of the slide could be considered but would be less effective than buttressing. Trenched drainage systems or vertical wells pumped during winter rainfall events may slow or stop slide movement in the short term. Large diameter vertical wells would maximize the number of fractures intercepted. Because threshold pore water pressures have remained fairly constant over the last five years of observation, erosion rates may be relatively low,; thus a drainage system may provide significant remediation before erosion causes movement. Installation of such a system could be justified from a research perspective in order to gain an understanding of the effectiveness of alternative dewatering schemes.

CONCLUSIONS AND RECOMMENDATIONS

Monitoring movement and pore water pressures at the Johnson Creek landslide continues to provide a unique opportunity to examine factors controlling movement of large translational landslides in sedimentary rock. The slide moves in response to intense rainfall that raises water pressure throughout the side over a period of 30–50 hours. The sequence of events that leads to movement starts with vertical infiltration through the unsaturated zone at ~50 mm/hr (~1.5–3.0 m depth in 30–50 hrs). The piezometric elevation slopes down the axis of the slide but the slide surface is nearly horizontal, so in this period of time infiltrating water can reach the water table only at the headwall graben. Infiltration rapidly raises pore water pressure in the graben; pressure is then transmitted down the axis of the slide at speeds of 1.4–2.5 m/hr in the upper part (between sites LT-3 and LT-2) and 3.5 m/hr to virtually instantaneous in the middle part of the slide between monitoring sites LT-2 and LT-1. Arrival time of this "wave" of pressure is similar at different levels in the saturated zone at both the middle and west monitoring sites. It arrives at the east site next to the graben ~1–3 hours after the start of most rainfall events. There is also little vertical hydraulic gradient at the middle and west sites. A flow net showed nearly horizontal flow roughly parallel to the slide plane. These observations and the rapidity of pressure transmission are consistent with a high effective hydraulic conductivity throughout the slide mass (Ellis and others, 2007a, 2007b). The lower piezometric head in the western part of the slide is probably indicative of better drainage there than to the east, possibly in response to a fault or internal slide structure that causes 2 m of down-the-east displacement between boreholes LT-1 and LT-2 (Landslide Technology, 2004; Ellis and others, 2007b).

Pore water pressure changes at the middle of the slide appeared to be a key control of movement. The middle monitoring site has head above the slide plane persistently higher than at sites to the east and west. Total movement there was a factor of 1.8 times that of the east site and a factor of 1.4 times that of the west site (Table 3). The slide begins to move en masse when threshold pressures are reached, the middle site outpacing the ones east and west when pore water pressure there rises above ~9.4–10.8 m head above the slide plane. Pore water pressure thresholds for movement at the site near the headwall graben varied much more widely than at the other two sites, consistent with passive response to movements in the middle. Stability analysis found that pore water pressure change from the middle observation site to the head of the slide accounted for 52 percent in change in factor of safety compared to 21 percent to the east site.

The lower part of the slide also plays an important role in stability. Pore water pressure at the western monitoring site, 62 percent of the way down the slide axis, appears to be a key control on slide movement. The largest, fastest displacement occurred January 31 to February 2, 2003, when pore water pressure at the west site rose as much as at the middle site. In all subsequent movement events, pressure changes at the west site have been no more than about one third of the responses at the middle site. Slide velocity during the 2003 event increased by an order of magnitude relative to all later events. The dramatic effect on stability of this unique rise in head at the west site was confirmed by the stability analysis finding that the slide from this site east accounts for 73 percent of the decrease in factor of safety for a given rise in pore water pressure (Appendix N). The conditions for accelerated movement were 0.84 m of rainfall in the previous 60 days and 62 hours of antecedent rain at a mean rate of 2.1 mm/hr. Other instances of rain at these intensities for 33 and 15 hours did not trigger the unique response at the west site, although in January of 2006 head rose as high as 10.9 m at the middle site. Antecedent movement in December 2002 of the west site 1 cm further than the middle site created extension between the two and possibly raised effective hydraulic conductivity. Increased hydraulic conductivity may have caused the unique early pressure response and increase in head at the west site. The large movement in January 2003 increased compression between the middle and west sites for the remainder of the observation period. This compression may have decreased the effective hydraulic conductivity in the western part of the slide and contributed to the lack of large movement events in subsequent years (Table 3).

Acquiring observational data to test these hypotheses should be a priority for further investigation. Monitoring one of the large movements with the vertical arrays of piezometers now installed will be vital. Measure-

ment of porosity and permeability of rocks and installation of additional inclinometers and piezometers, including innovative wireless piezometers below the slide plane, would greatly improve data quality. Installation should be aimed at other parts of the slide along strike and down the axis. Any new piezometers should be installed using the grouting procedure as opposed to sand-packed boreholes. Pore water pressure data from grouted piezometers are a more accurate measurement of pressure at the installed depth than measurements from piezometers installed in standard sand packs. Grouted piezometers installed at the same depth as adjacent sand-packed piezometers recorded water pressures 1-2 m higher. Sand-packed pressures were lower than the predicted by hydrostatic gradient at the installed depth.

Remediation of water pressures at the headwall graben by drainage through French drains or other means (e.g., vertical wells, sealing the surface) could be implemented on an experimental basis to evaluate alternative approaches. The high hydraulic conductivity of the slide mass should make dewatering schemes effective. Large-diameter vertical wells might be an efficient means of draining the networks of fractures that transmit pressure and water through the slide. Costs could be kept down by pumping only at a threshold of pore pressure or rainfall intensity.

Limit equilibrium stability analysis found that factor of safety (FOS) declines 2.3 percent for every meter of erosion from the passive wedge formed by the back-tilted toe of the slide (Landslide Technology, 2004). The same analysis found that a 1-m rise in head at the middle monitoring site caused a 2 percent decline in FOS and that the slide reaches instability when head rise at the middle site reaches 1.1 m above normal winter levels. Removal of 3 m from the toe could thus destabilize the slide during most of the winter season. Erosion would also be expected to destabilize the toe and possibly create extension in the lower part of the slide with attendant increase in hydraulic conductivity. Buttressing the slide with a revetment is therefore the most effective long-term remediation option. Buttressing eliminates erosion while stopping slide movement. The main environmental impacts of a buttress are (1) creating an unnatural feature at the shoreline, (2) causing loss of dry sand beach from scour and by fixing the shoreline in the face of rising sea level, and (3) cutting off sand supply from bluff erosion. There is little sand content in the current sea cliff (Appendix A), so loss of sand supply would be minimal. The other two impacts can only be mitigated by making the revetment as small as possible. The most cost-effective and environmentally benign option would be to buttress only the southern 30 percent of the slide where the largest, most damaging movement has occurred and where stability analysis indicates the least resistance to sliding (Appendix N). It is possible that buttressing this portion of the slide might improve stability of the rest of the slide. Determining this is an important research objective.

It may be that innovative erosion-control such as a dynamic revetment composed of hard rock cobbles can offer a significant increase in the factor of safety at reasonable cost and with low environmental impact. Dynamic revetments adjust in height in response to wave conditions, rising higher during large wave events. The mass of such a revetment would also help buttress the landslide, possibly increasing the factor of safety significantly. Further study of this option, perhaps with a demonstration project, would be worthy of consideration.

The analysis in this report is incomplete without a more accurate measure of wave erosion at the toe of the slide. Ground-based lidar surveys like those performed May 14, 2004, October 3-4, 2006, and April 3-4, 2007, should be completed annually or semiannually to accurately track erosion so this variable can be properly evaluated against theoretical predictions. Monitoring wave activity from offshore buoy data will allow empirical relationships to be established between erosion and wave strike that may allow erosion prediction in the future from the buoy data alone.

Until remediation is implemented, the current data stream of hourly rain gauge, piezometer, and extensometer data should be used to warn ODOT of impending slide movement. This type of system has been implemented along Interstate Highway 84 in the Columbia River Gorge. This system would require maintaining the current instrumentation and telecommunications links to the two dataloggers. Costs to the State of Oregon will be minimal for the next few years while USGS partners maintain the instrumentation. Table 9 lists possible threshold water pressures for such a system, but all that is needed is monitoring of the water pressure and movement at the key LT-2 site. The observed variability of thresholds for movement makes such a

Table 9. Raw water pressures associated with beginning and acceleration of landslide movement.

Piezometer	Raw Pressure (m) - Start of Movement	Raw Pressure (m) - Accelerated Movement
LT-1p (24.8-m depth)	4.6	7.4
LT-1a (24.08-m depth)	5.9	8.6
LT-2p (16.7-m depth)	6.8	9.8
LT-2a (16.76-m depth)	7.9	10.8
LT-3p (5.5-m depth)	3.0	4.8

These thresholds could be incorporated into a landslide warning system. Pressures are in meters of water above the piezometer tips as recorded by the dataloggers. Threshold values for start of movement are therefore different from those of Table 8. Pressures for start of movement are based on the mean values for start and stop of movement minus one standard deviation. Pressures for accelerated movement are based on peak pressures reached during the January 31 to February 3, 2003, event; as LT-1a and LT-2a piezometers were not installed at that time, values for those piezometers are estimated from values at LT-1p and LT-2p by adjusting for depth differences and then adding 1.85 m to the LT-1p value (for LT-1a) and 0.9 m to the LT-2p value (for LT-2a).

system unreliable for warning of small creeping movements, but still useful for the large movements like the one in 2003. Intense precipitation of ~2 mm/hr for ~60 hours and antecedent rain of ~0.8 m over 60 days were the key factors in triggering the largest slide displacement. When these thresholds are approached, the slide is capable of severe damage to the highway in less than 3 days.

ODOT should keep in mind that any warnings would be experimental at best and that such warnings should not be relied upon without other types of observations. A warning system based on this data collection system might give false alarms, or movement could still occur unexpectedly as a result of evolving internal slide forces, particularly wave erosion. Instrument failures, communications failures, or other factors could also cause the system to fail.

ACKNOWLEDGEMENTS

This project was funded by ODOT Miscellaneous Contract and Agreement, Project Name: Detailed Geotechnical Analysis of Large Translational Landslides in Seaward-Dipping Sedimentary Rocks. State Planning and Research Project 356. Funding for the project was provided to ODOT by the Federal Highway Administration.

In 2005 the essential labor and material support was provided by the U.S. Geological Survey (USGS) Landslide Hazards Program. William L. Ellis of the USGS, Denver, Colorado, office, supervised all telecommunications and instrumental upgrades to allow hourly collection of movement data that proved vital to the project. He made numerous trips from Denver to solve telecommunications issues. William H. Schulz of the USGS supervised drilling and installation of the 2006 piezometers. Rex Baum led the USGS team and made key recommendations that greatly improved the project plan. Thanks are owed to all the USGS partners for their valuable reviews and discussion of data. Special thanks are owed to William Schulz for his instruction in the interpretation of piezometer data from the unsaturated zone. Without this help, the paper could not have been written.

In addition to providing overall technical guidance to the project, ODOT loaned GeoKon LC-1 dataloggers and a Slope Indicator inclinometer cable, probe, and Datamate to the project. Len Saltekoff of ODOT provided estimates of the age of the Old Coast Highway. Jerry Stokes of ODOT provided estimates of average annual maintenance costs where the slide cuts Highway 101. ODOT supervised the drilling contractor for the 2006 boreholes and provided flaggers for highway crossings. Lincoln County also assisted by loaning roadside warning signs during the 2006 drilling.

Technical advisory committee (TAC) reviewers at various stages of the investigation were Michael T. Long, Steve Narkiewicz, Bernie Kleutsch, and Matthew Mabey of ODOT, and Yumei Wang and William J. Burns of DOGAMI. Numerous discussions with the TAC in meetings, by phone, and through e-mail were invaluable. Mike Long also encouraged us at the proposal stage and kindly arranged for acquisition of a 2004 scan of the slide toe using ground-based lidar. The 2004 scan was completed by David Wellman of D. Wellman Surveying L.L.C., Eugene, Oregon. Ranvir Singh of ODOT Geometronics supervised the 2006 and 2007 lidar scans of the slide toe using supplemental funding from ODOT Research.

Marshall Gannet of the USGS provided an invaluable review of initial hydrologic interpretations in the interim report. His discussions about the difference between lateral flow and lateral transmission of hydraulic pressure in causing head change were particularly useful.

Landslide Technology's team of geotechnical engineers and engineering geologists on the project included Charles M. Hammond, CEG; Andrew Vessely, CEG, PE; Jonathan Harris, PE; Erica Meyer, EIT; and Darren Beckstrand, GIT. Mr. Hammond was the geotechnical study project manager. Mr. Vessely provided senior oversight, managed the engineering analyses, reviewed the interim report, and provided key interpretations and advice. Mr. Harris managed the instrumentation and data analysis, installed dataloggers and the rain gauge, and assisted with the engineering analyses. Ms. Meyer performed the engineering analyses. Mr. Beckstrand performed the field inspection and assisted with initial data analysis in 2003.

Geo-Tech Explorations, Inc., of Tualatin, Oregon, performed the 2002-2003 geotechnical drilling and installed slope inclinometer casing and vibrating-wire piezometers under the direction of Landslide Technology. Slope Inclinometer Company supplied slope inclinometer casing and vibrating wire piezometers for the 2002-2003 work. The company also put us in touch with Erik Mikkelsen, who contributed an invaluable analysis of error in the water pressure data from the sand-packed piezometers.

Dennison Surveying Inc., of Newport, Oregon, was retained under DOGAMI contract 41120-080401 to survey the landslide topography and to establish permanent survey hubs for long-term monitoring.

REFERENCES

Collins, B. D., and Kayen, R., 2006, Land-based LIDAR mapping—a new surveying technique to shed light on rapid topographic change. U.S. Geological Survey Fact Sheet 2006-3111, 4 p.

Ellis, W. L., Priest, G. R., and Schulz, W. H., 2007a, Precipitation, pore pressure, and landslide movement—detailed observations at the Johnson Creek landslide, coastal Oregon: First North American Landslide Conference Landslides and Society: Integrated Science, Engineering, Management, and Mitigation, Vail, Colorado June 3–8, 2007a, Conference Proceedings.

Ellis, W. L., Schulz, W. H., Baum, R., and Priest, G. R., 2007b, Hydrogeologic investigations of the Johnson Creek landslide—recent data, results and future plans: 2007 Landslide Symposium: New Tools and Techniques for Developing Regional Hazard Maps and Future Risk Management Practices, Portland, Oreg., April 26–28, 2007.

Grathoff, G. H., 2005, Weathering mineralogy in dunal soils near Newport, Oregon: Oregon Society of Soil Scientists Annual Meeting, oral presentation.

Grathoff, G. H., Peterson, C. D., Beckstrand, D. L., 2001, Coastal dune soils in Oregon, USA, forming allophane and gibbsite: 12th International Clay Minerals conference, Bahía Blanca, Argentina, July 22–28, 2001.

Johnson, C. M., 2003, Iron mineralogy in the Newport dune sheet, Oregon coast: Portland State University M.S. thesis, 38 p. Web link: http://web.pdx.edu/~grathog/StudentWork/Catrina%20Johnson%20UG%20honors%20thesis%20SP03.pdf.

Kane, W. F., and Beck, T. J., 1996, Rapid slope monitoring: Civil Engineering, v. 66, no. 6, p. 56–58.

Landslide Technology, 2004, Geotechnical investigation, Johnson Creek landslide, Lincoln County, Oregon: Oregon Department of Geology and Mineral Industries Open-File Report O-04-05, 115 p.

Mikkelsen, P. E., and Green, G. E., 2003, Piezometers in fully grouted boreholes, Symposium on Field Measurements in Geomechanics, FMGM, Oslo, Norway, 10 p. Web link: http://www.slopeindicator.com/pdf/papers/piezometers-in-fully-grouted-boreholes.pdf .

Priest, G. R., and Allan, J. C., 2004, Evaluation of coastal erosion hazard zones along dune and bluff backed shorelines in Lincoln County, Oregon: Cascade Head to Seal Rock: Oregon Department of Geology and Mineral Industries Open-File Report O-04-09, 188 p.

Priest, G. R., Allen, J. C., Niem, A., Christie, S. R., and Dickenson, S. E., 2006, Interim report: Johnson Creek landslide project, Lincoln County, Oregon: Oregon Department of Geology and Mineral Industries Open-File Report O-06-02, 184 p.

Schulz, W. H., 2007, Hydrologic controls on translational bedrock landslides, coastal Oregon: Geological Society of America Abstracts with Programs, v. 39, no. 6, p. 362.

Schulz, W. H., and Ellis, W. L., 2007, Preliminary results of subsurface exploration and monitoring at the Johnson Creek landslide, Lincoln County, Oregon: U.S. Geological Survey Open-File Report 2007-1127, 11 p., 1 appendix. Web link: http://pubs.usgs.gov/of/2007/1127/.

Sera, M. N., 2003, Site assessment and remediation: CRC Press, Boca Ration, Fla., 1176 p.

Spencer, E., 1967, A method of analysis of the stability of embankments assuming parallel interslice forces: Geotechnique, v. 17, no. 1, p. 11–26.